Portland Cement Association

Research & Development Information

PCA R&D SN2821

The Development of a Rapid Test for Determining the Transport Properties of Concrete

by David Smith
University of New Brunswick

5420 Old Orchard Road
Skokie, Illinois 60077-1083
847.966.6200 Fax 847.966.9481

www.cement.org

The Development of a Rapid Test for Determining the Transport Properties of Concrete

By

David Smith

B.Sc.E., University of New Brunswick, 2004

A Thesis Submitted in Partial Fulfillment of
the Requirements for the Degree of

Masters of Science in Engineering

In the Graduate Academic Unit of Civil Engineering

Supervisor: Michael Thomas, Ph.D, Civil Engineering

Examining Board: Lloyd Waugh, Ph.D, Civil Engineering (Chair)
Theodore Bremner, Ph.D, Civil Engineering
Dr Guida Bendrich, Chemical Engineering

This Thesis is accepted by the
Dean of Graduate Studies

UNIVERSITY OF NEW BRUNSWICK
November, 2006

Abstract

Electrical resistivity techniques are used to give an indication of the relative permeability of concrete. The ASTM C 1202 (Standard Test Method for Electrical Indication of Concrete's Ability to Resist chloride Ion Penetration), more commonly known as the rapid chloride permeability test (RCPT), is widely specified as a quality control method in concrete construction. However, this test is time consuming and is highly dependant on the chemistry of the pore solution.

This test program studied the relationships between the RCP test and instantaneous resistivity measurements and the relationship between resistivity, or its inverse conductivity, and the rate of diffusion of chlorides into concrete.

Theoretically, conductivity and diffusion are linked by what is known as a formation factor in which, among other things, the resistivity of the pore solution must be known. The feasibility of two methods to obtain the pore solution conductivity was examined. It was hoped that the results obtained from the pore solution conductivity tests could be used to develop a new test to determine chloride diffusion coefficients.

Finally, factors such as presence of reinforcing steel and humidity were examined to determine their effect on concrete resistivity when surface measurements are taken on field structures.

Acknowledgements

Several people have helped me in the completion of this project and I would like to take this time to thank them. A special thanks to Dr. Michael Thomas for his encouragement, support and guidance throughout this project. Thanks is also due to the undergraduate and graduate students of the Materials Group for their help. I would also like to express my appreciation of the Civil Engineering Technical Staff and Faculty Shop for their ideas and great workmanship. Finally I would like to thank the Portland Cement Association for their financial contribution to this project.

Table of Contents

List of Figures

List of Tables

List of Symbols

A	=	Area (m^2)
a	=	Spacing between electrodes (mm)
C_i	=	Concentration of ion "i" (mol/m^3)
$C_{i(x,t)}$	=	Concentration of ion "i" and depth "x" at time "t" (mol/m^3)
$C_{i,o}$	=	Surface concentration of ion "i" (mol/m^3)
D	=	Diffusion coefficient (m^2/mol)
d	=	Diameter (m)
D_o	=	Free diffusion of ion in solution at infinite dilution (m^2/s)
erf	=	Error function
F	=	Faradays constant ($9.348x10^4$ J/V*mol)
FF	=	Formation Factor
G_i	=	Conductivity coefficient $(mol/l)^{-0.5}$
I	=	Current (A)
I_m	=	Ionic strength of solution (mol/m^3)
J	=	Flux of ions ($mol/m^2/s$)
J_c	=	Flux of ions due to convection (mol/m2/s)
J_D	=	Flux of ions due to diffusion (mol/m2/s)
J_M	=	Flux of ions due to migration (mol/m2/s)
J_T	=	Total flux of ions ($mol/m^2/s$)
K	=	Correction factor
L	=	Length (m)
λ_i	=	Equivalent conductivity of ion "i" at infinite dilution (m^2*S/mol)
R	=	Universal gas constant (8.314 J/(mol*K))
R	=	Resistance (Ω)
ρ	=	Resistivity (Ω-m)
ρ_m	=	Measured resistivity at given moisture content (Ω-m)
ρ_s	=	Measured resistivity of solution at saturation (Ω-m)
σ	=	Bulk conductivity (S/m)
σ_o	=	Conductivity of pore solution (S/m)
T	=	Temperature (K)
V_c	=	Volume of concrete (m^3)
v_i	=	Velocity of ion "i" diffusing through solution (m/s)
V_{wl}	=	Volume of water lost (m^3)
w_m	=	Weight of concrete at the time of measuring (
w_s	=	Weight of saturated concrete (
z_i	=	Valency of ion "i"

1.0 Introduction

The transport of chloride ions through concrete has very severe ramifications on the service life of reinforced concrete structures, not because of its effect on the concrete, but because of its effect on the reinforcing steel.

In a high alkaline environment, such as concrete, a passive layer is formed on the surface of reinforcing steel. This layer is a very dense, slowly reacting corrosion product that essentially prevents further corrosion of the steel bars. However, this layer can be broken down in one of two ways, carbonation or chloride attack.

Carbonation lowers the pH of the concrete to a level where the passive layer is no longer stable, allowing corrosion to occur. This attack is common in balconies, soffits and other exposed concrete that is sheltered from direct precipitation.

While corrosion due to carbonation occurs relatively infrequently, a much more prevalent problem is chloride induced corrosion in structures exposed to marine conditions and deicing salts. Once the chloride concentration at the steel has reached a sufficient level (chloride threshold) it will attack the passive layer and reduce its ability to protect the underlying steel. The volume of the corrosion products is much larger than that of the reactants, therefore the formation of these products produces expansive forces on the concrete. These forces lead to cracking, spalling and delaminations, severely reducing the service life of the structure.

Due to the risk of corrosion, many owners of new structures that will be exposed to chlorides, either through deicing salts or marine environments, have specified the use of

low permeability concrete to reduce the rate at which the chlorides ingress into the concrete, thus extending the life of their structure.

CSA A23.1-04 specifies that for exposure class C-1 (structurally reinforced concrete exposed to chlorides) the maximum water to cementitious materials ratio (w/cm) is 0.40 and the concrete must have less than 1500 coulombs passed in the ASTM C 1202, "Rapid Chloride Permeability Test (RCPT)" at 56 days. The C-XL class (structurally reinforced concrete exposed to severe chloride conditions) requirements are even more stringent with a w/cm of 0.37 or less and a RCPT requirement of less than 1000 coulombs at 56 days.

1.1. Problem Statement

With the widespread specification of high-performance, low-permeability concrete, it is necessary, for quality control measures, to have a test that gives an indication of the concrete's quality. The currently accepted method is ASTM C 1202 Standard Test method for Electrical Indication of Concrete's ability to Resist Chloride Ion Penetration, more commonly known as the Rapid Chloride Permeability Test (RCPT). While its name suggests it, the RCPT is anything but rapid. A full day is required to cut and prepare the samples, and another full day is required for testing. It is for this reason that there is a need for a new rapid test quality control and assurance test.

A second reason for the development of this test method is to have a portable test that can be used in the field. At present, many contracts specify that, if cylinders fail to meet the specified RCPT values, cores must be taken from the structure and tested. If there were a

reliable field test then there would be no need to drill holes in the new structure, or spend more time and money on laboratory testing.

A third, and more difficult, problem is the need for a rapid test to give an accurate prediction of the chloride diffusion coefficient of concrete. This value is vital in service life prediction of structures. The current method is a long, labour intensive test, and must be performed at several different ages to have confidence in predicting how the diffusion coefficient of that particular concrete will change with time.

1.2. Goals and Objectives

There were two main goals of this project. The first was to develop a rapid quality control test that could replace current tests. This test may also have use in the field, reducing the need for laboratory testing. The second goal was to examine the feasibility of using electrical resistivity tests to accurately predict the rate of diffusion of chlorides through concrete.

1.3. Objectives

To achieve the goals previously stated, the following objectives must be met.

1. Examine various electrical resistivity test methods to determine if all tests give similar results.
2. Determine if a relationship exists between resistivity and charge passed in the Rapid Chloride Permeability test.

3. If a strong relationship does exist, recommend ranges of resistivity to classify the risk of chloride penetration. These ranges would correspond to the ranges set out in the RCP test (ASTM C 1202).
4. Study the effect that cover depth of reinforcing steel has on the resistivity of saturated concrete when measured with the Wenner Probe.
5. Determine if probe alignment, with respect to the direction of the reinforcing steel, has an effect on surface resistivity measurements.
6. Determine if natural wetting and drying of field concrete has a significant effect on surface resistivity measurements.
7. Determine if a relationship exists between concrete resistivity and the rate of diffusion of chloride ions through concrete.
8. Study the effectiveness of two different methods to determine the conductivity of concrete pore solution.
9. Improve the relationship between resistivity and diffusion by the use of a formation factor, using results from the pore solution conductivity tests.
10. Compare diffusion coefficients determined by two different monitoring methods of the electrical migration test.
11. Compare diffusion coefficients obtained through electrical migration tests to those obtained from the bulk diffusion test.

1.4. Methods

To achieve the goals and objectives set out previously, five different electrical resistivity tests, as well as various ion transport tests were conducted on concrete with a wide range of maturity and composition.

Samples under two different moisture conditions (saturated and naturally exposed) as well as saturated concrete with reinforcing steel with varying cover depths were tested using a hand-held surface resistivity meter. This testing was conducted to determine if these variables significantly influence surface resistivity measurements.

Two different methods were used to measure the electrical conductivity of pore solution of concrete. These results were then used in the formation factor formula to attempt to improve the relationship between resistivity and the rate of diffusion of chloride ions through concrete.

A much more detailed description of the tests used can be found later in this document.

1.5. Scope

The large majority of the work done in this project was conducted on saturated concrete specimens under laboratory conditions. It is realized that many other factors influence resistivity, however it is not within the scope of this project to quantify the impact of these factors. However, once it was found that resistivity could be used as a quality control method, a small-scale study was conducted to determine if the depth of variation in surface saturation, due to natural exposure, was significant enough to impact the resistivity results obtained with the Wenner Probe. However, it was not within the scope of this project to develop a relationship between the degree of saturation and surface

resistivity measurements. It was also not the intention to determine to what depth natural wetting and drying affects the saturation condition of bulk field concrete.

A comparison of two methods for determining the diffusion coefficient of chlorides through concrete by electrical migration was conducted. However, this was by no means a comprehensive comparison of the two methods.

2.0 Literature Review

2.1. Chloride Transport

One of the major causes of deterioration of concrete marine and transportation structures is chloride-induced corrosion of reinforcing steel. It is, therefore, very important to understand the process by which chlorides can reach the reinforcing steel. There are three possible ways for chlorides to move into concrete: absorption, hydrostatic pressure and diffusion (Stanish, 1997).

Absorption is driven by moisture gradients meaning water, and whatever is dissolved in it, will travel from areas of high moisture content to areas of low moisture content. Therefore, atmospherically exposed concrete subjected to wetting and drying cycles is susceptible to chloride ingress by this method. In most exposure conditions the moisture gradient is typically restricted to a very small depth (below which the concrete is saturated) and is therefore not a major mechanism affecting the ingress of chlorides to the reinforcing steel. However, it does reduce the distance between the steel and the chloride front, thus reducing the time until the chlorides reach the steel by other transport mechanisms.

If a hydraulic head is applied to the face of a concrete structure, a hydraulic gradient is formed which will cause water flow, however it is rare that gradients of sufficiently high magnitude occur to produce significant flow rates in concrete.

Under most field conditions, in which the bulk of the concrete remains saturated, the most influential of the transport mechanisms is diffusion caused by concentration

gradients within the pore solution of the concrete. There is a strong driving force to gain concentration equilibrium within any substance.

2.1.1. Theory of Diffusion

The diffusion of chloride ions in saturated concrete under steady-state conditions is controlled by Fick's First Law that states;

$$J = D\frac{dC}{dx} \qquad \text{(Equation 1)}$$

Where:

J = Flux of chloride ions (mol/m^2/s)
D = diffusion coefficient (m^2/s)
C = is the concentration of chloride ions (mol/m^3)
x = position with respect to the surface of the concrete (m)

The effective diffusion coefficient takes into account the fact that the chlorides are not diffusing through a homogenous medium, rather through a porous cement matrix and the pore solution contained within. The use of an effective diffusion coefficient also acknowledges that, through hydration, the cement matrix is continually changing, especially at young ages.

Fick's First Law only applies when steady-state flow is occurring, meaning a constant gradient exists however chlorides have broken through to the other side of the concrete and all potential chloride binding has occurred. A more likely description of chloride diffusion in structural concrete would be the non-steady state described by Fick's Second Law:

$$\frac{\partial C}{\partial t} = D_{eff} \frac{\partial^2 C}{\partial x^2} \qquad \text{(Equation 2)}$$

Given boundary conditions of $C_{(x+0,\ t>0)} = C_0$, $C_{(x>0,\ t=0)} = 0$ and $C_{(x+\infty,\ t>0)} = 0$ the solution to this differential solution is (Crank, 1975):

$$\frac{C(x,t)}{C_0} = 1 - erf\left(\frac{x}{\sqrt{4 D_{eff} t}}\right) \qquad \text{(Equation 3)}$$

Where:

C_0 = Surface concentration (mol/m^3)
t = time (s)
C(x,t) = concentration at depth x at time t (mol/m^3)
erf = error function

Fick's First and Second Laws, as stated above, describe the rate at which a particle diffuses at a given temperature. However, the rate of diffusion for a particular system is highly dependant on temperature. Because the diffusion rate is dependant on the interaction of molecules, the higher the temperature, and therefore the higher the energy, of a molecule, the faster the rate of diffusion. This temperature dependence is described the Arrhenius Equation:

$$D = D_0 e^{-\frac{E_A}{RT}}$$

where:

D = Diffusion coefficient (m^2/s)
D_0 = Maximum diffusion coefficient at infinite temperature (m^2/s)
E_A = Activation energy (J/mole)
T = Temperature (K)
R = Universal gas constant (8.314 J/mol*K)

2.1.2. Properties Affecting Diffusion

The pore structure of the cement paste, which dictates the rate of diffusion of ions through the concrete, is affected by several factors, including age, water to cementitious materials ratio (w/cm), use of mineral admixtures, the temperature at which the concrete is cured and the propensity of the cement paste to bind chlorides (which is controlled to a large extent by the C_3A content of the cement).

The age, or more importantly the degree of hydration, significantly affects the diffusion rate of ions through concrete. The more fully hydrated the cement paste, the more poorly connected and tortuous the pores in the matrix, making it more difficult for the ions to pass through the paste. The rate of change in the pore structure is very high at early ages and continually drops off as the degree of hydration increases.

Supplementary cementing materials (SCMs), in the long run, have very significant benefits in reducing the permeability of concrete. These materials react in a secondary reaction called the pozzolanic reaction. The siliceous portions of the SCMs react with the relatively porous calcium hydroxide (CH), a by-product of the hydration of portland cement, and produces calcium silicate hydrates (C-S-H) which render the concrete less porous. CH is a dense material that forms early in the hydration process. It is relatively soluble and reacts with the pozzolan to form a needle like shield in the pore structure, rendering the concrete less permeable to the flow of water. SCMs can also have a beneficial effect by simply acting as fillers, blocking the pore matrix.

The use of SCMs affects the rate of diffusion at early ages in different ways depending on the reactivity of the material used. For example, silica fume has a very fine particle size and reacts very quickly with the CH and its benefits can be seen at very early ages. Fly

ash, on the other hand, has a relatively slow pozzolanic reaction and consequently may have a detrimental effect on the pore structure at early ages, however, by the age of one year, concrete containing fly ash typically has equaled or surpassed concrete with silica fume added and most certainly concrete with no SCMs.

The temperature at which concrete is cured also affects the rate of diffusion. Concrete cured at elevated temperatures will experience accelerated hydration and, at young ages, will exhibit lower diffusion rates than identical concrete cured at lower temperatures. However, at later ages when concrete cured at a lower temperature has a chance to catch up, it will typically have a lower diffusion rate. This is because accelerated curing leads to a coarser pore structure and possible micro-cracking of the cement paste matrix (Stanish, 1997).

Cement that has a high capacity to bind chloride in the matrix will obviously reduce the diffusion coefficient if measured during non steady state conditions. However, if steady state has been achieved there will be no effect on the diffusion rate by chloride binding other than the fact the binding of the chlorides will render the concrete less permeable, a result of the matrix being slightly more dense.

The C_3A content of the cement used is the major determining factor in the amount of chlorides that are chemically bound in the matrix. Chlorides are chemically bound when they react with the calcium aluminates in the cement paste and form Freidel's salt (Csizmadia et al, 2000).

2.1.3. Bulk Diffusion Test

A common way to determine the diffusion coefficient of concrete is to use ASTM C 1556 Standard Test Method for Determining the Apparent Chloride Diffusion Coefficient of Cementitious Mixtures by Bulk Diffusion. This procedure consists of immersing the specimen in saturated calcium hydroxide solution until a constant weight has been achieved and then and sealing all but one face of a 100mm diameter by 75mm thick concrete disc. The sample is then submerged in a 2.8M NaCl solution for a minimum of 35 days. After the soak period, the sample is incrementally ground parallel to the surface using a milling machine or a lathe. A common depth for each pass is 1mm. The dust samples from each increment are collected and analyzed to determine the chloride content. The error function solution of Fick's Second Law is then fitted to the data and a diffusion coefficient and a surface concentration are determined by iteration.

2.2. Electrical Migration

The understanding of diffusion of chloride ions through concrete is very important, however, because the diffusion rate is so slow, it takes a very long time to conduct tests. Consequently, faster methods have been developed which use an electrical gradient to supplement the driving force of the concentration gradient. The total flux of chlorides through concrete can be described as the sum of the flux induced by a concentration gradient, the flux induced by an electrical gradient and the flux induced by the moisture gradient. Therefore, the total flux of the chlorides through the concrete is (Stanish, 2002):

$$J_T = J_D + J_M + \mathrm{J_C} \qquad \text{(Equation 4)}$$

where:

J_T = total flux
J_D = flux due to diffusion
J_M = flux due to migration
J_c = flux due to convection

J_D can be found using Fick's First Law as described in the previous section and J_M can be determined using the Nernst – Planck equation shown below.

$$-J(x) = \frac{zF}{RT} DC \frac{\partial V}{\partial x} \qquad \text{(Equation 5)}$$

Where:

J(x) = flux (mol/m^2/s)
C = concentration (mol/m^3)
D = diffusion coefficient (m^2/s)
z_i = valence number of ion "i"
F = Faraday's constant 9.348x10^4[J/(V*mol)]
U = potential (V)
R = gas constant 8.314 [J/(mol*K)]
T = temperature (K)
x = distance from surface

Combining the terms for diffusion, migration and convection the following equation is obtained:

$$J(x) = D \frac{\partial c}{\partial x} + \frac{zF}{RT} DC \frac{\partial V}{\partial x} + Cv(x) \qquad \text{(Equation 6)}$$

The first term, $D\frac{\partial C}{\partial x}$, is the flux due to the concentration gradient, $\frac{zF}{RT}DC\frac{\partial V}{\partial x}$ is the flux due to the electrical gradient and $Cv(x)$ is the contribution due to convection. In steady-state migration, where the diffusion and convection components are much smaller than the migration component and can be neglected, Equation 6 can be simplified to:

$$J(x) = DC\frac{zF}{RT}\frac{\Delta V}{\Delta x} \qquad \text{(Equation 7)}$$

Typically, when determining the flux of chlorides through concrete, the increase in concentration of the chlorides on the downstream portion of the cell is monitored. However, depending on the age and composition of the concrete it may still take a substantial amount of time for steady state flow to occur, even if an electrical gradient is applied. To reduce the time needed to establish the steady state flux of chlorides through concrete, a method was proposed by Truc (1999) in which the decrease in chloride concentration of the upstream reservoir is to be monitored. Truc argued that, once chloride binding in the outermost layer of the concrete had occurred, the flow through that portion of concrete would be at steady state. Therefore, the decrease in the concentration in the upstream reservoir, from that point on, would equal the increase in concentration in the downstream reservoir once steady state flow through the entire specimen was established. In theory this proposal makes sense, however the major issue in using this method is accurately measuring very small changes in high concentration chloride solutions, which can be quite difficult with the equipment typically found in a concrete testing facility.

2.3. Electrical Resistivity – Theory

Electrical resistivity is a normalized measure of a materials ability to resist the passage of electrical current. The electrical current is passed by the ions in the pore solution of the concrete – the cement matrix acts as an insulator – so it is therefore reasonable to assume that the current would follow a similar path as any ions as they move into the concrete.

Resistivity is measured by applying a known current or voltage and measuring the effect the concrete has on the other, a resistance can then be calculated by use of Ohm's Law. A more in-depth discussion of testing methods can be found later in this document. Ohm's law states that:

$$V = IR \qquad \text{(Equation 8)}$$

where:

V = electrical potential across the sample (V)
I = current passed through the sample (A)
R = Resistance (Ω)

The resistance determined above is then normalized by the following equation resulting in a resistivity value.

$$\rho = R\frac{A}{L} \qquad \text{(Equation 9)}$$

where:

ρ = Resistivity (Ω-m)
A = cross-sectional area of sample (m)
L = length of sample (m)

2.3.1. Formation Factor

The bulk resistivity, or its inverse conductivity, of a porous material can be related to diffusion through what is known as a formation factor, initially developed by the petroleum industry for determining the bulk conductivity of the rocks from which oil was to be extracted. This principle can be applied to any porous material containing liquid, such as concrete. The formation factor is defined as:

$$FF = \frac{\sigma}{\sigma_0} = \frac{D}{D_0} \qquad \text{(Equation 10)}$$

therefore;

$$D = \frac{D_0 \sigma}{\sigma_0} \qquad \text{(Equation 11)}$$

where:

σ = bulk conductivity of porous material in Siemens/meter (S/m)
σ_0 = conductivity of pore solution (S/m)
D = diffusion coefficient (factor of interest) (m^2/s)
D_0 = free diffusion of chloride in solution of infinite dilution (m^2/s)

The bulk conductivity of the porous material can be easily measured by the techniques described below and the free diffusivity of chlorides can be determined from physical tables. The conductivity of the pore solution is the most difficult of the factors to determine. To determine the conductivity the pore solution can be pressed from the concrete and chemically analyzed or measured in-situ with a conductivity probe, or the concrete can be dried out and the pore solution replaced with a solution of known conductivity as suggested by Streicher and Alexander (1995). Each of these methods have their drawbacks.

Pore solution extraction requires a compression-testing machine with a capacity of 7 – 10 MN, a special press, and the ability to carry out chemical analysis, a combination only found in a few laboratories in North America. Even if a laboratory has all three components, extraction could prove very difficult depending on the degree of hydration and the w/cm of the concrete.

The replacement of the pore solution with a solution of known conductivity requires several days of sample conditioning which may or may not be effective on low permeability concrete. This method also does not account for the ions that precipitated out during the drying period and would be subsequently dissolved in the new solution changing the conductivity of the known solution (Stanish 1997).

The in-situ measurement of the pore solution using a conductivity probe has not been attempted to the author's knowledge. This would require establishing a small reservoir in the sample and inserting a microprobe (i.e. $\leq$ 1mm in diameter) to determine the conductivity of the solution in the reservoir. The technique requires that the solution in the reservoir comes to equilibrium with the pore solution and the measurement does not disturb the solution composition (e.g. by carbonation). This technique is explained as part of this thesis.

2.3.2. Calculating Pore Solution Conductivity

The resistivity of pore solution can be measured directly by use of a conductivity probe or it can be calculated, if the concentrations of the constituent ions are known. Like solids, aqueous solutions obey Ohm's law, where the voltage (V), current (I) and resistance of a system are related by:

$$V = IR \qquad \text{(Equation 12)}$$

At any concentration, the equivalent conductance of an aqueous electrolytic solution (λ_e) is described in terms of one mole of electrolyte placed between 2 parallel plate electrodes 1 cm apart.

In an aqueous solution the concentration of the ions has a significant impact on its electrical conductance. Most of the equations have been developed for solutions of low concentrations (Horvath, 1985). At higher concentrations most of the equations developed lose their accuracy.

The conductivity of an aqueous solution can be calculated as a weighted sum of the equivalent conductivity, λ_i, of the ions in solution (Snyder 2003). This solution is presented below:

$$\sigma_o = \sum z_i c_i \lambda_i \qquad \text{(Equation 13)}$$

where:

σ_o = calculated conductivity of pore solution (S/m)
z_i = valency of species
c_i = concentration of species (mol/m^3)
λ_i = equivalent conductivity of ion *i* at infinite dilution (m^{2}S/mol)

λ_i can then be calculated by:

$$\lambda_i = \frac{\lambda_i^o}{1 + G_i I_m^{1/2}} \qquad \text{(Equation 14)}$$

where:

λ_i^o = equivalent conductivity of ionic species at infinite dilution (cm^2 S/mol) (Table 2.1)

G_i = conductivity coefficient $(mol/l)^{-0.5}$ (Table 2.1)

I_m = Ionic strength of solution

and I_m is defined as;

$$I_m = \frac{1}{2}\sum_i z_i^2 c_i \qquad \text{(Equation 15)}$$

Table 2.1: Equivalent Conductivity at Infinite Dilution and Conductivity Coefficients at 25°C (Snyder, 2003)

Species	$z\lambda^o$ (m^2 S/mol)	G $(mol/l)^{-0.5}$)
OH^-	0.0198	0.353
K^+	0.00735	0.548
Na^+	0.00501	0.733
Ca^{2+}	0.00590	0.771
SO_4^{2-}	0.00790	0.877

2.4. Factors Affecting Resistivity

The electrical resistivity of concrete is highly dependent on several factors including moisture content, temperature, presence of reinforcing steel, pore structure and pore solution which will be discussed next.

2.4.1. Moisture Content

As previously discussed, it is the pore solution of the concrete that transfers applied electrical current during resistivity testing. It would therefore follow that the degree of saturation of the concrete would have a significant effect on resistivity measurements. In

other words, identical concrete at different moisture contents will exhibit substantially different resistivity readings.

Su et al (2002) conducted testing in which the resistivity, by four point Wenner Probe, was measured on concrete subjected to various drying conditions (saturated, air dried for 4-8 hr and then oven dried for at least 1 hr). To account for geometrical influences as described by Morris et al (1995), the resistivity measurements were normalized by:

$$\rho = \frac{\rho_m}{\rho_s} \qquad \text{(Equation 16)}$$

where ρ_m and ρ_s are the measured resistivity at a certain moisture condition and the measured resistivity of saturated concrete respectively.

The water loss ratio (V_{wl}) was calculated using:

$$V_{wl} = \frac{(w_s - w_m)}{V_c} \qquad \text{(Equation 17)}$$

where w_s is the weight of saturated concrete, w_m is the weight of concrete at time of measuring, and V_c is the volume of concrete.

In this study concrete with w/cm of 0.45, 0.55 and 0.65 were tested. Results show that for a water loss of 9 percent a five-fold increase in resistivity is experienced.

Saleem et al (1995) have also demonstrated the extreme dependence of resistivity on moisture content and ionic species present in the pore solution (Figure 2.1). As can be seen here, there is little change in resistivity above 4% moisture content, however there is a significant impact below this value.

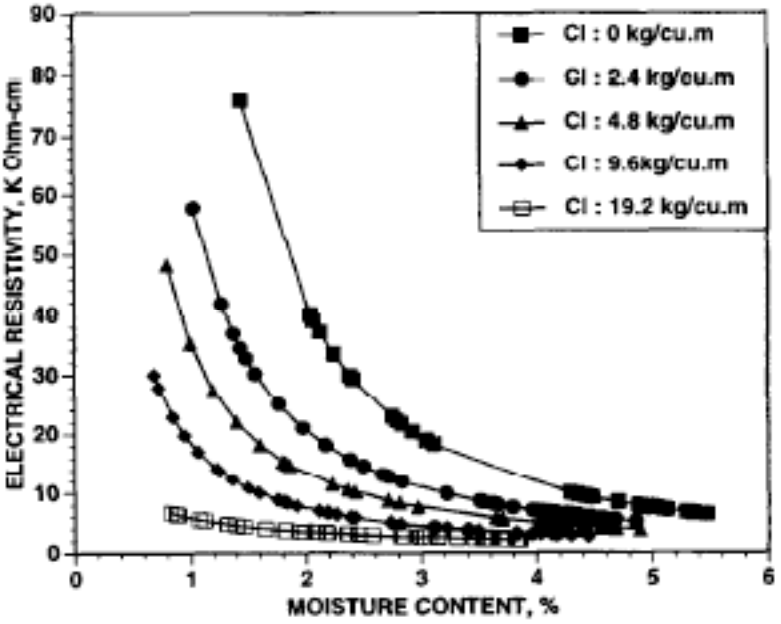

Figure 2.1: Relationship Between Resistivity and Moisture in Chloride Contaminated Concrete (Saleem et al, 1995)

2.4.2. Temperature

The temperature of the concrete is another factor that has a major effect on the resistivity. This influence is due to the change of viscosity of the pore solution, thus changing the mobility of the ions in solution that carry the charge. This relationship can be described by the law of Rasch and Hinrichsen (Whiting and Nagi, 2003) which is as follows:

$$\rho_2 = \rho_1 e^{A(\frac{1}{T_2}-\frac{1}{T_1})} \qquad \text{(Equation 18)}$$

where:

ρ_1 = resistivity at T_1

ρ_2 = resistivity at T_2

T_1, T_2 = temperatures (Kelvin)

A = constant

Hope and Ip (1985) conducted work that shows the temperature dependency of resistivity (Figure 2.2). Samples were conditioned to 75% relative humidity by placing prisms in desiccators over saturated salt solutions and applying a partial vacuum. The samples were left in this condition until hygral equilibrium was achieved. As can be seen in Figure 2.2, an increase in temperature results in a decrease in the resistivity of the concrete. It should also be noted that the resistivity increases with the water cement ratio, which is opposite to the trend exhibited in saturated concrete, however no explanation was given as to why this is so (Hope and Ip, 1985).

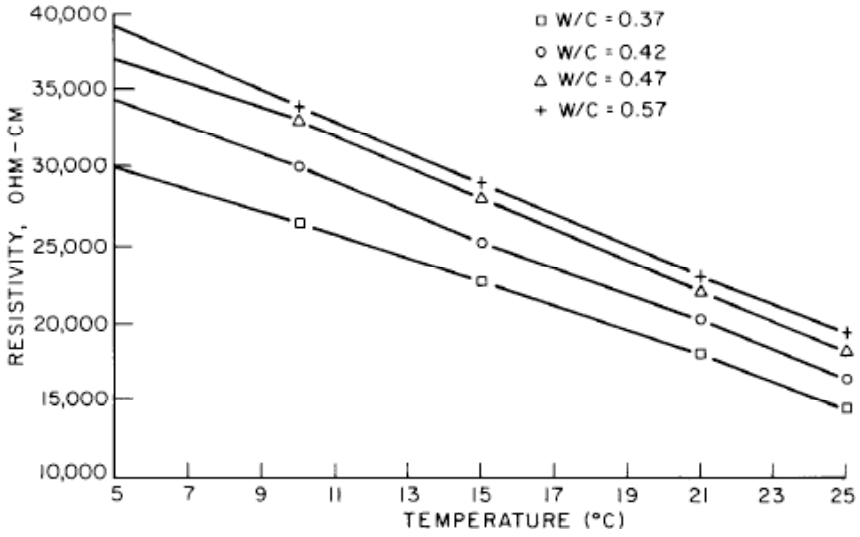

Figure 2.2: Influence of Temperature and w/c on Resistivity of Prisms and 75% R.H. (Hope and Ip, 1985)

To compensate for this effect of temperature on resistivity, a temperature reduction curve has been developed by Spencer (1937) and later added to by Woelfl and Lauer (1979) using data from Monfore (1968) (found in Whiting 2003). The close fit of the data (Figure 2.3) indicates that this could be a useful tool for normalizing resistivity data to a standard temperature.

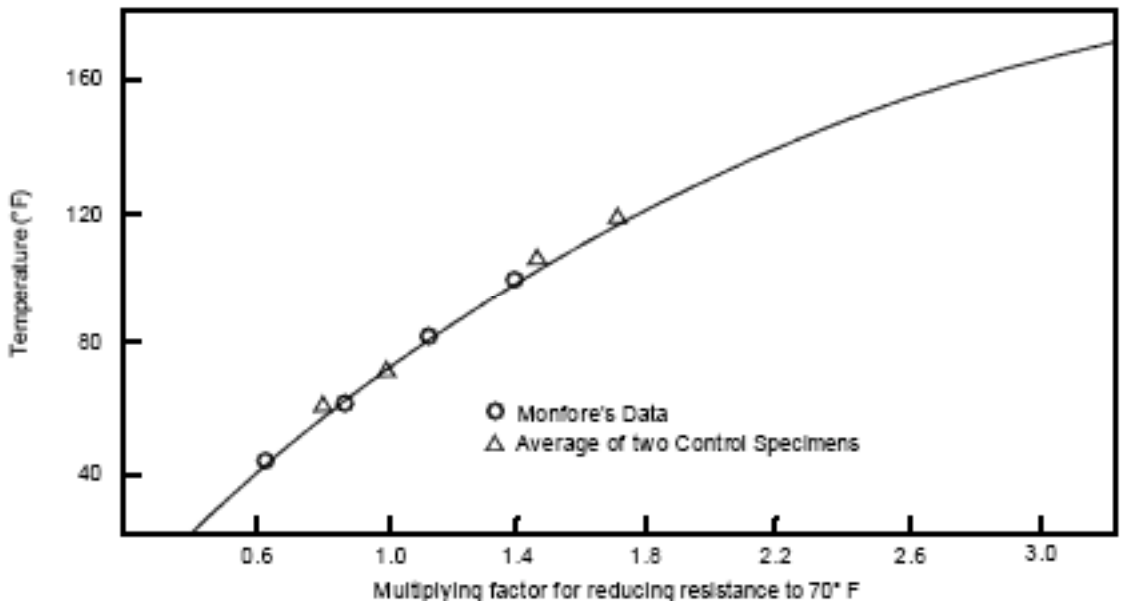

Figure 2.3: Temperature reduction curve for electrical resistivity (Whiting and Nagi 2003)

2.4.3. Presence of Reinforcing Steel

The principle of measuring the electrical resistivity of concrete is to pass a known electrical current through the concrete and measure the voltage drop that occurs over a given distance due to the resistive force of the medium through which the current travels. Reinforcing steel has a much lower resistance to electrical current than concrete, so therefore, if reinforcing steel is present close enough to the location of testing, it will act as a short circuit, greatly reducing the voltage drop that would otherwise occur. The work of Hope and Ip, (1985) using pairs of embedded electrodes, illustrates this point very well (Figure 2.4). In this experiment electrodes were placed in the concrete with the configuration shown in the inset of Figure 2.4. The resistivity was then measured, in increasing distance from the left hand edge of the specimen, between pairs of electrodes (A-B, C-D and E-F). The resulting measurements are found in the graph in Figure 2.4.

It has been found that, for the Wenner probe at least, the depth of influence is equal to the spacing of the electrodes measuring the potential drop (Morris et al, 1996). It could therefore be assumed that as long as the cover depth is greater than the tip spacing of the probe there will be no reduction of in resistivity. Also, the minimum spacing of the probe tips should be 1.5 to 2 times the size of the maximum size aggregate (Morris, 1996).

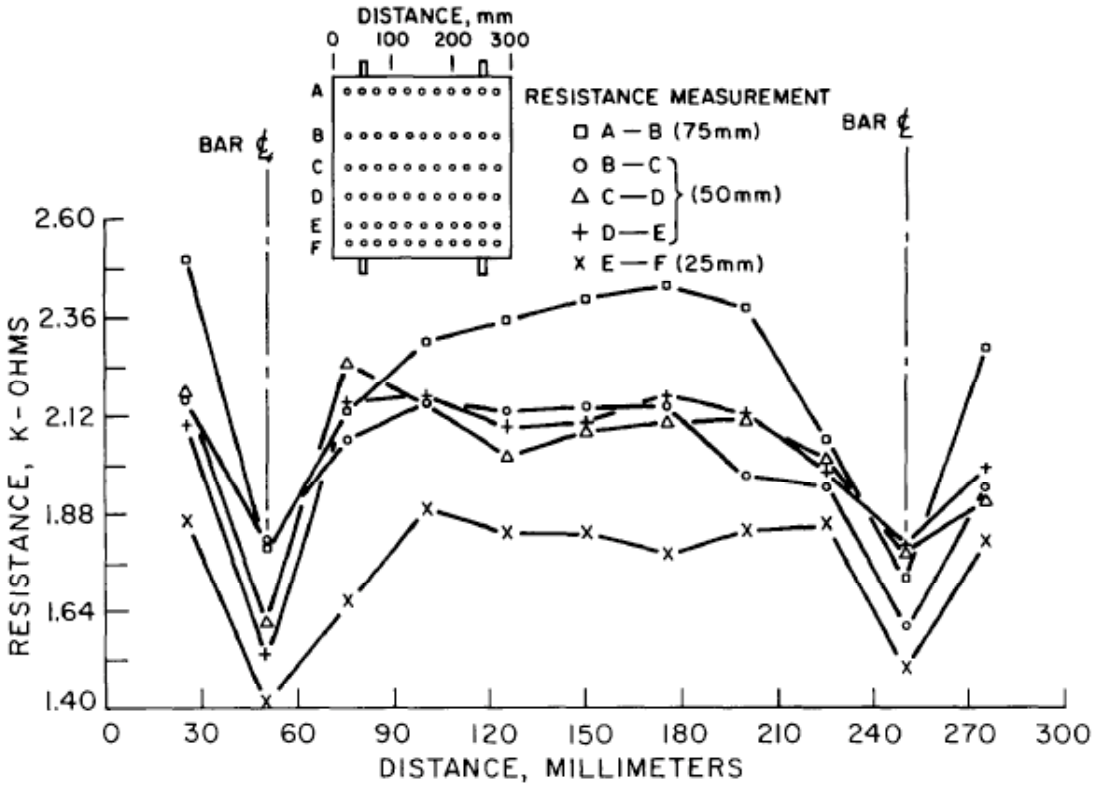

Figure 2.4: Influence of proximity of reinforcing steel on measured resistance (Hope and Ip, 1985)

2.4.4. Pore Solution Composition

With an increase of ions in solution comes an increase in the solutions ability to conduct an electrical current. This is due to the reduced average distance that ions must travel in solution to transfer the electrical charge. Saleem et al (1995) showed that with an

increase in contaminants in the pore solution, in this case chloride and sulfate, there is a decrease in the resistivity of the concrete (Figure 2.1 and Figure 2.5) for chloride and sulfate, respectively.

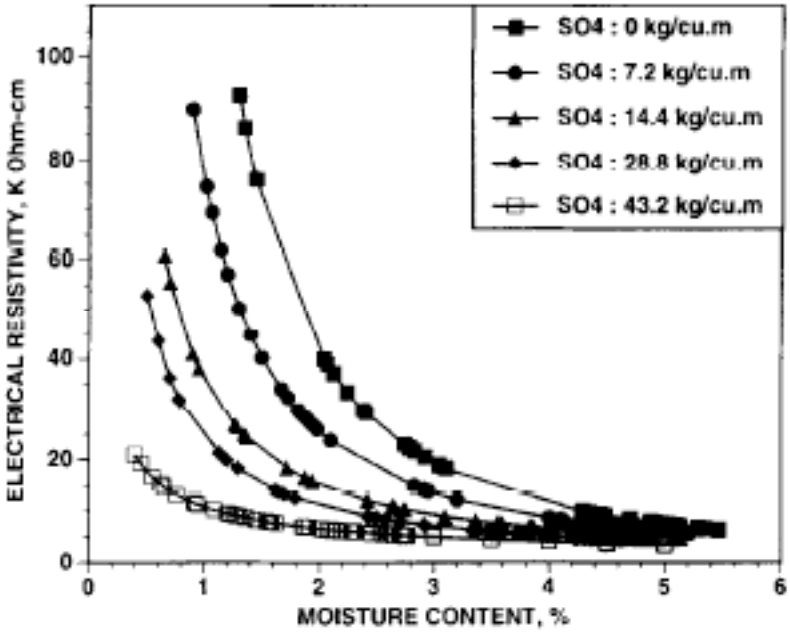

Figure 2.5: Relationship between moisture montent and resistivity in sulfate contaminated concrete (Saleem et al, 1995)

2.4.5. Polarization

When DC currents are applied to concrete a chemical reaction occurs at the electrodes which can cause a voltage drop, in addition to the drop caused by the paste matrix. the reactions that may occur are (Hansson, 1983):

$$2H_2O + 2e^- \leftrightarrow H_2 + 2\ OH^- \qquad \text{(Equation 19)}$$

$$4OH^- \leftrightarrow O_2 + 2H_2O + 4e^- \qquad \text{(Equation 20)}$$

These reactions cause a build up of a polarized layer near the electrodes causing a back emf, in turn increasing the bulk voltage drop across the sample. It is generally thought that these reactions do not have time to set up if an alternating current is used at the proper frequency (Hansson, 1983). One way to overcome the voltage drop due to polarization when using a DC power supply is to use a method developed by Monfore in which the current is read at various voltages and the slope of the best fit line through the data is take as the resistance (Hansson, 1983).

Figure 2.6 gives an example of the Monfore method. In this case, the voltage drop caused by polarization is the intercept of the best-fit line (1.45 V) and the resistance used in the resistivity calculation is the slope (1513 Ω).

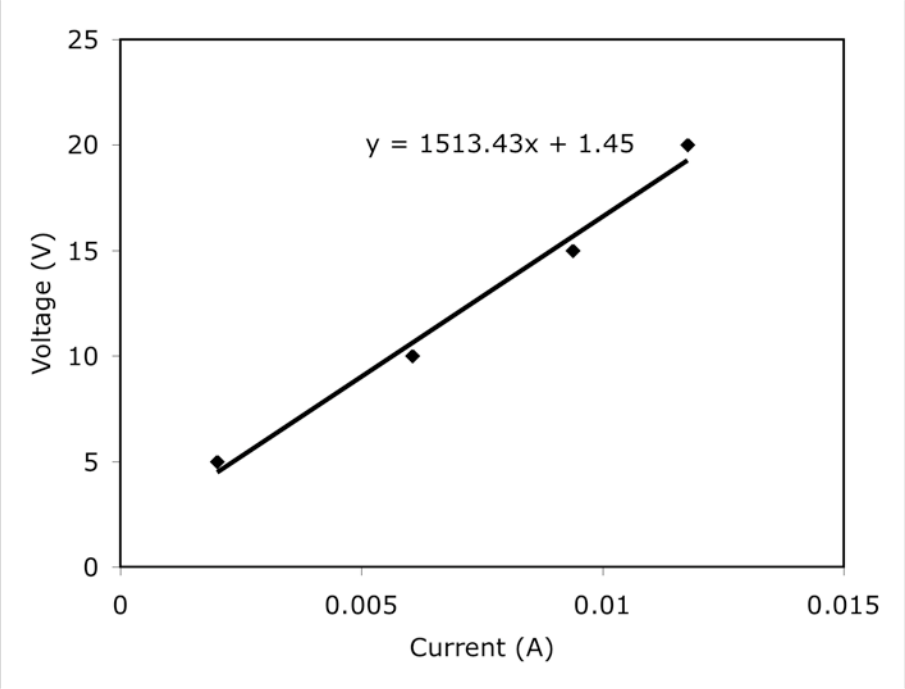

Figure 2.6: Example of Monfore method

2.5. Electrical Resistivity – Test Methods

2.5.1. Parallel Electrodes

One common way to measure the bulk resistivity of concrete is to sandwich the sample between two electrodes as shown in Figure 2.7. One of the electrodes is attached to the negative pole of a power supply and the other electrode is attached to the positive. A constant current is applied to the system and the voltage drop across the sample is measured. A bulk resistivity can then be determined using Equation 9. This method is typically used on cylinders or cores taken from structures. It is a very simple method that requires minimal testing equipment and time.

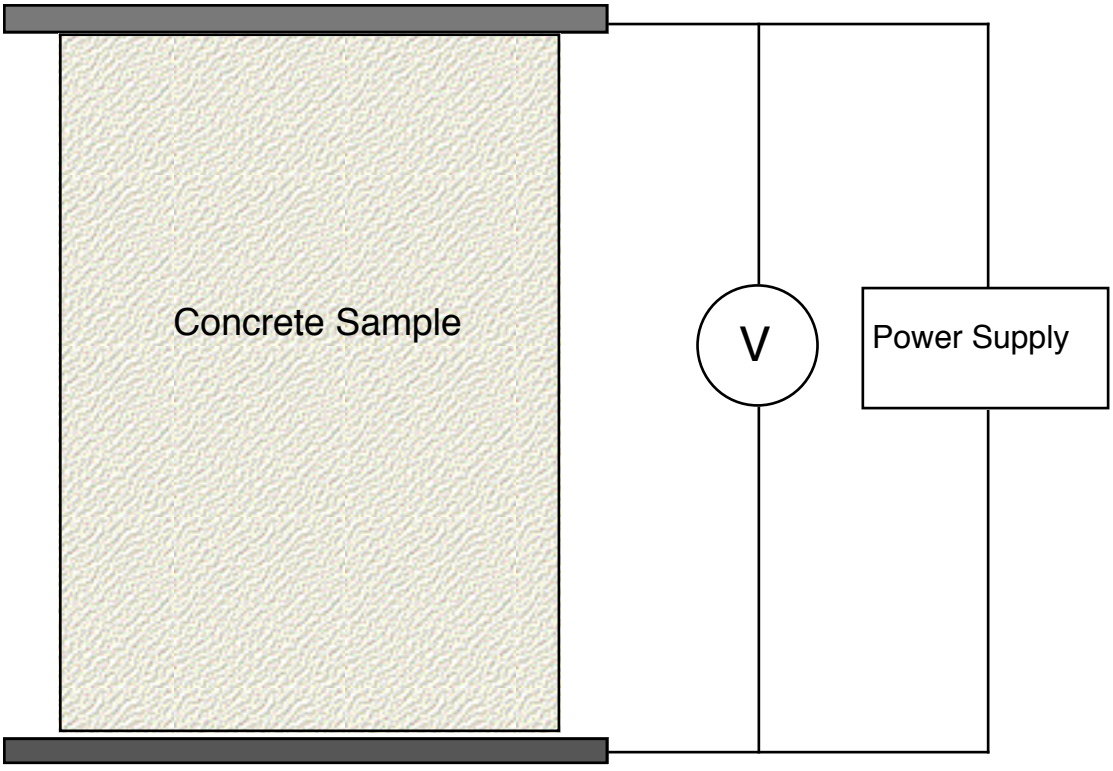

Figure 2.7: Parallel plate resistivity schematic

2.5.2. Single Electrode

This method uses a small metallic disc placed on the concrete surface as the electrode and reinforcing steel bar as the counter-electrode. The resistivity is then calculated using the following equation (Bloomfield, 1997).

$$\rho = 2Rd \qquad \text{(Equation 21)}$$

where d is the diameter of the metallic disc and R is the measured resistance.

This technique has the advantage of eliminating the influence of the reinforcing bar by incorporating it into the system, however it is very sensitive to contact resistance (Bloomfield, 1997).

2.5.3. Two-Point Probe

This technique consists of passing a known current between the two points and measuring the drop in voltage however, this technique has two major drawbacks that limit its effectiveness.

The first is that resistivity is influenced primarily by the concrete immediately around the tips of the electrode. Therefore, if the electrode is placed directly over an aggregate, which has a much higher resistivity than concrete, the reading will be much higher than the true resistivity of the concrete (Whiting and Nagi 2003)

The second is the fact that holes 6.5mm in diameter and 8mm deep (recommended) need to be drilled into the concrete (Whiting, 2003). This is both time consuming and esthetically displeasing on concrete structures and owners may not agree to the use of this method.

2.5.4. Four-Point (Wenner) Probe

A Wenner probe (Figure 2.8) consists of four points spaced at an equal distance *a*. A current is driven between the two outer most points and the corresponding voltage drop is measured between the inner two. Because the voltage drop is measured at different points from the current supply there is less influence of the concrete immediately surrounding the points as is the case with the two-point probe.

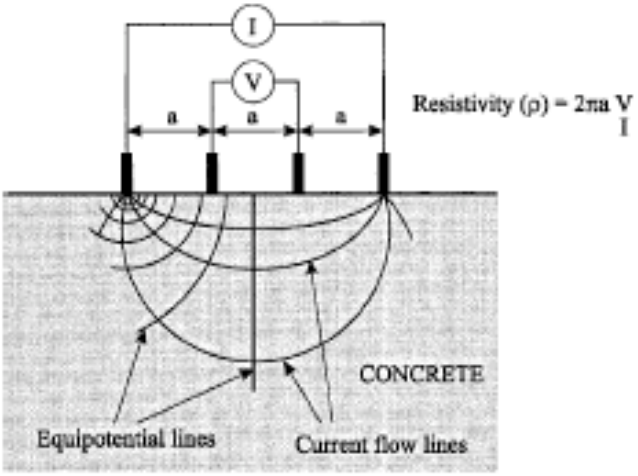

Figure 2.8: Four point Wenner Probe

To determine the resistivity of concrete (ρ) using the Wenner probe the following equation is used:

$$\rho = \frac{2\pi a \frac{V}{I}}{K} \qquad \text{(Equation 22)}$$

where:

a = spacing between points (mm)
V = potential between inner points (V)

I = current passed between outer points (A)

K = correction factor

When the probe is applied to a specimen with dimensions much greater than *a*, and there is no interference from reinforcing steel, the correction factor is 1. If this is not the case, then the correction factor must be determined. Morris *et al.* (1995) conducted a study to determine correction factors for various sized cylinders. The results of this work are shown in Figure 2.9. The concrete tested had low resistivity and the graphs developed may lose accuracy as the resistivity increases.

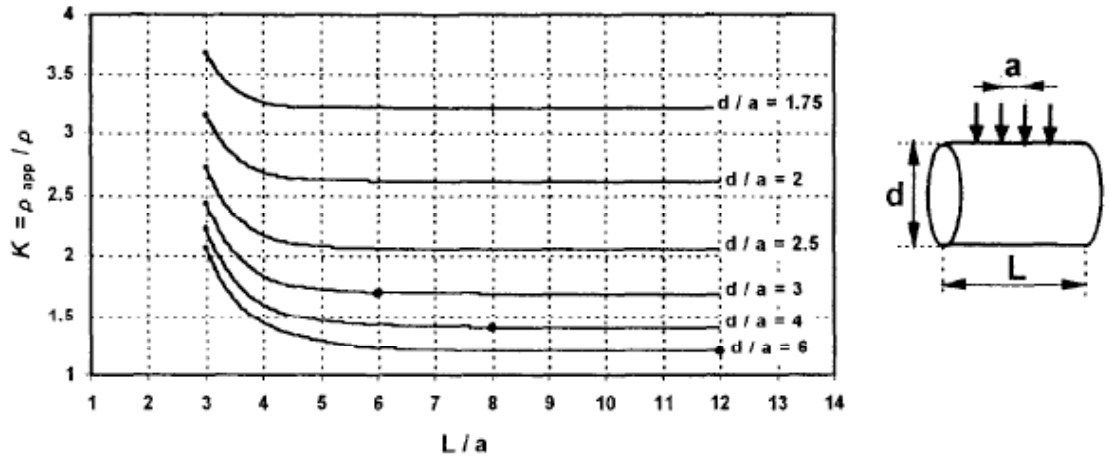

Figure 2.9: Correction factors for cylinders tested with Wenner Probe (Morris et al, 1995)

2.5.5. Rapid Chloride Permeability Test

The Rapid Chloride Permeability Test (RCPT) (ASTM C 1202 Standard Test Method for Electrical Indication of Concrete's Ability to Resist Chloride Ion Penetration) is truly an electrical conductance test, rather than a chloride ion penetration test. This test gives an indirect indication of the permeability of the concrete.

The test consists of sandwiching a 95mm diameter x 50mm thick disc between two reservoirs, one containing 3% NaCl solution and the other a 0.3N NaOH solution. If samples with diameters other than 95mm are tested then the results are normalized to 95mm. A 60V potential is then applied across the sample for 6h. Current readings are taken every 30 minutes, at minimum, and then the total charge passed in Coulombs is calculated by integrating the Current vs. Time graph developed from the readings taken. Table 2.2 gives an indication of the risk of chloride penetrability with regards to charge passed.

Table 2.2: Chloride ion penetrability based on charge passed (ASTM C 1202)

Charge Passed (Coulombs)	Chloride Ion Penetrability
>4000	High
2000-4000	Moderate
1000-2000	Low
100-1000	Very Low
<100	Negligible

This test is widely used as both a test for qualifying concrete mixes and as a quality control measure in construction as it is relatively quick. However, there is a belief that the results obtained from this test depend more on the composition of the pore solution than on the pore structure and gives little information about the permeability of the concrete.

Shi, (2004) presented data that shows mineral admixtures such as silica fume, fly ash and ground granulated blast furnace slag (GGBS) can lower the conductivity of the pore solution, relative to a control of 100% Portland cement, by up to 80% which can have a

severe impact on concretes ability to pass an electrical charge. It was also found that chemical admixtures, and the alkali content of the cement and aggregates could greatly modify the conductivity of the pore solution without significantly changing the pore structure of the cement matrix. Therefore it is not possible to use the RCPT to gain a good indication of the permeability of a concrete, compared to another, if different materials are used. This is also true for all other resistivity tests and it is therefore necessary to account for the resistivity of the pore solutions by one of the methods described previously.

Another problem with the RCP test is the tendency for heat to be generated when low quality concrete is tested (Stanish, 1997). As the temperature of the concrete increases, the resistivity decreases (Figure 2.2) and therefore inflated results will be obtained. The lack of heat generation is one advantage of instantaneous resistivity tests.

Another drawback to the RCPT is its repeatability, or lack thereof. The precision statement given in the ASTM test procedure indicates that there is a possible variance for a single operator of 42% and an intra-laboratory variance of up to 51%. This huge variance in test results does not instill confidence in this method.

Despite the drawbacks outlined above, this test can be useful as a quality control method, as long as similar concretes are compared.

2.6. Summary

The bulk diffusion test is probably the best test for determining a concrete's resistance to the penetration of chlorides because it involves only diffusion, the main transport mechanism in field concrete. This test is fine for research or pre-qualifying mixes but it

is much too long to be used effectively as a quality control and quality assurance method. However, resistivity tests may be a satisfactory alternative for determining the transport properties of concrete for quality control purposes.

While it is common to use the RCP test for quality control, its six-hour testing period serves no advantage over instantaneous resistivity measurements, and may even be less accurate due to heating effects if poor quality concrete is tested.

The four point Wenner probe has an advantage over most resistivity tests in that it is portable and can be applied to the surface of a structure, meaning there is no need to take cores from the structure for laboratory testing.

Bulk resistivity measurements cannot provide an accurate enough estimate of the diffusion coefficient of a particular concrete because of pore solution effects, however if the resistivity or composition of the pore solution can be determined, the apparent diffusion coefficient ($D_{a)}$ can be predicted. This ability to predict D_a using instantaneous methods could greatly reduce time and effort required for service life modeling of concrete structures.

Migration tests can be used to determine the diffusion coefficient by using the change in concentration in the downstream cell after steady state has been reached. Some research also suggests that faster results can be obtained by monitoring the change in concentration in the upstream cell, however this has not been investigated beyond initial study, to the author's knowledge.

3.0 Laboratory Research

Concrete samples were tested from four different sources, a) samples cast by the author for this testing program, b) samples cast by Evans (1997), c) cores taken from high-volume fly ash concrete pavements in Wisconsin (Naik et al, 2004) and d) cores taken from concrete elements on the University of New Brunswick (UNB) Materials Group's exposure site. The elements were part of another research project in which the author participated. The information contained in sections 3.1 and 3.2 represent the samples cast by the author, section 3.3 represent samples cast by Evans, section 3.4 represent the pavement cores and finally section 3.5 represents the structures on the UNB exposure site.

3.1. Methodology

Concrete samples were produced with a wide range of mixture proportions. These mixes were selected to represent concretes with a wide range of permeability and electrical conductivity properties. Samples were also used from other research programs to ensure that the effect of maturity was captured.

3.2. Materials and Mixture Proportions

3.2.1. Cementitious Materials

Chemical compositions for all cementitious materials used can be found in Table 3.2.

The cement used met the criteria for Type GU cement set out in CSA A3001-03 and for Type I cement set out by ASTM C 150. The Bogue potential composition is listed in Table 3.1.

Table 3.1: Bogue potential composition

Bogue Potential Composition	(%)
Tricalcium Silicate (C_3S)	59.53
Dicalcium Silicate (C_2S)	12.60
Tricalcium Aluminate (C_3A)	6.96
Tetracalcium Aluminoferrite (C_4AF)	9.31

All supplementary cementing materials used in this program met the requirements of CSA A3001-03 and their chemical compositions can be found in Table 3.2. The silica fume was undensified silica fume from Beaucour, Quebec and the fly ash was a Class F ash from the Belledune Generating Station in New Brunswick.

Table 3.2: Chemical compositions of cementitious materials

Chemical Composition (%)	Cement	Fly Ash	Silica Fume
SiO_2	20.08	57.36	96.7
Al_2O_3	4.58	20.18	0.3
Fe_2O_3	3.06	10.25	0.1
CaO	63.09	2.42	0.4
MgO	2.37	2.12	0.3
Na_2O	0.20	1.02	0.1
K_2O	0.78	2.15	0.7
P_2O_5	0.13	0.18	0.1
TiO_2	0.21	0.89	0.0
SO_3	3.35	1.14	0.09
Mn_2O_3	0.21	0.07	0.0
SrO	0.12	0.05	0.0
NaO_e	0.71	2.43	0.56
LOI	1.45	1.82	2.35

3.2.2. Aggregates

The coarse aggregate used was from the Blagdon Quarry with a maximum nominal size of 19 mm. It has a specific gravity of 2.68 and a water absorption value of 0.65%. The fine aggregate used was Zeeland sand. This has a specific gravity of 2.60 and a water absorption value of 1.32%. Both sources are local to Fredericton and meet the requirements of CSA A23.1-04.

3.2.3. Admixtures

A normal and a high-range water-reducing admixture were used in varying amounts to achieve a target slump of between 100mm and 150mm. The normal range water reducer meets the requirements of ASTM C 494 for a Type A water reducer and the high-range water reducer meets the specifications of ASTM C 494 Type F high-range water reducer.

3.2.4. Preparation

Concrete was mixed in a counter-current pan mixer for a total of 5 minutes. The materials were added in the order of coarse aggregate, cementitious materials and fine aggregate. The mixer was then switched on and the materials were allowed to mix dry for one minute. Water was then added over a one-minute period and the mix was allowed to mix for another minute. The mixer was then switched off and the concrete was allowed to sit for another minute. Superplastizer was then added, if needed, and the concrete was allowed to mix for another minute. The concrete was then discharged and placed in molds.

3.2.5. Casting

100mm x 200mm cylinders were produced from six different mixes; the mixture proportions are presented in Table 3.3. All casting was performed in accordance with ASTM C 192 / C 192M.

Table 3.3: Mixture proportions – Laboratory Study

Material	0.37PC	0.37SF	0.37SF/CNI	0.6PC	0.37SF/FA	0.37FA
Cement	405	373	373	267	304	284
Silica Fume (kg/m^3)	-	32	32	-	20	-
Fly Ash (kg/m^3)	-	-	-	-	81	122
Water (kg/m^3)	150	150	150	160	150	150
w/cm	0.37	0.37	0.37	0.60	0.37	0.37
Coarse Aggregate (kg/m^3)	1100	1100	1100	1100	1100	1100
Fine Aggregate (kg/m^3)	783	771	771	870	755	752
Calcium Nitrite Corrosion Inhibitor (l/m^3)	-	-	30	-	-	-
Water Reducer (ml/100 kg CM)	250	250	250	-	250	250
Super Plastizer (ml/100 kg CM)	600	600	600	300	600	300

* All proportions given are for saturated surface dry condition

Additional specimens were cast according to the mix design of 0.37PC and 0.37SF to examine the effect of humidity, the presence of reinforcing steel and the in-situ measurement of pore solution.

Paste samples were cast for pore solution extraction that had the same proportions of cement, SCMs water and CNI as the mixes in Table 3.3.

3.3. Samples from Evans (1997)

Samples used in this program that were produced by Evans (1997) were 100mm x 200mm cylinders and were approximately 11 years old at the time of testing. A summary of the mix designs can be found in Table 3.4.

Table 3.4: Mix proportions – Chris Evans

	CESF	CIJ25	CE40FS	CE56FS
T10SF Cement (kg/m^3)	450	375	330	242
Fly Ash (kg/m^3)	-	125	220	208
Water (kg/m^3)	135	120	130	130
w/cm	0.30	0.24	0.24	0.24
Water Reducer (ml/100kg cementitious)	180	175	180	193
Super Plastizer (ml/100kg cementitious)	203	250	203	214
Air Entraining Admixture (ml/100kg cementitious)	10	22	20	35

3.4. Samples from Pavement Cores

These samples were taken from cores cut from pavements in Wisconsin. The cores were cut in July 2005, at which time the age of the pavements ranged from 11 to 21 years of age. Specimens A-1 to F-6 were made with fly ash (Class F and Class C) from the Pleasant Prairie Power Plant and PW-1 was made with fly ash (Class C only) from the Port Washington Power Plant. Little information was given on the fly ash from the Port Washington Power Plant. The mix design and other pertinent information for the pavement cores can be found in Table 3.6. The chemical analyses of the fly ashes used can be found in Table 3.5. All information in Table 3.5 and Table 3.6 was taken from (Naik et al, 2004). This series of specimens will be called FAPC from this point on.

Table 3.5: Figure 3.1: Chemical composition of fly ash – FAPC

Chemical Composition	Class F Fly Ash (%)	Class C Fly Ash (%)
Silicon dioxide (SiO_2)	51.4	32.9
Aluminum oxide (Al_2O_3)	26.3	19.4
Iron oxide (Fe_2O_3)	15.3	15.4
Total $SiO_2 + Al_2O_3 + Fe_2O_3$	93.0	57.7
Sulfur trioxide (SO_3)	1.4	3.8
Calcium oxide (CaO)	3.6	28.9
Magnesium oxide (MgO)	1.1	4.8
Titanium oxide (TiO_2)	1.1	1.6
Potassium oxide (K_2O)	1.9	0.3
Sodium oxide (Na_2O)	1.0	2.0
Moisture content (%)	0.7	0.8
NaO_e	2.3	2.2
Loss on ignition	6.5	0.6

Table 3.6: Mixture proportions – FAPC

Mixture No.	A-1	B-5	C-4	D-2	E-3	F-6	PW-1
Class C fly ash (%)	70	50	19	-	-	-	50
Class F fly ash (%)	-	-	-	67	53	35	-
Cement (kg/m^3)	101	175	285	133	181	271	178
Fly ash (kg/m^3)	234	175	65	267	208	145	178
Water (kg/m^3)	N.A.*	92	101	125	119	98	131
w/cm	N.A.*	0.26	0.29	0.31	0.31	0.27	
Fine Aggregate (kg/m^3)	884	742	813	837	837	914	712
Coarse Aggregate (kg/m^3)	1086	1086	1145	1127	1127	1095	1146
Water Reducing Admixture (ml/m^3)	310	0	0	0	0	0	NA*
Superplastizer (ml/m^3)	0	N.A.*	0	217	178	194	NA*
Air Entraining Admixture (ml/m^3)	426	464	271	1238	1238	580	NA*
Slump (mm)	-	70	51	44	57	64	NA*
Air Content (%)	5-6	5	6	5	5.8	5	NA*
Air Temperature (^{o}C)	-	28.3	24.4	12.2	11.1	35	NA*
Concrete Temperature (^{o}C)	-	31.1	28.9	17.0	17.8	31.7	NA*
Concrete Density (kg/m^3)	-	2352	2304	2339	2339	2308	NA*
Date Cast	1984	1990	1990	1991	1991	1990	1994

*Not Available

3.5. Samples from Field Study

These specimens were cast in October 2005 and coring and sample preparation was conducted the day before the samples were tested. Testing dates include 28, 56, 90, and 180 days of age.

Two mixes were cast, one was high performance concrete (DOTH) and the other mix was a regular portland cement (DOTL). These mixes were designed to meet the C-XL and C-2 designations respectfully, as stated CSA A23.1. The mix proportions can be found in Table 3.7.

For each mix, a wall section and a slab section were cast. The slabs (Figure 3.1 and Figure 3.3) were 1 m x 1.75 m x 0.25 m thick. The wall sections (Figure 3.2 and Figure 3.4) were cast in the shape of a T. The plan view of this element can be seen in Figure 3.5 and had a height of 1m. Cores taken from the wall elements will have a WC designation and those taken from the slab will have a SC designation.

Table 3.7: Mix proportions – Exposure Site

	DOTH	DOTL
T-GUb-SF Cement (kg/m^3)	425	-
T-GU Cement (kg.m^3)	-	396
Coarse Aggregate (kg/m^3)	1044	1060
Fine Aggregate (kg/m^3)	660	680
Water (kg/m^3)	140	160
w/cm	0.33	0.40
Air Entraining Admixture (ml/100kg cementitious)	63	37
Water Reducer (ml/100kg cementitious)	280	280
Super Plastizer (ml/100kg cementitious)	1465	-
Corrosion Inhibitor (ml/100kg cementitious)	3660	-

Figure 3.1: Photograph of slab from DOTH mix

Figure 3.2: Photograph of wall section from DOTH mix

Figure 3.3: Photograph of slab from DOTL mix

Figure 3.4: Photograph of wall section from DOTL mix

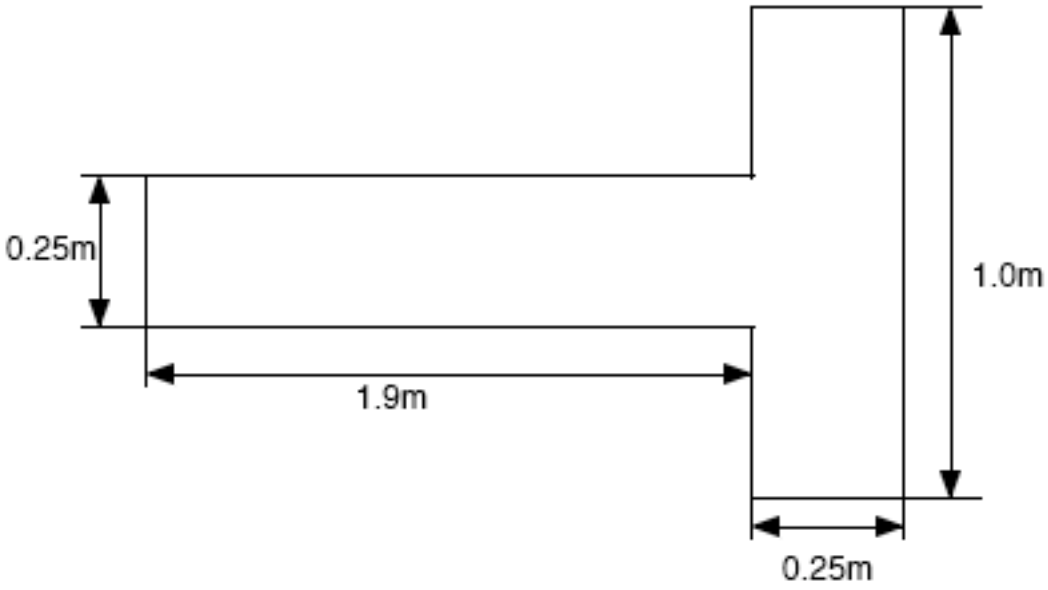

Figure 3.5: T-section (plan)

3.6. Testing

A summary of the tests performed in this program can be found in Table 3.8.

Table 3.8: Summary of tests performed

Samples	Test	Age Tested	Notes
0.37PC to 0.37FA	RCPT	28, 90, 180, and 365 days	
	Parallel Plate AC Resistivity (50mm and 200mm)	28, 90, 180, and 365 days	
	Wenner Probe Resistivity	28, 90, 180, and 365 days	
	RCPT Cell Resistivity	28, 90, 180, and 365 days	
	Electrical Migration	28 days	Permeability too low to achieve steady state in reasonable time in samples greater than 28 days old.
	Bulk Diffusion	28, 90, 180, and 365 days	
	Compressive Strength	28 days	
	Extracted Pore Solution Resistivity	28 days	
0.37PC and 0.37SF	In-situ Pore Solution	Periodically	
	Effect of Humidity on Resistivity	Periodically	
Exposure Site Structures	RCPT	28, 56, 90, and 180 days	
	Parallel Plate AC Resistivity (50mm and 200mm)	28, 56, 90, and 180 days	
	Wenner Probe on Structure	28 days	
	Wenner Probe Resistivity	28, 56, 90, and 180 days	
	RCPT Cell Resistivity	28, 56, 90, and 180 days	
Evans (1997)	RCPT	~11 years	
	Parallel Plate AC Resistivity (50mm and 200mm)	~11 years	
	Wenner Probe Resistivity	~11 years	
	RCPT Cell Resistivity	~11 years	
	Bulk Diffusion	~11 years	
Pavement Cores (Naik et al, 2004)	RCPT	11-21 years	
	Parallel Plate AC Resistivity (50mm and 200mm)	11-21 years	
	Wenner Probe Resistivity	11-21 years	
	RCPT Cell Resistivity	11-21 years	
	Bulk Diffusion	11-21 years	

3.6.1. Rapid Chloride Permeability Test

The Rapid Chloride Permeability test was conducted in accordance with ASTM C 1202-97.

3.6.2. AC – Cell Resistivity

The AC – Cell resistivity test consisted of measuring the resistivity of the sample in the RCPT cell just prior to conducting the ASTM C 1202 test. This was done by hooking the AC resistivity meter into the two terminals of the cells, applying a constant current of 100μA and measuring the voltage drop across the sample. A schematic of the AC resistivity meter can be found in Appendix A.

3.6.3. DC – Cell Resistivity

DC – Cell resistivity was determined by taking the initial current reading from the RCPT after the relaxation period of approximately a minute and calculating resistivity using Equation 9. When the power is switched on the polar molecules within the pore solution and cement matrix are aligning. The time needed for this to occur is called the relaxation period.

3.6.4. Parallel Plate AC Resistivity

The AC parallel plate resistivity test was conducted on 200mm cylinders (//Plate-200mm) that were end ground to improve contact with the plates and on 50mm samples (//Plate-50mm) prior to being tested in the ASTM C 1202 test. The same 200mm samples were tested at each age, however different 50mm samples were tested at each age. The samples were sandwiched between two stainless steel electrodes. A conductive gel was

applied to the electrodes to ensure uniform contact between the electrode and concrete. A constant current was then applied and the voltage drop across the sample was measured. Typically 100μA was used as the constant current value, however if the voltage drop across the sample exceeded 2000mV a lower value was used. This is because the maximum value able to be read by the meter is 2000mV.

3.6.5. Wenner Probe Resistivity

This test was conducted in accordance with the Florida Method of Test For Concrete Resistivity as an Electrical Indicator of its Permeability Designation: FM 5-578 Jan. 27, 2004. Please see Appendix B for a detailed description of the test procedure. A correction factor of 2.7 (determined from Figure 2.9) was used for all Wenner probe analysis in this thesis.

3.6.6. Electrical Migration

The electrical migration testing apparatus, consisting of an upstream and downstream reservoirs and an electrical power source, is shown in Figure 3.6

Samples were moist cured until time of testing. 50mm thick discs were cut from 100mm diameter cylinders and the vacuum saturated in 0.3M NaOH solution. During the saturation process the discs were placed in a desiccator and covered with solution. A vacuum pump was then run for one hour at which time the valves on the dessicator were closed and the vacuum was maintained for another 4 hours. The vacuum was then relieved and the samples remained in the NaOH solution over night. The samples were then sealed into the migration cells (Figure 3.6) and the reservoirs were then filled. The upstream reservoir was filled with 2.75l of 0.3M NaOH + 0.5M NaCl solution while the

downstream reservoir was filled with 2.75l of 0.3M NaOH solution. A power supply was then connected to the sample such that the negative pole was attached to the upstream cell and the positive pole was attached to the downstream cell. The power supply was adjusted so that the voltage drop across the sample was approximately 20V. Samples both of the upstream and downstream reservoirs were taken periodically and analyzed for chloride content. The test was run until steady-state chloride flow was achieved. A constant slope of the chloride content vs. time graph (Figure 3.7) indicates that steady state flux has been achieved.

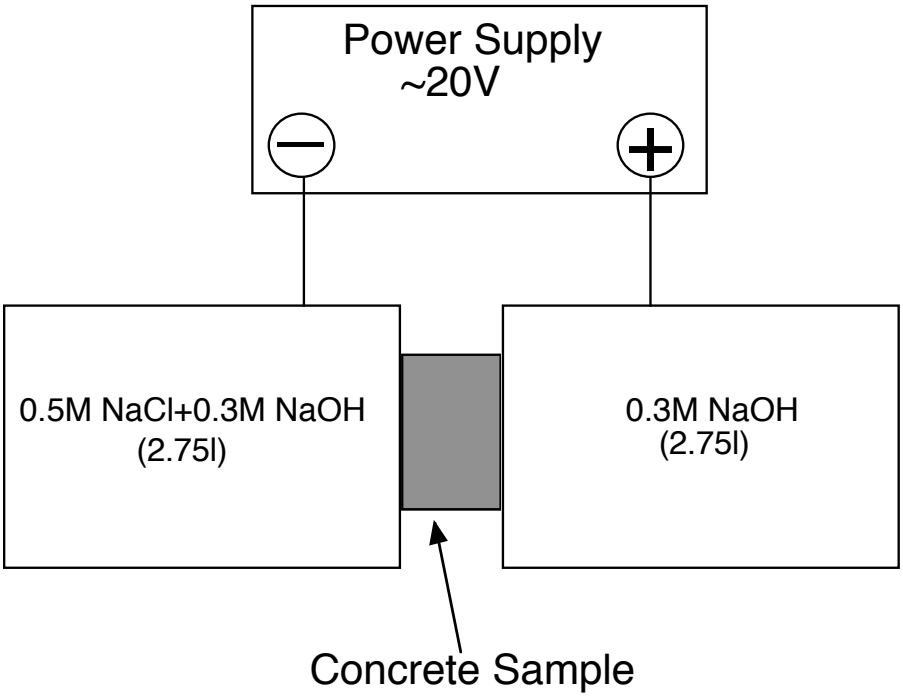

Figure 3.6: Typical migration cell

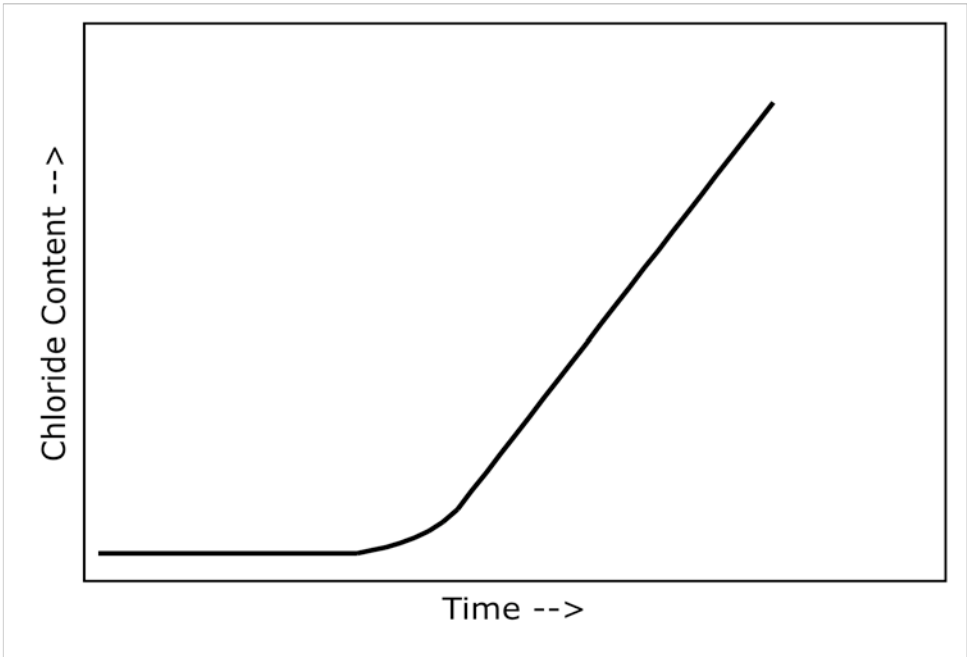

Figure 3.7: Typical Migration Profile (Downstream)

3.6.7. Bulk Diffusion

This test was done in accordance with ASTM C 1556 – 03. The duration of the soak period for the UNB Laboratory samples and the Evans samples was 40 days, while a 90 day duration was used for the Pavement Core samples.

The data collected from chloride analysis was entered into a Excel spreadsheet and the diffusion coefficient and surface concentration are determined by fitting the non-steady state solution of Fick's Second Law to the data. An example of this spreadsheet can be seen below.

0.37SF/FA		
Depth (m)	Measured	Fitted
0.0005	0.680%	0.703%
0.0015	0.591%	0.550%
0.0025	0.416%	0.412%
0.0035	0.278%	0.293%
0.0045	0.184%	0.199%
0.0055	0.115%	0.128%
0.0065	0.087%	0.078%
0.0075	0.050%	0.045%
0.0085	0.040%	0.024%
0.0095	0.026%	0.013%
C_s (%)		0.8400%
D_a (m^2/s)		2.03E-12
R^2		0.998

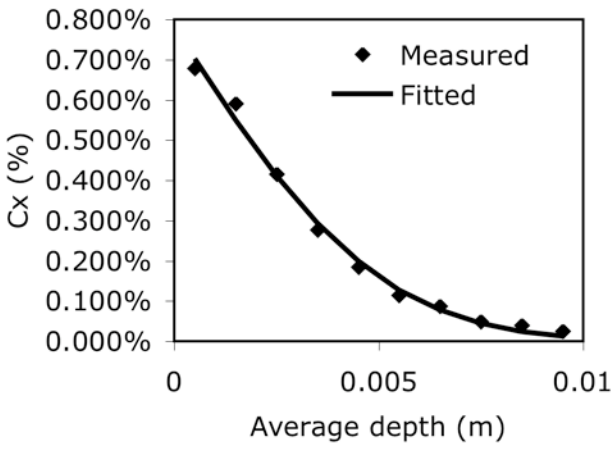

3.6.8. Compressive Strength

This testing was carried out in accordance with ASTM C 39-/C 39M – 01.

3.6.9. Extracted Pore Solution Resistivity

For this test, paste samples were prepared according to Table 3.9. Once mixed the paste was placed in molds and rotated for 24 hours to prevent segregation. The paste samples were allowed to cure for a period of 28 days and then the pore solution was extracted.

The paste samples were put into a high-pressure pore press cylindrical chamber 50mm in diameter and 90mm in length. The samples were pressed under high pressure (1400-2100MPa). The pore solutions were collected in a small vial. After the extraction, the pore solutions were diluted. The OH^- concentration was measured immediately by titration against 0.01N HCl solution with phenolphthalein as the indicator. The other ions, including Na, K Si, Ca, SO_4 and NO_3, were analyzed by Ion Chromatography (IC) or Inductively Coupled Plasma Emission Spectrometry (ICP-ES).

Table 3.9: Mix proportions for paste specimens

Material	0.37PC	0.37SF	0.37SF/CNI	0.6PC	0.37SF/FA	0.37FA
Cement	405	373	373	267	304	284
Silica Fume (kg/m^3)	-	32	32	-	20	-
Fly Ash (kg/m^3)	-	-	-	-	81	122
Water (kg/m^3)	150	150	150	160	150	150
CNI	-	-	30	-	-	-
w/cm	0.37	0.37	0.37	0.60	0.37	0.37

3.6.10. Internal Pore Solution Resistivity

This procedure was conducted on samples from mixes 0.37PC and 0.37SF, which were approximately 180 days old. Two cylinders from each mix were tested. 16mm diameter holes were drilled approximately 50mm into the curved surface of the cylinder, equidistance from each end. The cylinders were then sealed on the side with the ends left unsealed. Distilled water was then placed in the holes and the initial resistivity of the solution was measured with a resistivity probe. The hole was then sealed at the surface and the cylinders were stored in a 100% humidity room at 21 ^{o}C. The resistivity of the pore solution was measured periodically until equilibrium was reached. A diagram of the specimen can be seen in Figure 3.8 and a photo of the specimen during testing can be seen in Figure 3.9. 50mm samples were then cut from either side of the hole and were tested by the //Plate-50mm resistivity method described previously. It was intended to also use a microprobe with a diameter of approximately 1-mm which would have required much smaller reservoirs (i.e.≤5mm in diameter) however, problems were

encountered locating or manufacturing such probes (the possibility of manufacturing these probes is still being investigated).

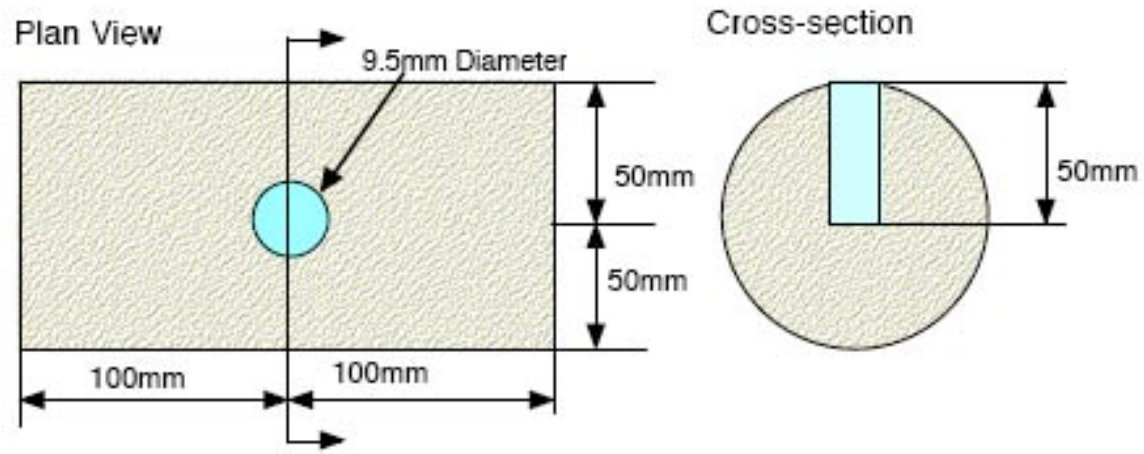

Figure 3.8: Insitu solution specimen diagram

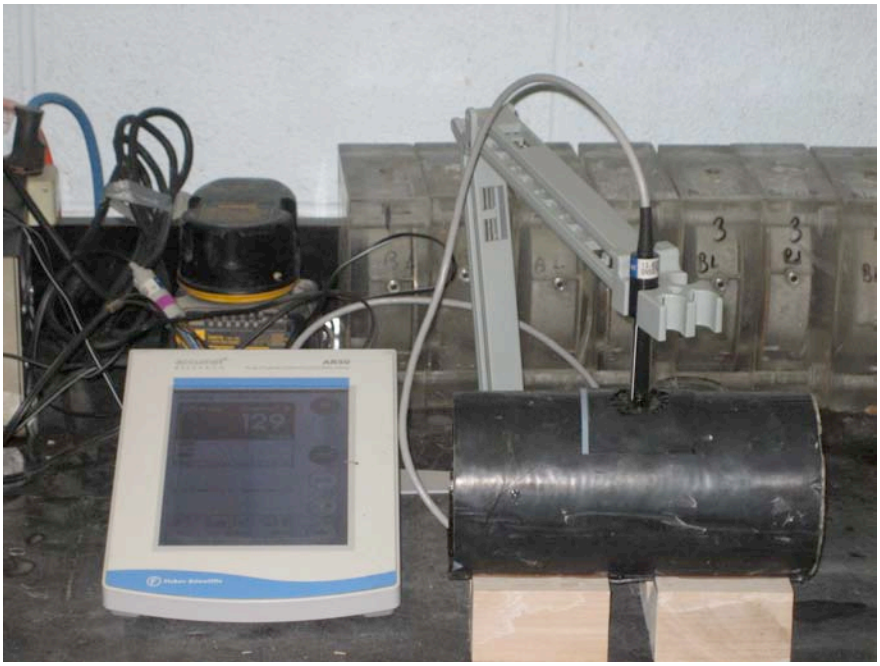

Figure 3.9: In-situ Pore Solution Measurement

3.6.11. Effect of Rebar on Resistivity

For this portion of the program 250 x 250 x 100 mm blocks (Figure 3.10) were cast from 0.37PC and 0.37SF. Three lengths of 15-mm rebar were placed parallel to each other at quarter points for four blocks with cover depths of 25, 50, 75 or 100 mm. A block with a depth of 125mm was cast for the block with 100mm of cover. A control block with no rebar was also cast. The blocks were stored under water when not being tested

The resistivity of the blocks was tested using the Wenner Probe method. Six readings were taken for each block, with the exception of the control for which only three readings were taken. Readings were taken directly over, parallel each of the three bars and then three readings were taken perpendicular to the bars.

Figure 3.10: Resistivity block to test the effect of reinforcing steel (50mm cover depth)

3.6.12. Effect of Humidity on Resistivity

0.4m x 0.4m x 0.7m (Figure 3.11) blocks were cast with the mix proportions of 0.37PC and 0.37SF described in Table 3.3, however the cement used was from St. Lawrence Cement Plant. The blocks were moist cured for 7 days and then placed on the University of New Brunswick Materials Group exposure site. Wenner Probe measurements were then taken daily at nine points (three on North face, three on top and three on South face), taking note of rainfall since the last reading. Four cylinders were also cast for each mix, two were stored outside on the exposure site with the blocks, and two were stored under water in the lab. Wenner probe measurements were also taken on these cylinders.

Figure 3.11: Effect of humidity block on exposure site

4.0 Summary of Results

A summary of mix-designs and results for concrete cast for this testing program can be found in Table 4.1 to Table 4.3

4.1. Compressive Strength

Figure 4.1 and Table 4.1: Data Summary – UNB Laboratory Specimens gives the compressive strength of all mixes at 28 days of age. The results were as expected with the mixes containing silica fume (0.37SF & 0.37SF/CNI) having the highest strengths. This is due to the large surface area of the silica fume, which allows the pozzolanic reaction to happen much more quickly than in concrete containing fly ash. As expected, the control mix with a w/cm of 0.6 had the lowest strength. It can also be seen that the mix containing only fly ash (0.37FA) as a SCM has a lower strength than the control mix with similar w/cm. This is typical of fly ash concrete, and at later ages this trend will be reversed as the pozzolanic reaction has time to occur.

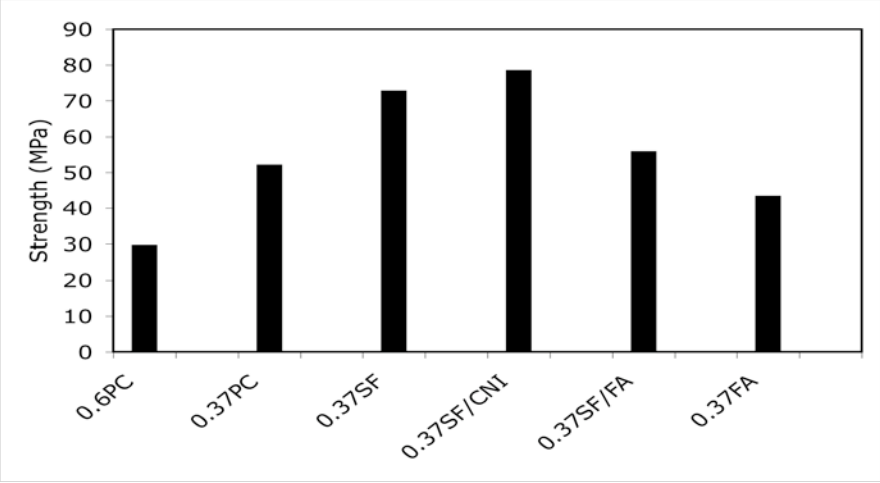

Figure 4.1 Results for 28d compressive strength – UNB Laboratory samples

Table 4.1: Data Summary – UNB Laboratory Specimens

Mix ID	w/cm	SF (%)	FA (%)	CNI (%) (l/m^3)	Age (d)	Strength (MPa)	Resistivity (Ω-m) Wenner	//Plate-200	//Plate-50	AC – Cell	DC – Cell	Diffusion Coefficient (m^2/s) Bulk Diffusion	Migration Up	Migration Down	RCPT (Coulombs)
0.37PC	0.37	0	0	0	28	52	82	82	69	74	72	4.38E-12	3.18E-13	1.08E-12	2376
					90	-	118	147	103	110	95	5.72E-12	-	-	2218
					180	-	146	159	118	110	110	2.07E-12	-	-	1408
					365	-	116	137	108	103	107	1.17E-12	-	-	1869
).37SF	0.37	8	0	0	28	73	542	257	207	211	291	1.37E-12	1.23E-13	3.98E-13	902
					90	-	860	899	688	785	678	1.36E-12	-	-	430
					180	-	1043	1056	794	725	725	2.84E-12	-	-	364
					365	-	751	820	878	770	805	1.04E-12	-	-	240
0.37SF?CNI	0.37	8	0	30	28	79	205	173	199	223	184	1.43E-12	2.73E-13	4.31E-13	975
					90	-	478	534	337	476	357	2.09E-12	-	-	503
					180	-	613	617	554	512	524	7.09E-13	-	-	316
					365	-	471	516	514	456	488	7.12E-13	-	-	422
0.6PC	0.6	0	0	0	28	30	58	50	48	45	44	5.57E-12	1.75E-12	4.76E-12	4796
					90	-	64	105	40	47	45	1.82E-E-11	-	2.59E-11	5234
					180	-	70	79	58	54	53	1.54E-11	-	-	2938
					365	-	66	90	65	65	64	4.62E-12	-	-	4922
0.37SF/FA	0.37	5	20	0	28	56	132	135	121	96	102	2.03E-12	-	-	2055
					90	-	427	450	341	335	335	3.88E-12	-	-	567
					180	-	620	792	522	535	563	1.68E-12	-	-	260
					365	-	724	883	852	806	834	2.99E-13	-	-	236
).37FA	0.37	0	25	0	28	43	39	45	41	42	39	6.11E-12	-	8.44E-13	5472
					90	-	111	118	110	103	105	3.08E-12	-		2204
					180	-	240	305	202	194	194	3.74E-12	-		774
					365	-	286	523	491	471	471	5.62E-13	-		350

Table 4.2: Data Summary – CE and FAPC

SPECIMEN ID	Age (years)	Wenner (Ω-M)	// Plate (50mm) (Ω-m)	AC – Cell (50mm) (Ω-m)	DC – Cell (50mm) (Ω-m)	RCPT (Coulombs)	Bulk Diffusion Coefficient (m^2/s)
CE56FS	11	6497	8660	5410	4189	32	3.22E-12
CE56FS-MDAT	11	5534	7964	4716	3324	52	4.55E-13
CE40	11	5585	6850	4189	4620	132	1.32E-12
CE40FS-MDAT	11	4084	6553	4051	4467	23	3.22E-13
CIJ25-MDAT	11	2464	3652	2124	2233	215	7.03E-13
CESF1	11	364	295	302	272	687	6.05E-12
CESF1-MDAT	11	302	336	234	239	740	1.84E-11†
CESF2	11	492	384	267	323	665	3.65E-12
E-3	14	1750	2427	2221	2772	81	5.22E-13
D-2	14	2099	4296	2009	4712	41	3.32E-13
F-6	15	*	1483	1362	1428	149	5.44E-13
B-5	15	*	1288	1073	1193	142	5.29E-13
C-4	15	*	404	372	386	482	3.66E-13
A-1	21	1577	1613	1376	1496	123	8.92E-13
PW-1	11	917	1434	1126	1346	133	1.11E-12

*Specimens too short to measure with Wenner Probe †Poor profile obtained

The samples from Evans were collected from the University of Toronto at two different times. The specimens with the designation MDAT indicate samples stored over water after collected from the University of Toronto. The ones with out the MDAT designation indicate the samples were stored under water.

Table 4.3: Data Summary – Exposure Site

	Age (d)	SPECIMEN ID	Wenner (Ω-M)	// Plate (50mm) (Ω-m)	AC – Cell (50mm) (Ω-m)	DC – Cell (50mm) (Ω-m)	RCPT (coulombs
DOTH	28	WC7	110	95	94	78	2011
		WC28	84	74	74	113	2504
		SC7	95	78	79	93	2000
		SC28	59	47	45	54	4366
		C	91	74	78	72	2696
	56	WC7	150	139	135	154	947
		WC56	100	81	78	91	1636
		SC7	171	129	125	143	1065
		SC56	66	56	51	56	2413
		C	169	121	110	120	1005
	90	WC7	224	222	191	223	624
		WC90	102	113	94	113	1101
		SC7	267	206	194	235	606
		SC90	66	68	60	70	1721
		C	225	160	160	189	781
	180	WC7	X	X	X	X	X
		WC180	152	159	116	119	1616
		SC7	X	X	X	X	X
		SC180	117	120	89	94	1843
		C	319	386	281	293	710
DOTL	28	WC7	53	55	44	48	2971
		WC28	67	46	40	38	3492
		SC7	61	44	40	49	4011
		SC28	74	49	30	44	3716
		C	52	44	37	55	3405
	56	WC7	60	52	47	55	2933
		WC56	50	40	40	43	3371
		SC7	71	53	51	58	2895
		SC56	53	37	33	54	3694
		C	56	42	40	67	2604
	90	WC7	59	58	53	54	2278
		WC90	46	46	36	43	2633
		SC7	58	52	48	53	2414
		SC90	43	39	35	40	3620
		C	56	41	38	45	2990
	180	WC7	X	X	X	X	X
		WC180	56	62	41	46	3846
		SC7	X	X	X	X	X
		SC180	60	62	44	49	3274
		C	53	57	43	52	5274

WC = Wall Core, SC = Slab Core, C = Cylinder, Number in ID indicates age in days core was taken

4.2. Rapid Chloride Permeability (RCP)

Figure 4.2 displays the results obtained from the ASTM C 1202 test, which measures the amount of charge passed over a six-hour period. As can be seen all mixes exhibit a general downward trend in the amount of electrical charge passed with an increase in time (with the exception of 0.37PC, 0.37SF and 0.6PC between 180 and 365 days). This downward trend is expected because as the cement paste hydrates the pores become less well connected and therefore more resistant to the passage of electrical current. The two control mixes (0.37PC and 0.6PC) show little improvement over the results obtained at 28 day testing. This is most likely due to the fact that the large majority of the cement has hydrated by this age, leaving little potential for improvement.

The dramatic improvement of the concrete containing fly ash (0.37SF/FA and 0.37FA) should also be noted. Due to the replacement of cement by fly ash and a slow pozzolanic reaction, early age results for concretes containing fly ash are typically higher than the control mix in the RCP test but perform much better at later ages. The addition of 5% silica fume in mix 0.37SF/FA seems to have offset the initial discrepancy. The mixes containing fly ash show the most improvement with time, indicating that, time allowing, the inclusion of fly ash is a good method to increase the discontinuity of the pore structure of cement paste

A slight increase in the amount of charge passed can be observed between testing conducted at 180 and 365 days for mixes 0.37PC, 0.37SF/CNI and 0.6PC. It is not known why this increase has occurred. It is recommended that testing at 2-year testing be conducted to see if this trend continues.

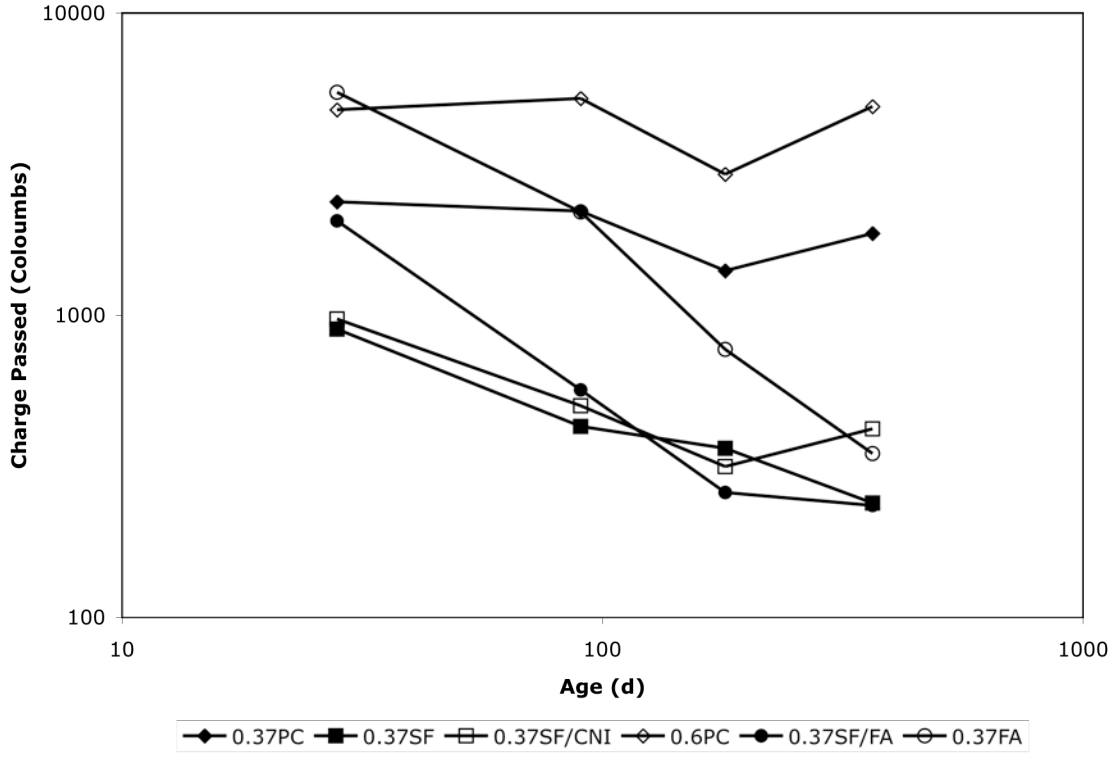

Figure 4.2: Charge Passed vs. Time for rapid chloride permeability test

4.3. Resistivity

The results obtained from the various resistivity tests can be seen in Figure 4.3 through Figure 4.7. All tests followed similar trends and gave expected results.

As expected, mixes 0.37PC, 0.6PC and 0.37FA had the lowest resistivity at 28 days. The mixes containing only Portland cement as the cementing material gained very little after 28 days of age, while mixes containing fly ash continually improved.

Mixes containing silica fume (0.37SF and 0.37SF/CNI) had higher 28-day results than the other mixes. The resistivity of these mixes increased until testing at 90 days then little improvement was seen after that. This is typical of concrete containing silica fume.

Because the pozzolanic reaction with silica fume is so rapid, high resistivity and strength results can be achieved at early ages, however most of the potential for improvement has been realized by 28 to 90 days of age.

The consistent equal distance between the graphs of 0.37SF and 37SF/CNI indicate that calcium nitrite corrosion inhibitor does lower the resistivity of concrete, however it is by a consistent amount each time.

As with the RCP test, the addition of silica fume in 0.37SF/FA showed a positive effect when compared to 0.37FA at 28 days of age. The lines of the two mixes are pretty close to parallel, reconfirming that most of the effect of silica fume is seen at early ages and the effect of fly ash is seen at later ages.

The dramatic increase in resistivity of 0.37FA should be noted. As is typical, at early ages the mix containing only fly ash as a SCM was the worst performer, however by the 365 day mark it had made significant gains. This is due to the slow pozzolanic reaction experienced by fly ash. The upward slope of the graph also indicates that the maximum potential of the mix had not been reached at that time the last testing occurred (1 year).

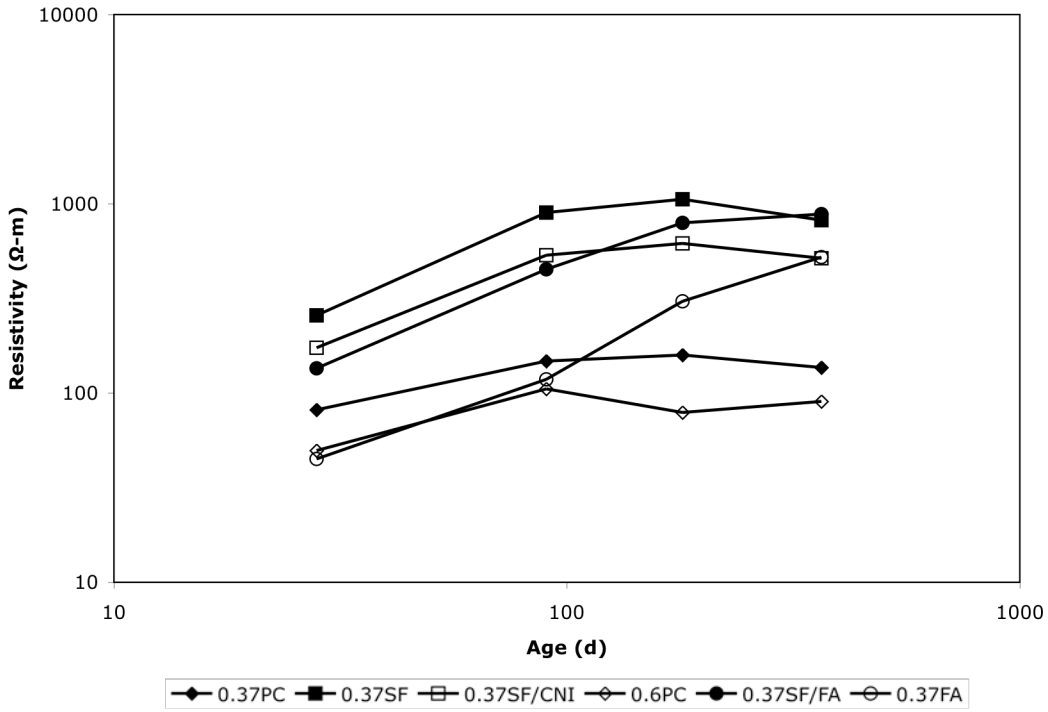

Figure 4.3: Change in resistivity with time for //Plate-200mm test

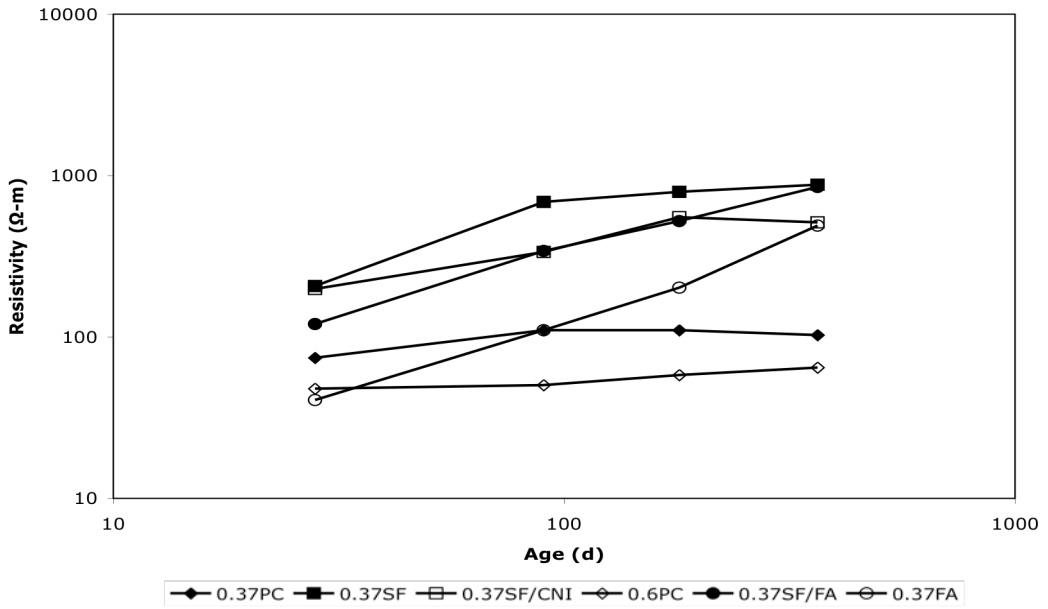

Figure 4.4: Change in resistivity with time for //Plate-50mm test

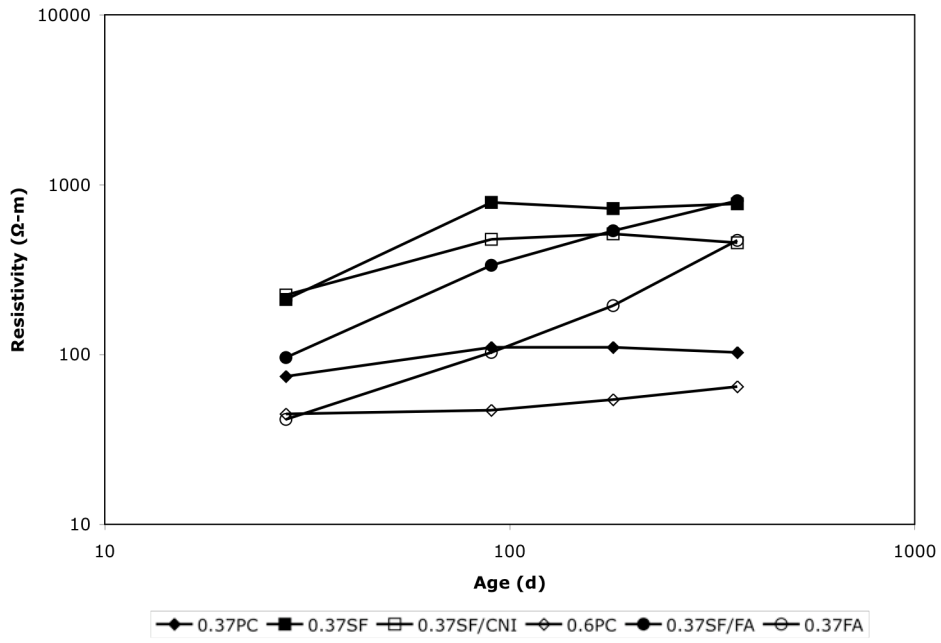

Figure 4.5: Change in resistivity with time AC-Cell test

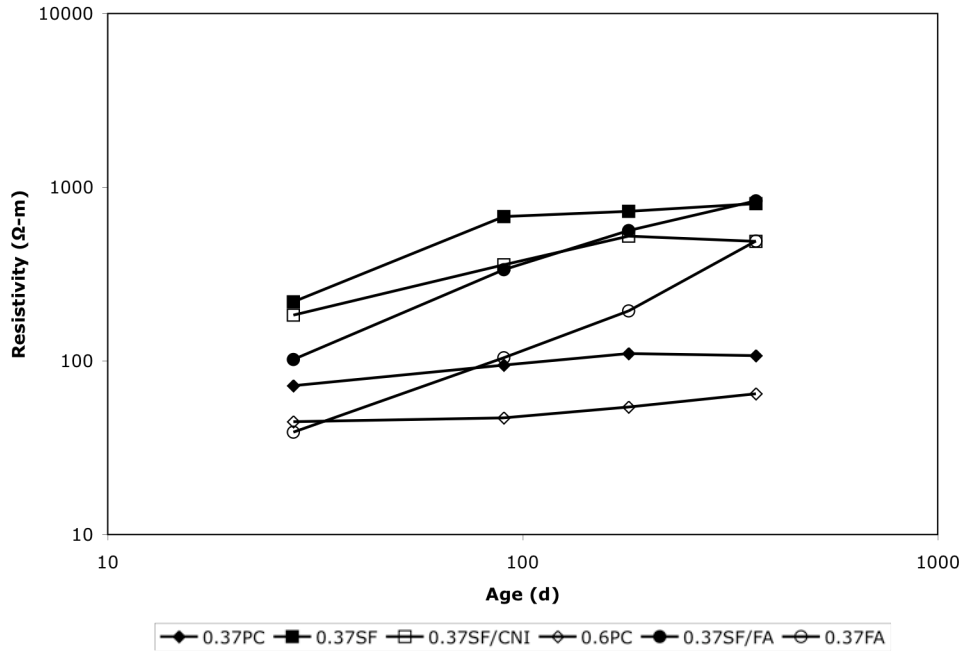

Figure 4.6: Change in resistivity with time DC-Cell test

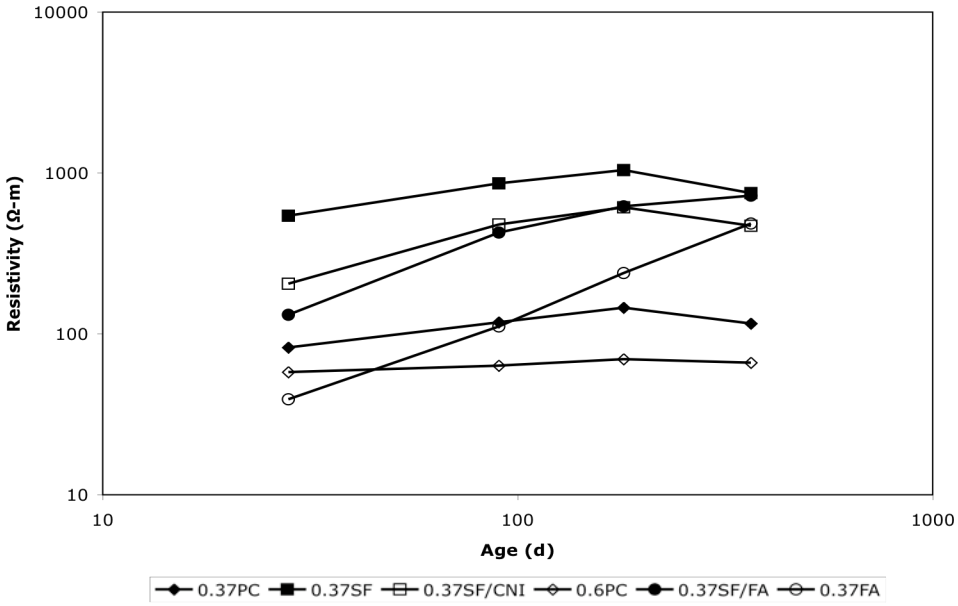

Figure 4.7: Change in resistivity with time for Wenner Probe test

4.4. Diffusion

The effect of time on the apparent diffusion coefficient determined by the bulk diffusion test of the various mixes can be seen in Figure 4.8. A general decreasing trend of diffusion coefficients, from the 90-day testing onwards, is present, but is not as well defined as was expected. It was also observed that all coefficients determined at the age of 28 days do not fit with this trend. It is not known why this has occurred but it is possible that there was an experimental error with the 28-day tests.

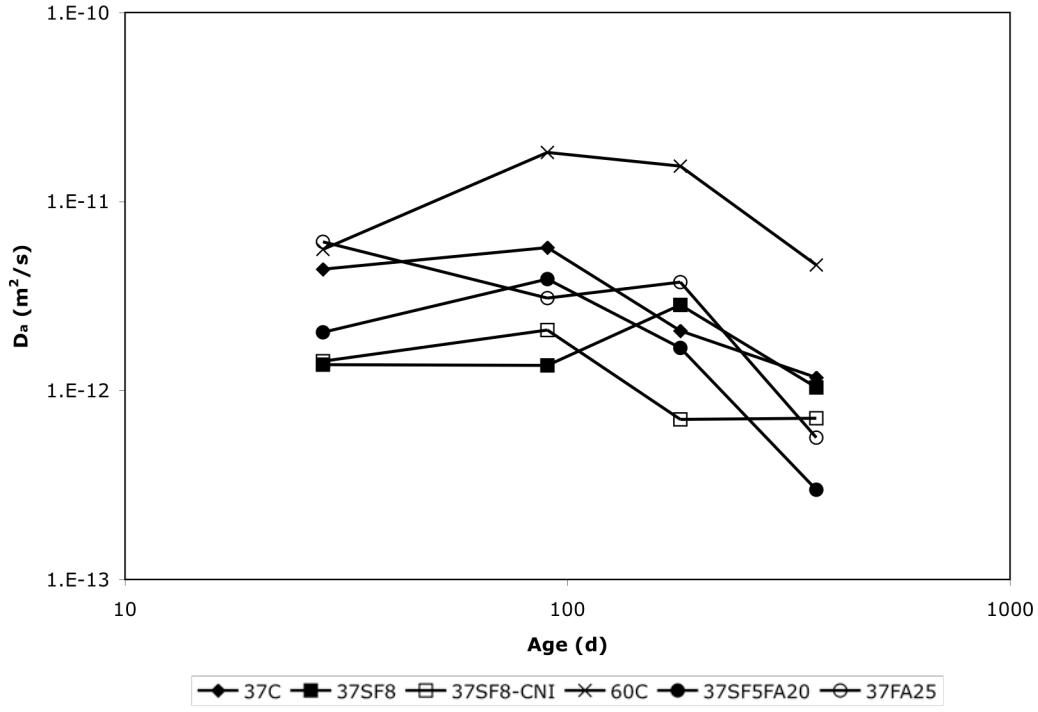

Figure 4.8: Change in D_a with time for Bulk Diffusion test

4.5. Migration

Figure 4.9 and Figure 4.10 show an example of the change in chloride content over time for downstream and upstream cells respectively. As can be seen in Figure 4.9, a chloride flux (slope of the graph after steady-state has been achieved) can easily be determined from this graph. However, there appears to be no consistent decline in the chloride content of the upstream cell making the determination of a flux less accurate.

The diffusion coefficients were calculated using the slope of the best-fit line through the data (flux) after steady-state flux had occurred and a diffusion coefficient was calculated using Equation 7. It was assumed that steady-state flow in the upstream cell had occurred immediately after the start of the test as suggested by Truc (2000).

As can be seen in Figure 4.11 the diffusion coefficients determined through the upstream and downstream monitoring give similar results. When compared to the results from the bulk diffusion test the diffusion coefficients determined both, on average, predict a slower rate of chloride transport. It should be noted that there is not a well-defined consistent decrease in the chloride content of the upstream cell. It is recommended that the upstream and downstream methods be more fully investigated.

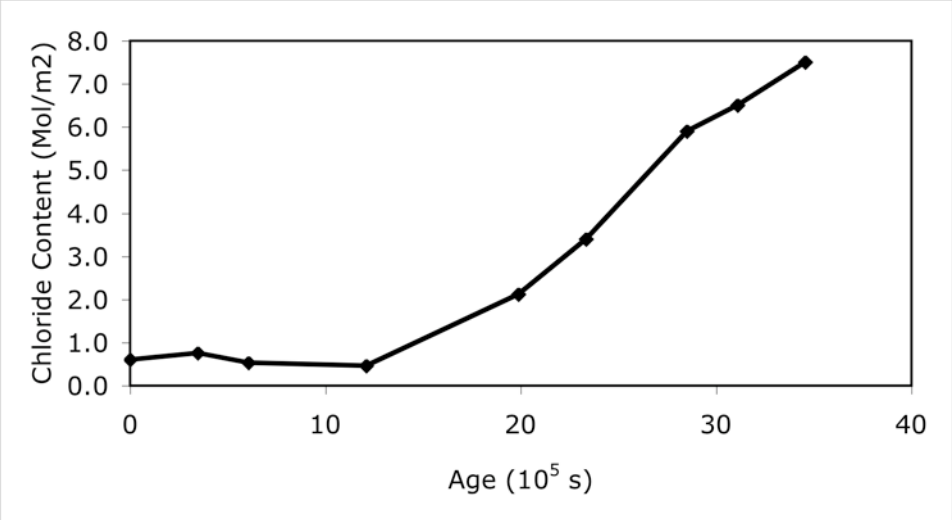

Figure 4.9: Downstream change in chloride concentration for 0.37SF/CNI-28d

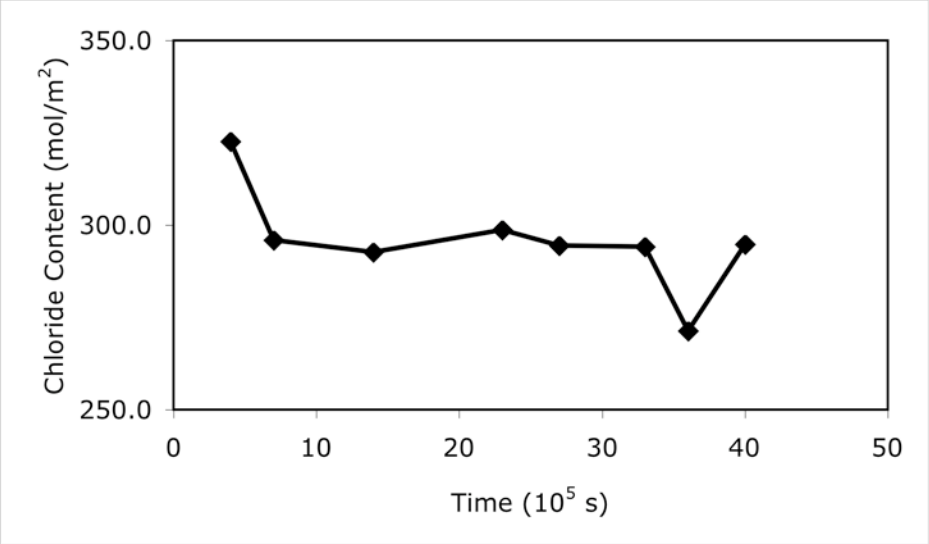

Figure 4.10: Upstream change in concentration for 0.37SF/CNI-28d

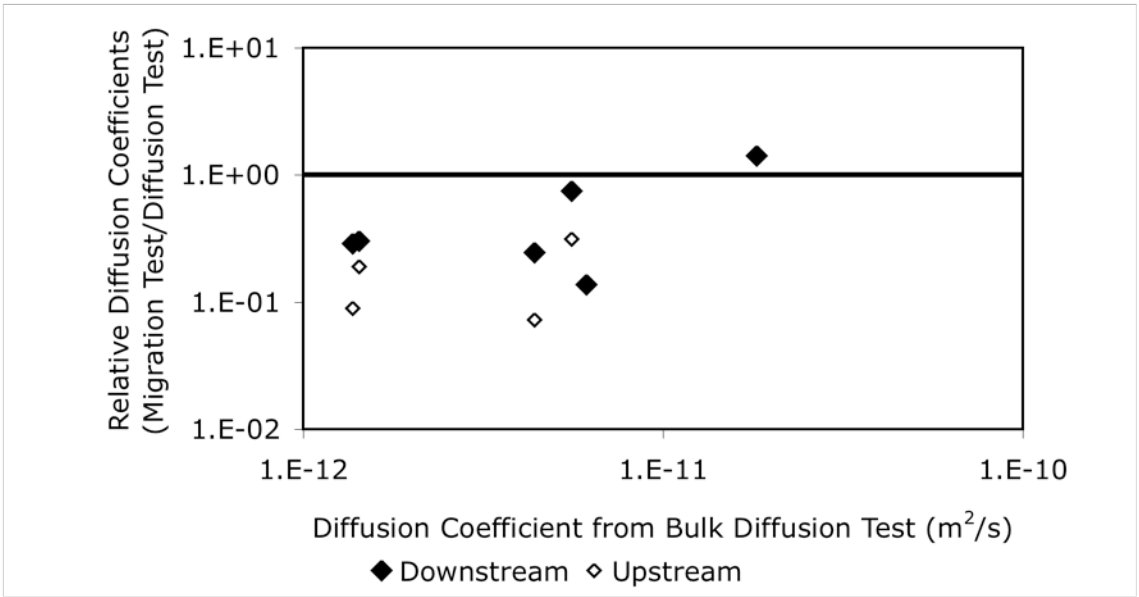

Figure 4.11: Diffusion Coefficients from upstream and downstream migration tests

4.6. Effect of Rebar on Resistivity

The resistivity of the blocks was measured with a Wenner Probe (that has an inter-point spacing of 50mm) aligned both parallel and perpendicular to the reinforcing steel.

Figure 4.12 to Figure 4.19 display the effect of cover depth over reinforcing and measurement direction steel on surface resistivity measurements. The graphs display the ratio of measurements taken on a control block with no reinforcing steel and measurements taken on blocks with varying cover depths over rebar. A ratio of 1.0 indicates that there is no effect on the resistivity measurements by the reinforcing steel.

The graphs indicate that there is an effect on the resistivity up to a cover depth of 50mm (equal to the tip spacing of the probe). Literature indicates that rebar influences resistivity measurements taken by Wenner Probes up to a cover depth equal to the spacing of the points on the probe, which is supported by the results from this study. Up

to this cover depth there is a significant influence when measuring parallel to the steel bars. This influence is greatly reduced when measurements were taken perpendicular to the steel, however there appears to some influence. When the cover depth is greater than the probe spacing there is very little difference between measurement directions, however the ratio remains below 1.0, significantly in the case of 0.37PC-100mm. This discrepancy is most likely due to measurement errors or differences in the resistivity of the concrete in the reinforced vs. control block. While an obvious solution to negate the influence of reinforcing steel on Wenner Probe measurements would be to reduce the point spacing, one must be careful not to reduce it too much. It is recommended that the inter-point spacing be greater than 1.5 times the maximum aggregate size to eliminate major influences by the aggregate (Morris,1996). Also since the depth of influence of the probe is approximately equal to the inter-point spacing, the spacing cannot be too small if a reading that is representative of the bulk concrete is to be obtained.

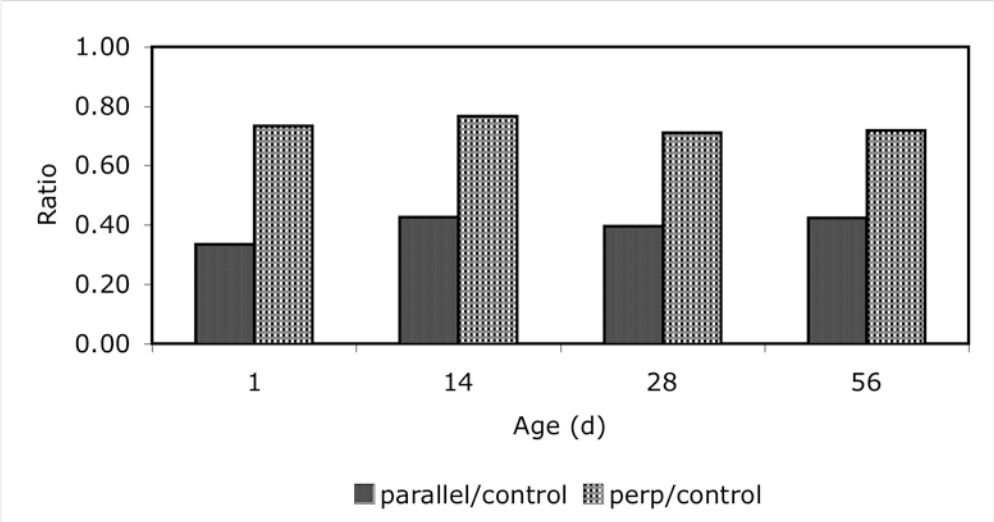

Figure 4.12: Resistivity ratio for 0.37PC-25mm

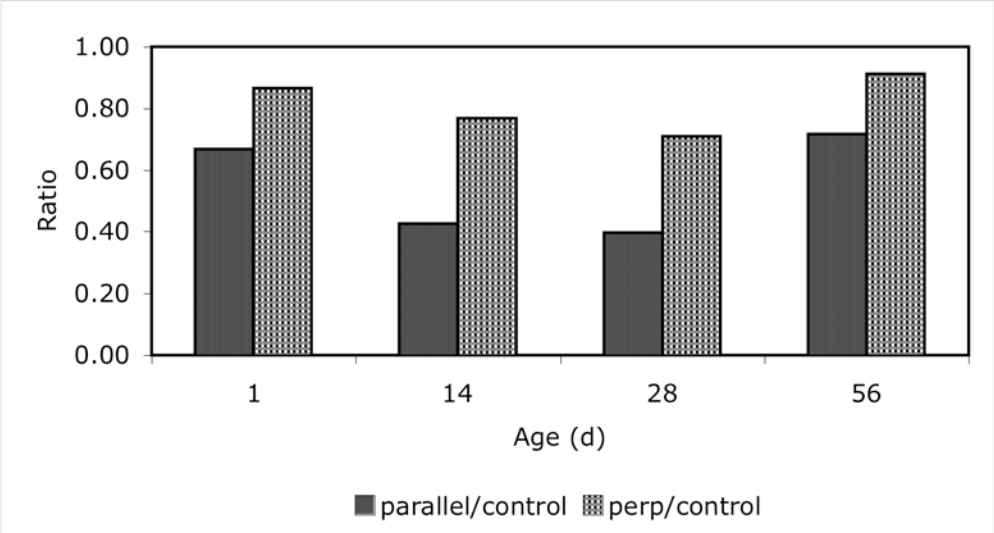

Figure 4.13: Resistivity ratio for 0.37PC-50mm

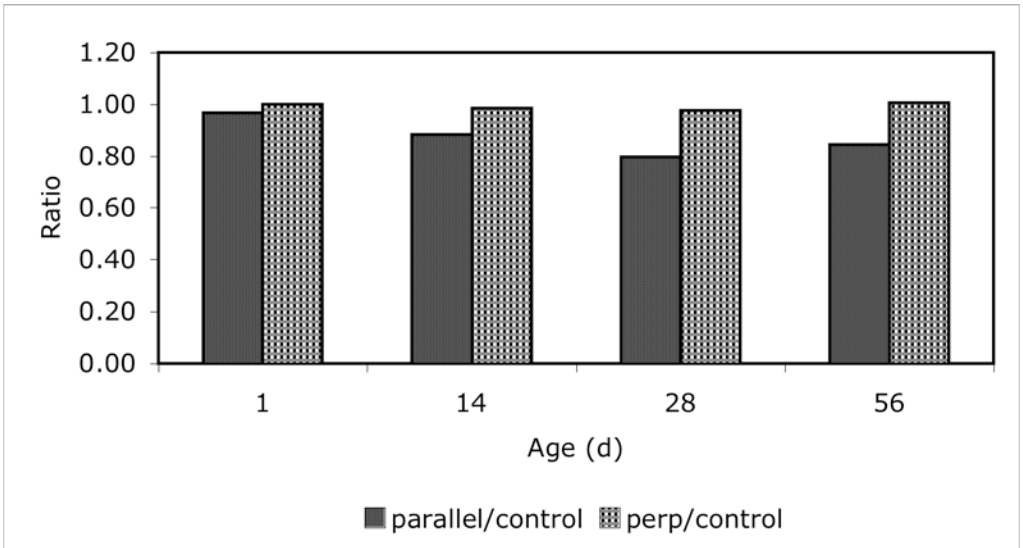

Figure 4.14: Resistivity ratio for 0.37PC-75mm

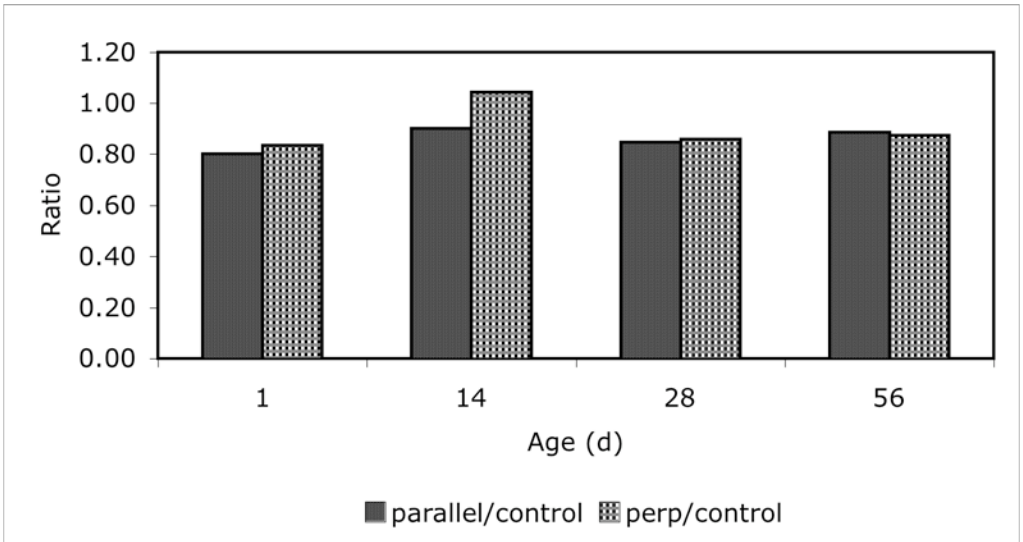

Figure 4.15: Resistivity ratio for 0.37PC-100mm

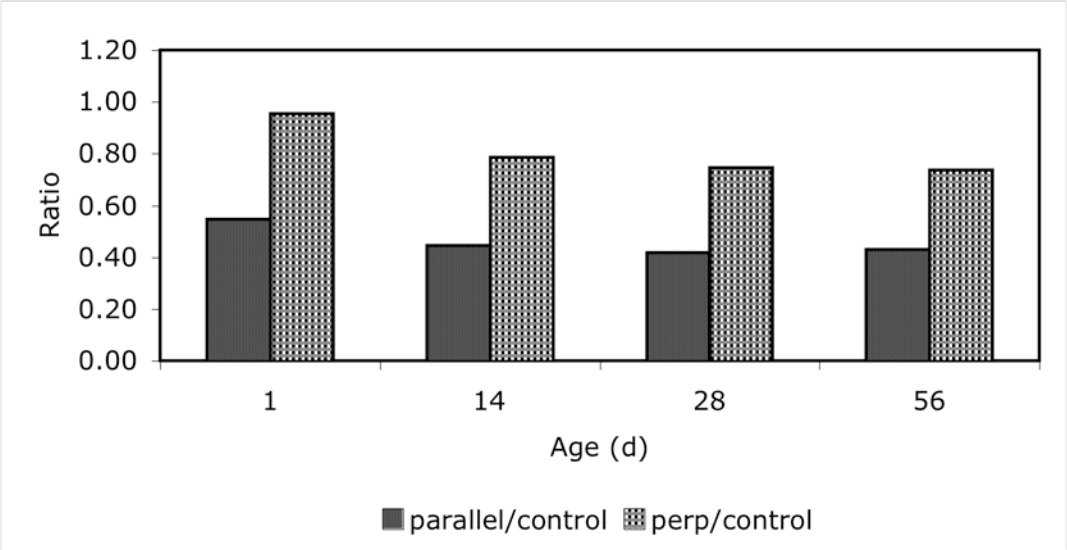

Figure 4.16: Resistivity ratio for 0.37SF-25mm

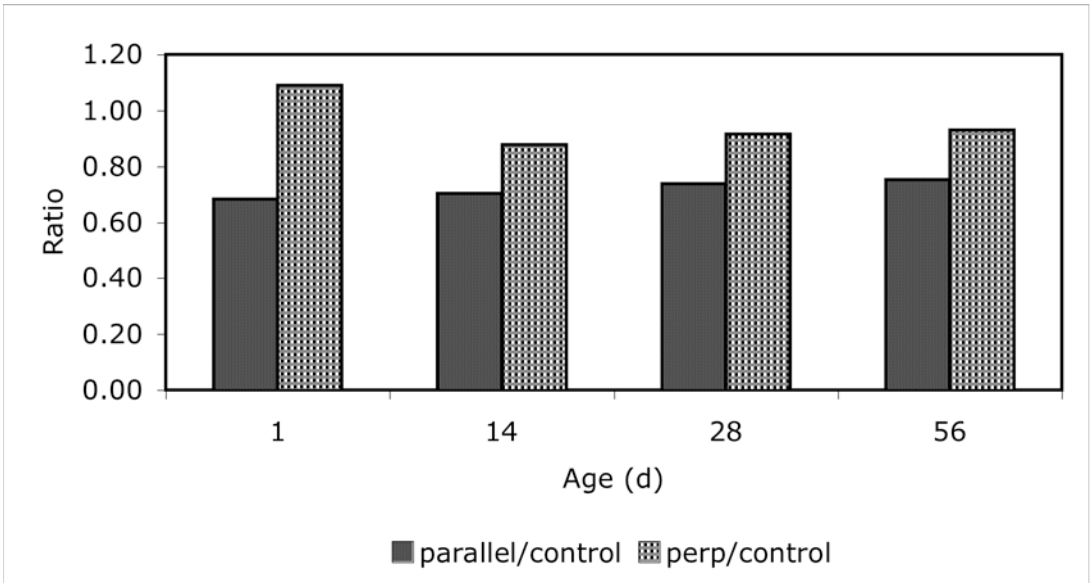

Figure 4.17: Resistivity ratio for 0.37SF-50mm

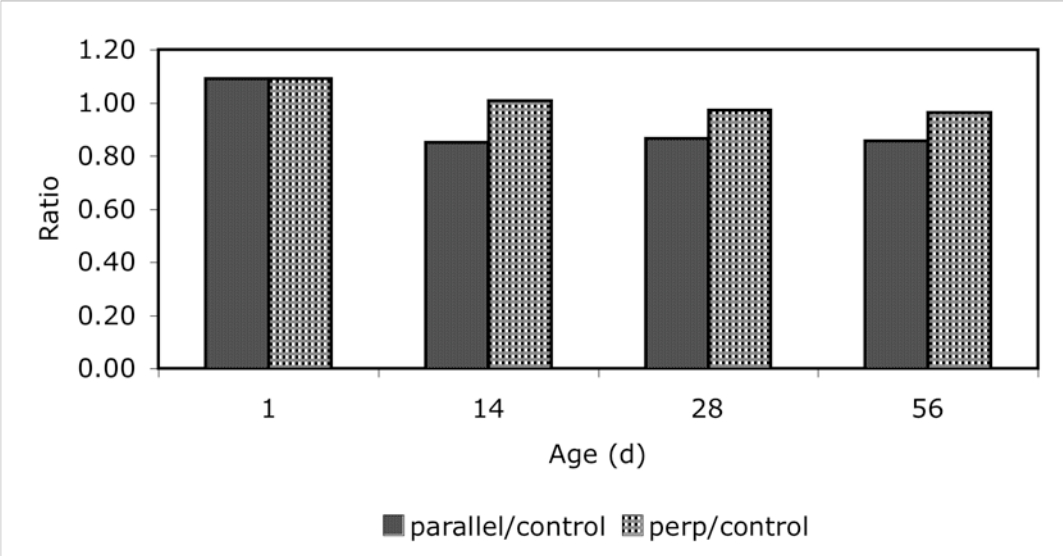

Figure 4.18: Resistivity ratio for 0.37SF-75mm

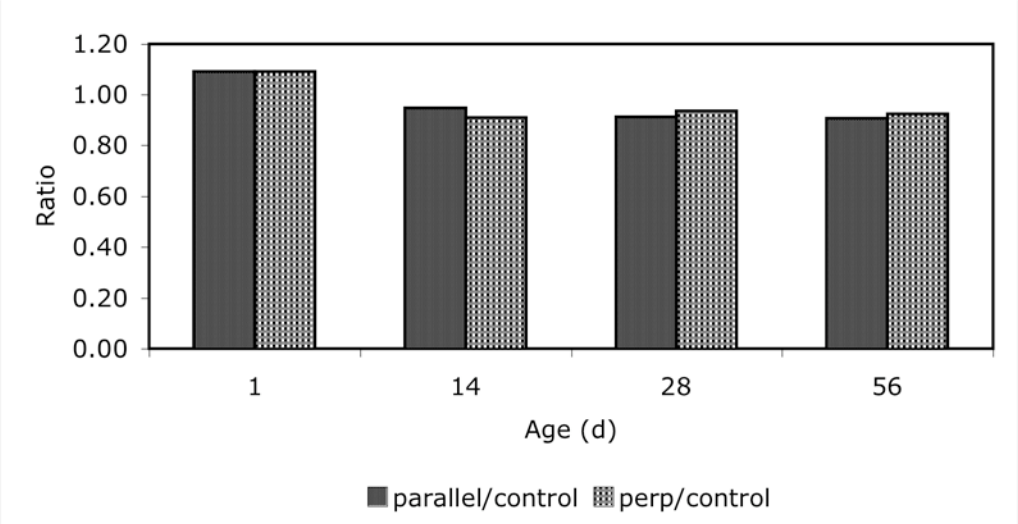

Figure 4.19: Resistivity ratio for 0.37SF-100mm

4.7. In-situ Measurement of Pore Solution

Figure 4.20 shows the change in the in-situ pore solution resistivity measurements of the concrete tested. It appears as though the resistivity of the solution in the reservoir equilibrated at approximately 50 days after testing started. As can be seen in the graph, the resistivity of both solutions is quite high, a resistivity of approximately 1 Ω-m was expected. The bulk resistivity was measured on either side of reservoir after monitoring of the in-situ solution was complete. The bulk resistivity for 0.37PC and 0.37SF were 112 Ω-m and 819 Ω-m respectively.

Table 4.4 gives composition of the solution that was extracted from the reservoir. The concentrations of sodium, potassium, calcium and hydroxide ions are much lower than one would expect, in some cases on the order of 10 times.

Given the high resistivity and the low concentrations of ions in solution it is quite apparent that the solution in the reservoir had not come to equilibrium with the pore solution of the concrete. The reason for this may be due to the fact that the test was started when the concrete was approximately 180 days old, and the volume of solution was too large. The volume of the reservoir was approximately 3.5ml, due to the size of the conductivity probe available, which is a substantial volume of solution to try to equilibrate with the pore solution contained within a cylinder. If the test had been started when the concrete was new, and the volume of the reservoir was smaller then equilibrium may have been achievable.

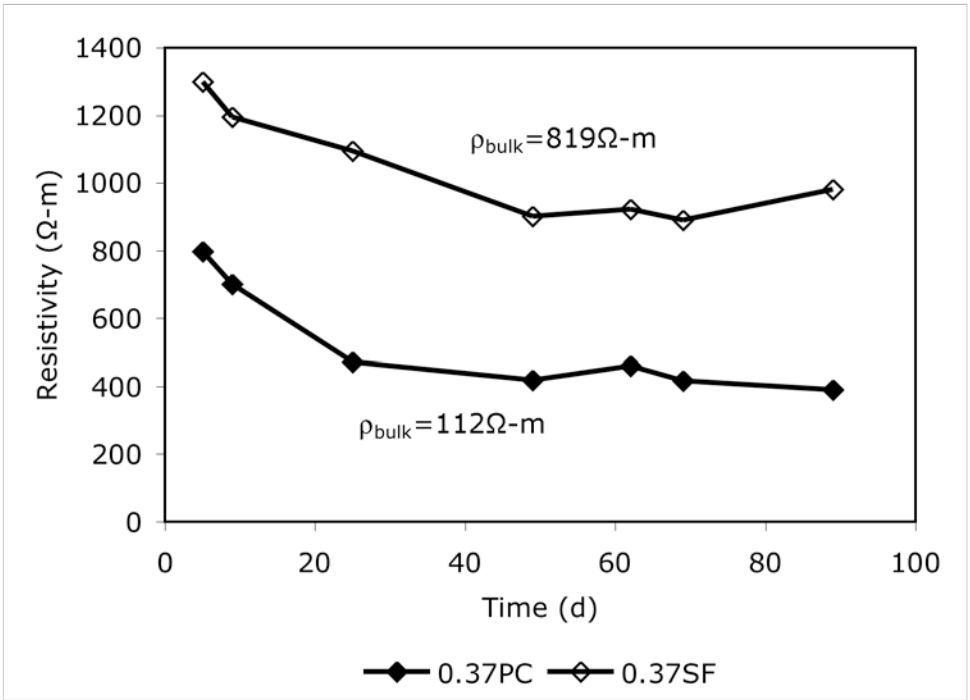

Figure 4.20: In-situ solution measurements

Table 4.4: In-situ solution composition

	OH^- (mol/l)	Na^+ (mol/l)	K^+ (mol/l)	Ca^{2+} (mol/l)
0.37PC	0.1375	0.016	0.0259	0.004
0.37SF	0.043	0.016	0.0218	0.003

4.8. Effect of Humidity on Resistivity

Figure 4.21 and Figure 4.22 display the change in resistivity over time of blocks and cylinders stored on the UNB exposure site and cylinders stored under water at standard lab conditions. During this testing there were two periods of rainfall, both indicated on the graphs. Measurements were taken within 24 hours of the rainfall; other measurements were taken periodically during good weather. As expected there is

reasonably good agreement between the blocks and the cylinders stored on the exposure site. Also, when the concrete on the exposure site was subjected to extended drying periods the resistivity was higher than the resistivity of the cylinders stored in the lab. It should be noted however, that the resistivity of the concrete on the exposure site after the large rainfall (40mm) was approximately the same as the lab stored cylinders. This indicates that the saturation condition of the concrete stored on the exposure site does vary enough to substantially alter surface resistivity measurements. It is obvious that more work needs to be done to quantify the extent that direct exposure to the environment has on the moisture condition, and in turn the resistivity measured by surface techniques, before the Wenner Probe can be used on structures as a quality control tool.

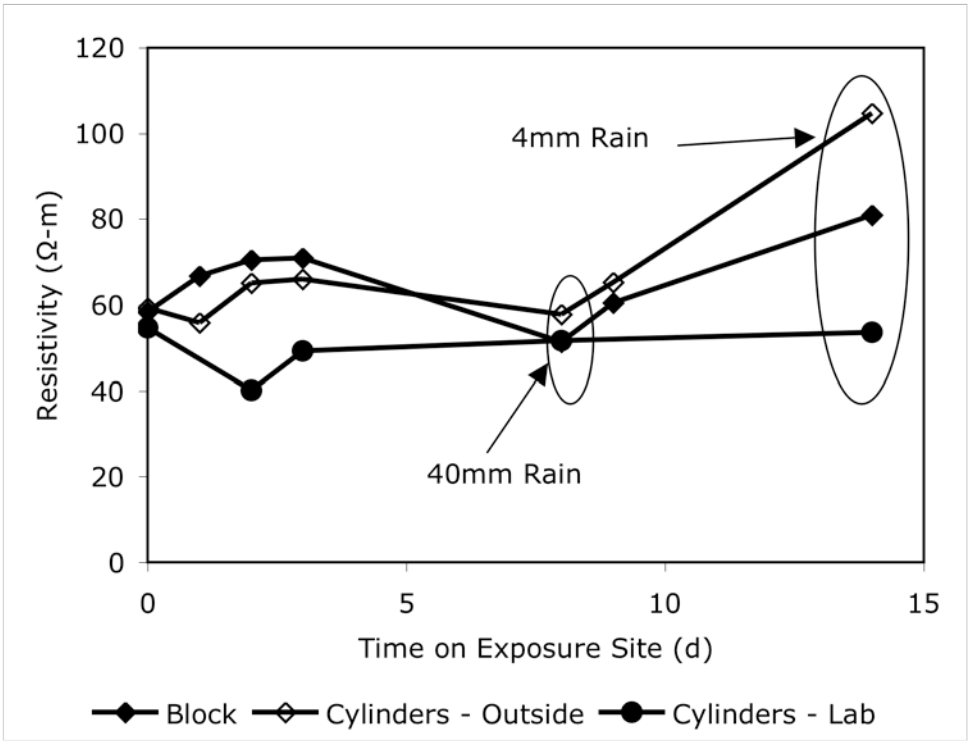

Figure 4.21: Effect of humidity on resistivity for 0.37PC

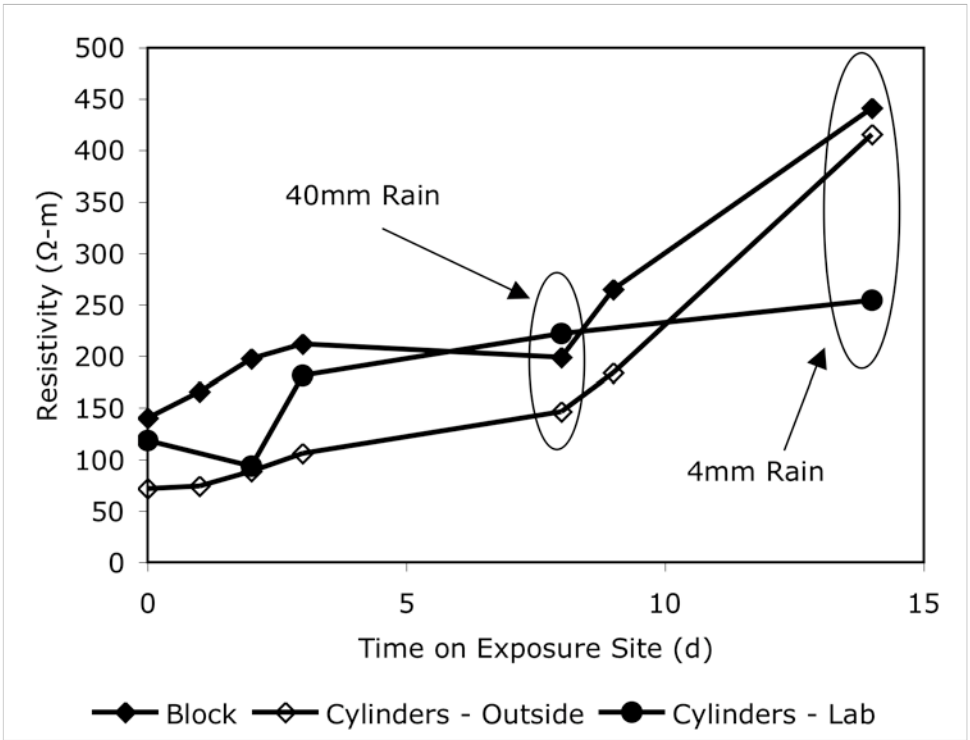

Figure 4.22: Effect of humidity on resistivity for 0.37SF

5.0 Discussion of Results

5.1. Comparison of Resistivity Tests

Table 5.1 gives the average resistivity relative to the other tests conducted, and Figure 5.1 to Figure 5.6 show graphical comparisons of the five different resistivity tests carried out for this program. All tests have been described previously. It should be noted from Table 5.1 that the Wenner Probe and the //Plate-200 consistently have a higher average relative resistivity. Generally there is good agreement between the tests, however as the resistivity of the concrete increases there seems to be more scatter in the data. The results from testing carried out on the FAPC series (Figure 5.5) the agree well with each other with the exception of the //Plate-50mm and the DC-Cell tests for mix D-2.

The data from the CE series which has the most highly resistive concrete tested in this program shows a large amount of scatter. It is also noted that the resistivity measured by the //Plate – 50mm test are consistently, and substantially higher than the results from the other tests conducted on the same sample. All testing for the CE series was not conducted on the same day, however all //Plate – 50mm testing was on the same day. If there was a problem with the resistivity meter the day the //Plate – 50mm tests were conducted it may result in a higher measurement. That being said, there were no observed problems with any of the testing equipment on the day of testing.

Table 5.1: Average relative resistivity

Denominator	Numerator				
	Wenner	//Plate-200	//Plate-50	AC-Cell	DC-Cell
Wenner	1.0	1.1	1.0	0.8	0.9
//Plate-200	1.0	1.0	0.8	0.8	0.8
//Plate-50	1.1	1.3	1.0	0.9	1.0
AC-Cell	1.2	1.3	1.2	1.0	1.0
DC-Cell	1.1	1.3	1.1	0.9	1.0

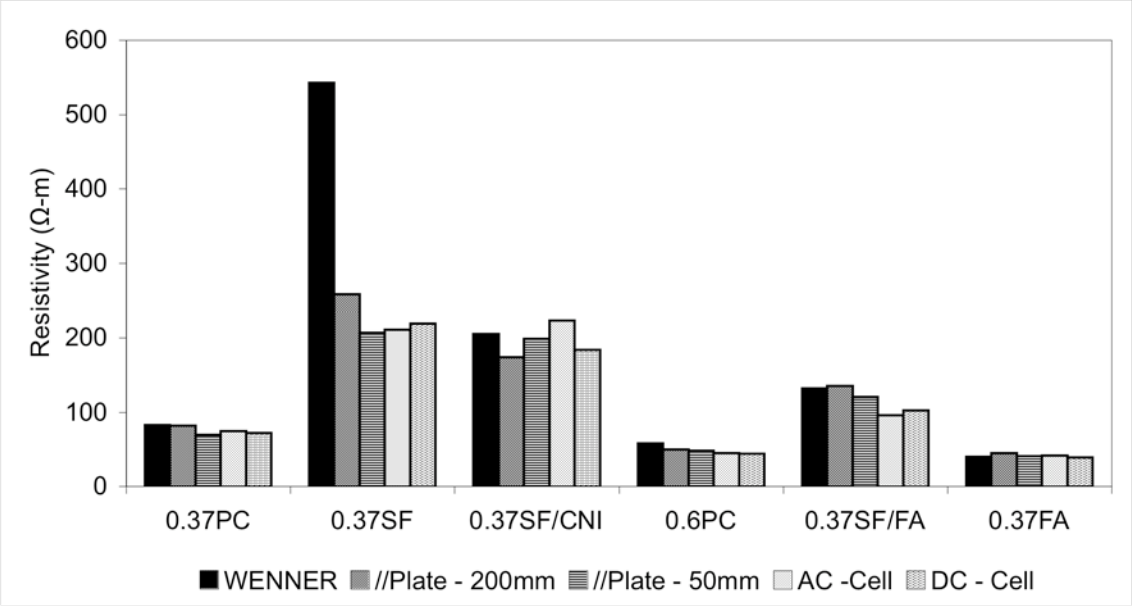

Figure 5.1: Comparison of results from various tests for Laboratory Study - 28d

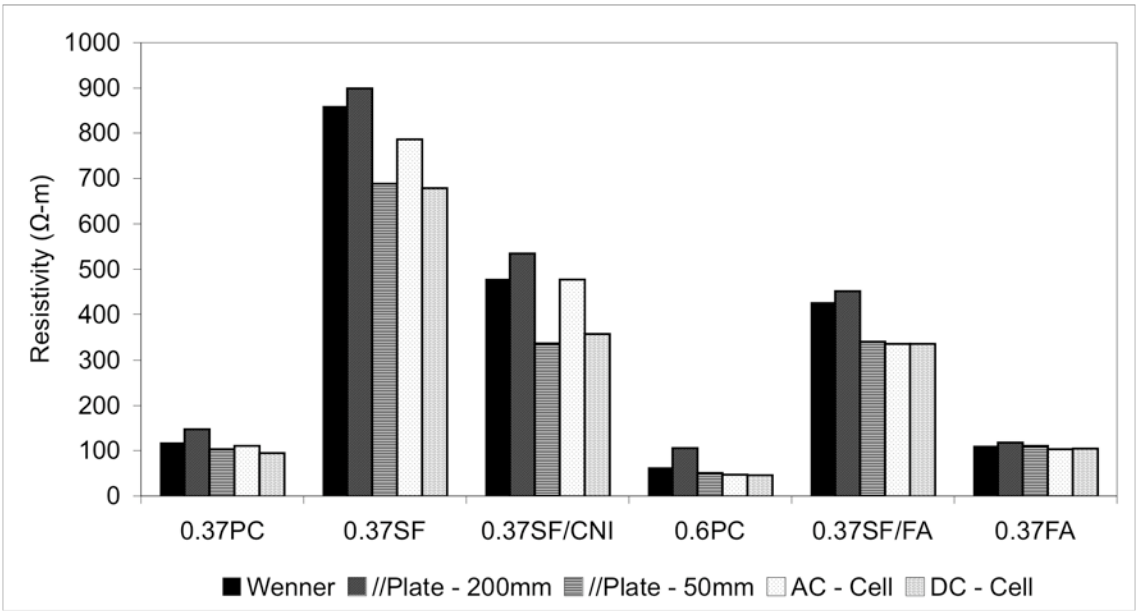

Figure 5.2: Comparison of results from various tests for Laboratory Study - 90d

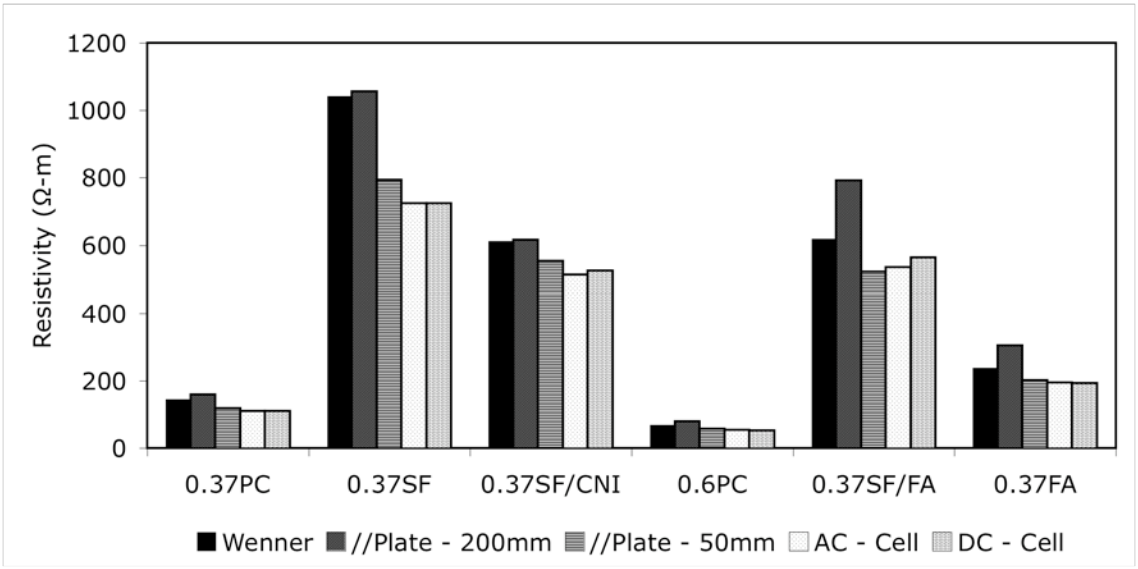

Figure 5.3: Comparison of results from various tests for Laboratory Study - 180d

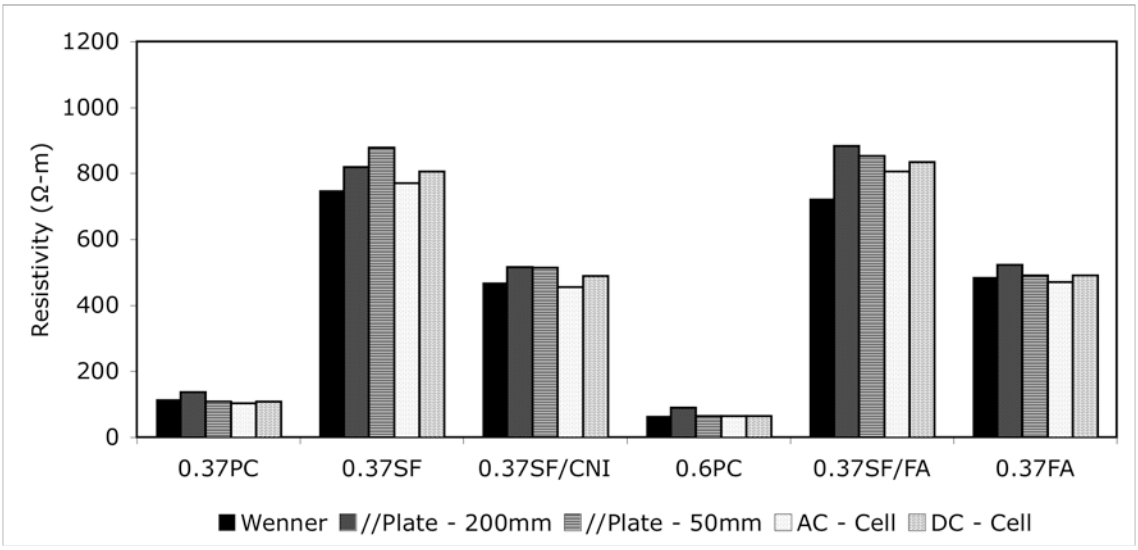

Figure 5.4: Comparison of results from various tests for Laboratory Study - 365d

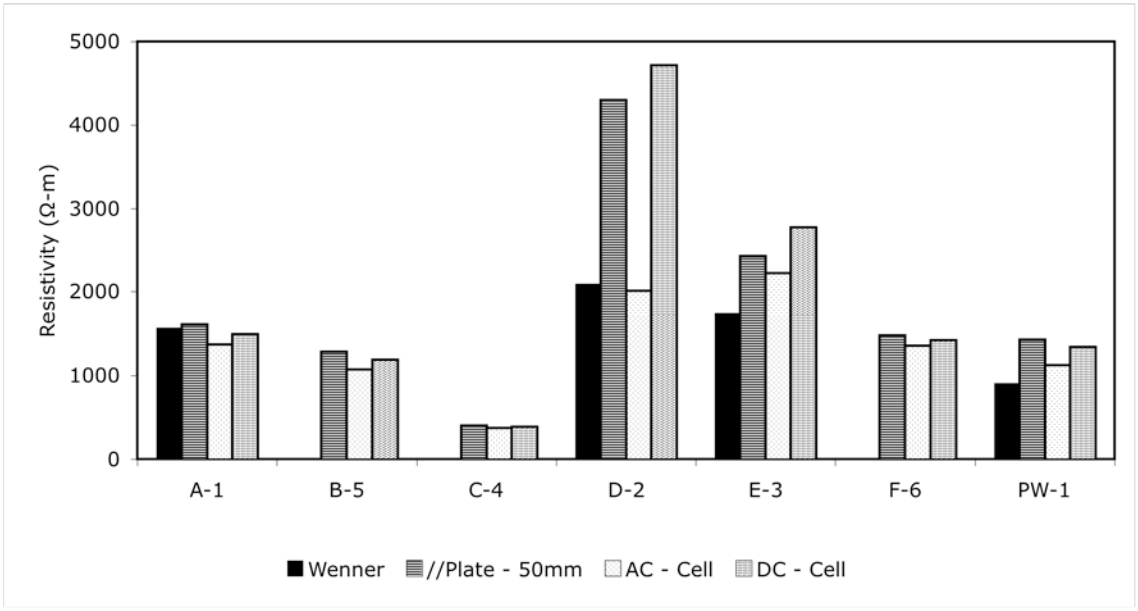

Figure 5.5: Comparison of results from various tests for FAPC series

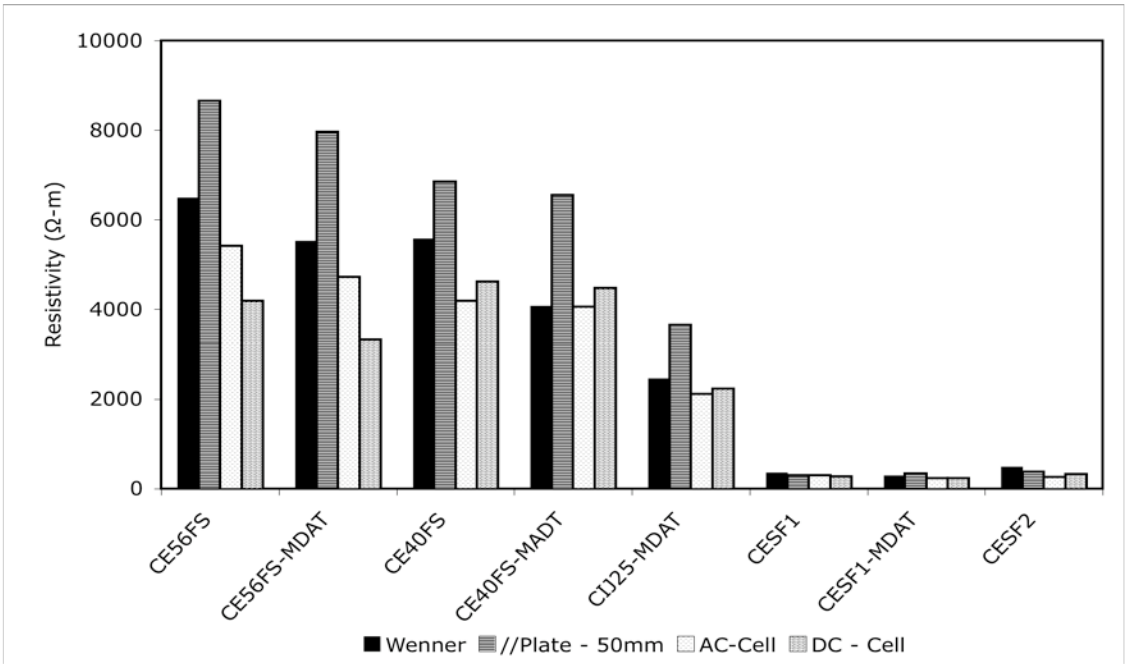

Figure 5.6: Comparison of results from various tests for Evans series

5.2. Resistivity – RCPT

Figure 5.7 to Figure 5.11 display the relationship between the various resistivity tests and the amount of charge passed in the RCP test. The Rapid Chloride Permeability test is actually a test that measures the electrical conductivity of the concrete. The general relationship between resistivity (in Ω-m) and the RCP (in Coulombs) test is:

$$\text{charge passed} = a\ (\text{resistivity})^{b} \qquad \text{(Equation 23)}$$

where a accounts for the 6-hour duration of the RCP test, and b is -1.

It would therefore be reasonable to assume that the best-fit curve through the data would be a power curve with an exponent of -1. After examining the equations of the best-fit lines, summarized in Table 5.2, it can be seen that all of the exponents are quite close to

the expected -1 value. //Plate – 200mm has the exponent closest to -1, however this test was conducted only on the concrete from the Laboratory Study due to the inconsistent length of the samples from the other series. Table 5.3 gives the coefficients, exponents and correlation coefficients of the best-fit lines when only the data from the Laboratory Study is considered. As can be seen, all values agree very well with each other so it is obvious that the higher resistivity values cause the best-fit line to have a shallower slope.

Table 5.2: Resistivity-RCPT Regression Information –All Results

	Wenner	//Plate – 200mm	//Plate – 50mm	AC – Cell	DC - Cell
Coefficient	157792	315882	98259	109110	132009
Exponent	-0.9506	-1.0395	-0.875	-0.9182	-0.9407
R^2	0.93	0.93	0.94	0.94	0.96

Table 5.3: Resistivity-RCPT Regression Information – Laboratory Study Only

	Wenner	//Plate – 200mm	//Plate – 50mm	AC – Cell	DC – Cell
Coefficient	250300	315882	239538	222083	216701
Exponent	-1.0103	-1.0395	-1.0289	-1.0178	-1.0175
R^2	0.9277	0.93	0.9598	0.9561	0.966

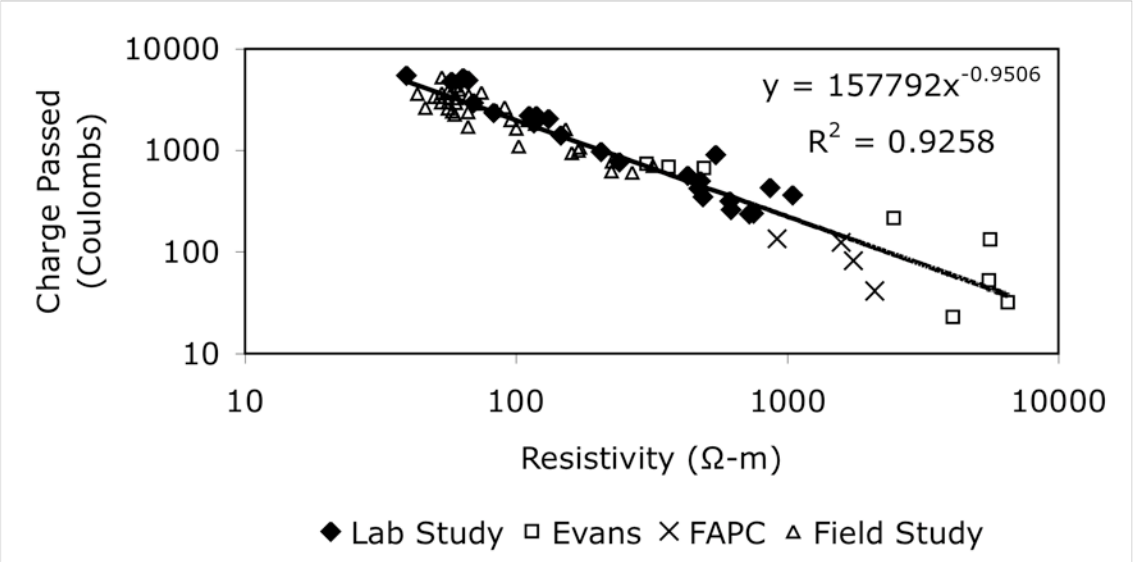

Figure 5.7: RCPT – resistivity correlation for Wenner Probe

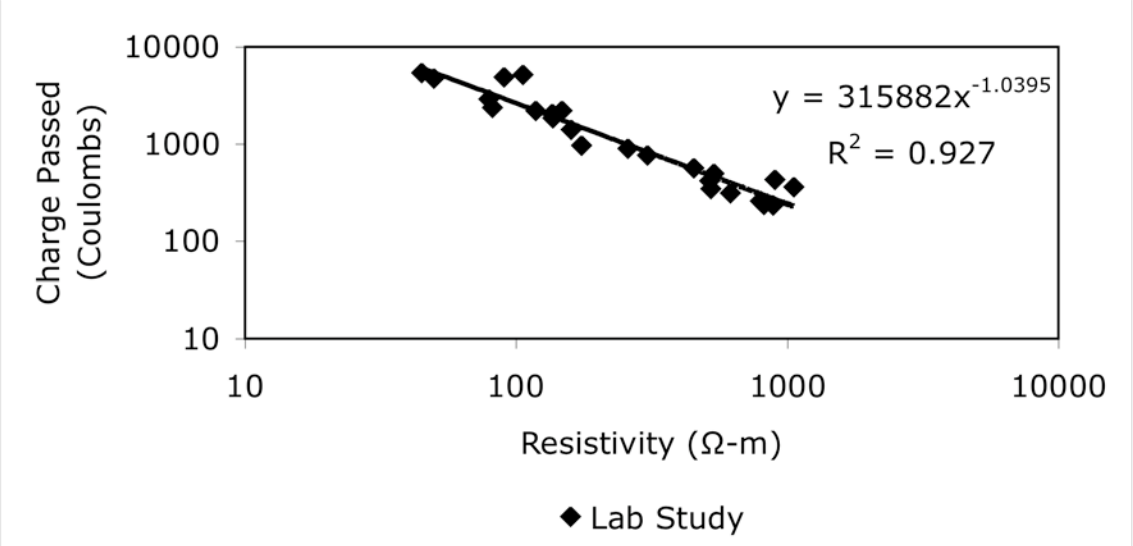

Figure 5.8: RCPT – resistivity correlation for //Plate-200mm

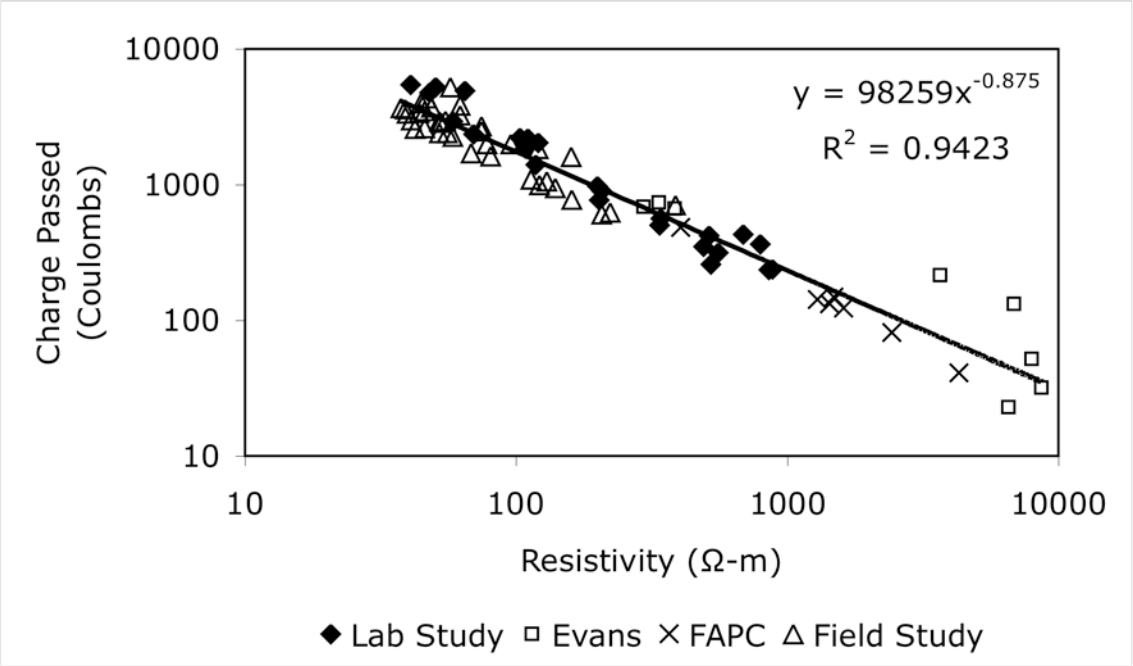

Figure 5.9: RCPT – resistivity correlation for //Plate-50mm

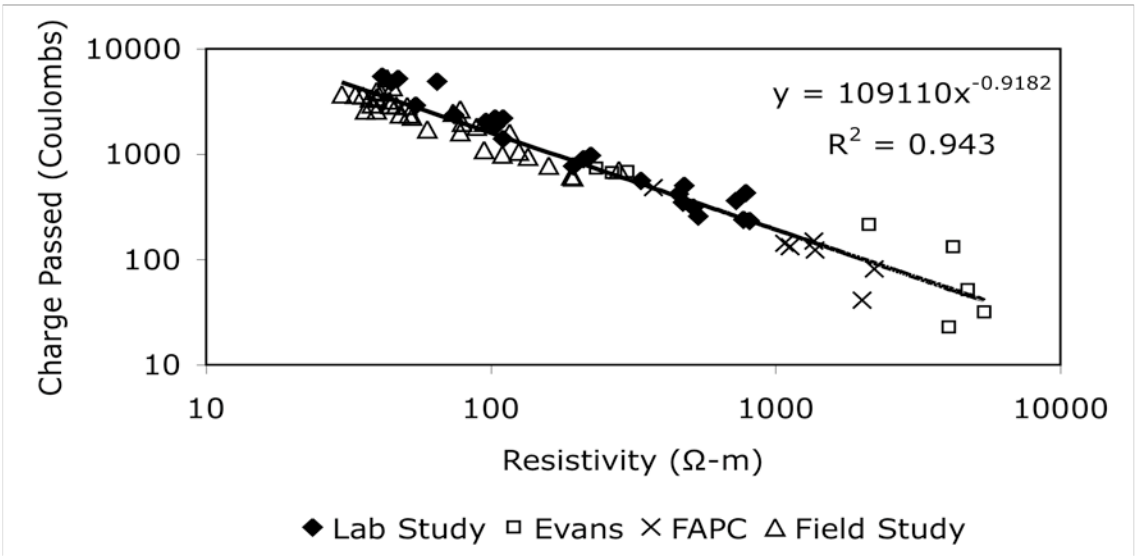

Figure 5.10: RCPT – resistivity correlation for AC-Cell

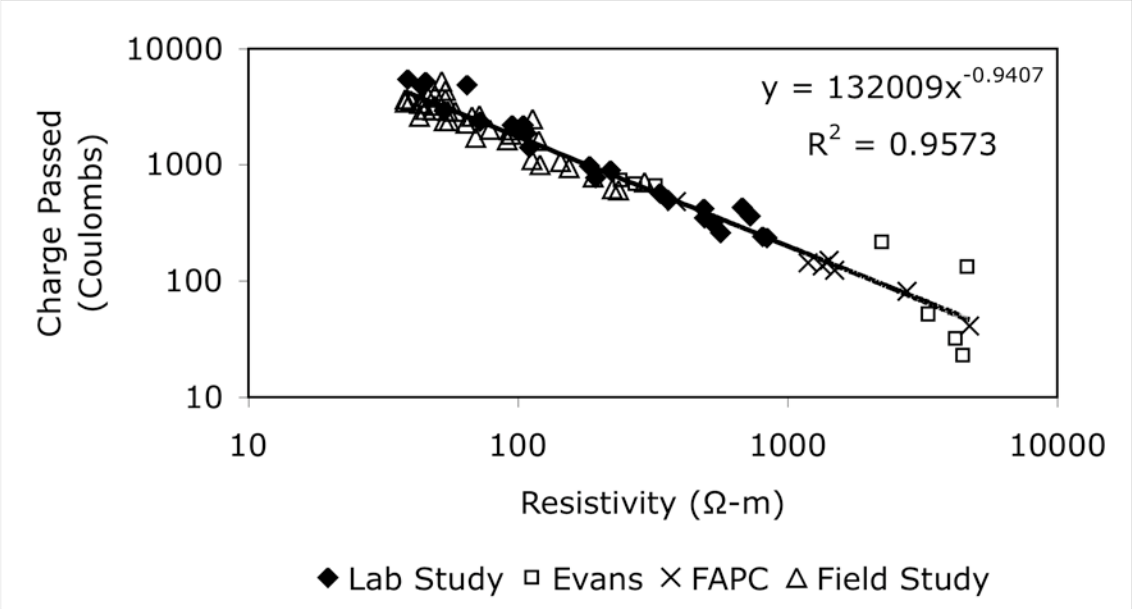

Figure 5.11: RCPT – resistivity correlation for DC-Cell

5.3. Comparison with other Data

Figure 5.12 shows the relationship between resistivity and charge passed in the RCP test from three independent studies. Series Smith indicates data from this research program, while the Burden and Obla series' were taken from Burden (2006) and Obla (2003) respectively. The resistivity results from the Smith series were obtained using the Wenner Probe method while Burden used the DC-Cell method and Obla used the Monfore method. All methods used have been described previously.

As can be seen, there is a very strong agreement between the three data sets. This indicates that resistivity techniques can be used for quality control and assurance with the same confidence as the RCP test, especially when the resistivity of the concrete is below 1000 Ω-m.

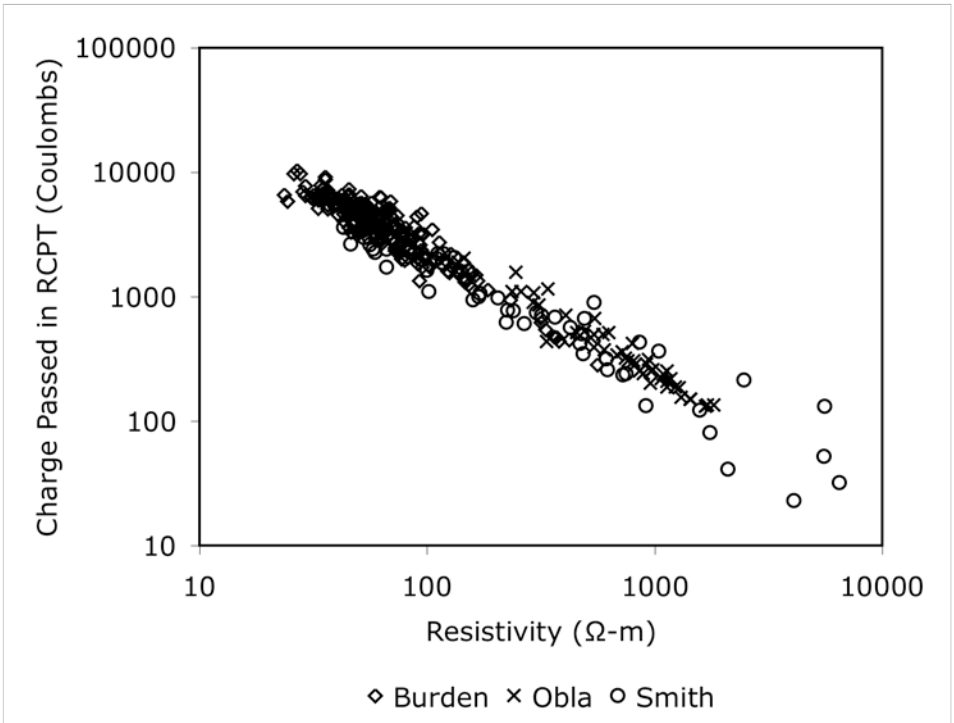

Figure 5.12: Comparison of relationship between resistivity and charge passed for Burden, Obla and Smith

5.4. Diffusion – RCPT Comparison

Figure 5.13 shows the relationship between diffusion coefficient and the amount of charge passed during the ASTM C 1202 test.

As can be seen from the plots, there is a general upward relationship between increasing diffusion coefficients and increasing charge passed. However, this relationship is not well enough defined to use as a prediction model.

The reason for the large scatter of data is most likely the fact that the ASTM 1202 test is essentially a conductivity test in which both the pore structure and the conductivity of the

pore solution are major factors impacting results, while only the pore structure has a major impact of the diffusion coefficient.

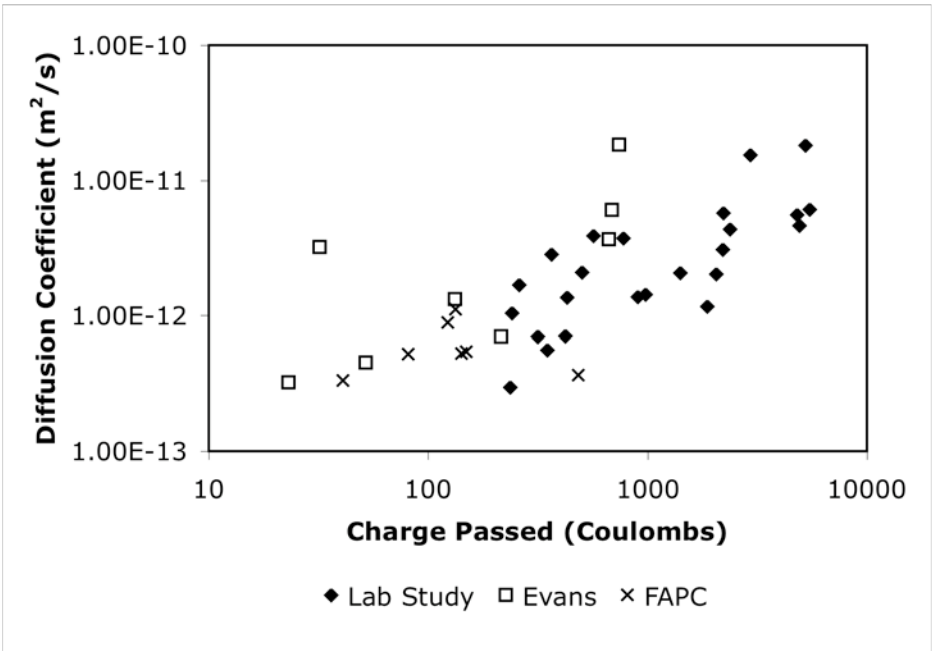

Figure 5.13: Relationship between diffusion coefficient and charge passed

5.5. Comparison of Formation Factors

The conductivity of pore solution extracted from paste samples, described in section 3.2.5 of this thesis, was calculated using Equations 13-15 as set forth by Snyder (2003). The pore solution was extracted when the paste was 28 days old. It was assumed that the composition of the pore solution changed little after 28 days. This assumption may not hold completely true, especially for those containing fly ash, however due to the difficulty in extracting pore solution from mature, low w/cm pastes this assumption had to be made. The conductivity of these pore solutions are presented in Table 5.4

Table 5.4: Pore solution conductivity of paste samples

Mix ID	0.37PC	0.37SF	0.37SF/CNI	0.6PC	0.37SF/FA	0.37FA
Conductivity (S/m)	1.39	0.77	0.39	0.12	0.47	0.68

Diffusion coefficients were then calculated for the concrete made in the Laboratory Study using Equation 11.

Figure 5.14 to Figure 5.18 show diffusion coefficients measured from the bulk diffusion test plotted against diffusion coefficients calculated using the formation factor theory. As can be seen, the correlation between measured and calculated diffusion coefficients is very poor. The calculated diffusion coefficients are much higher than the measured coefficients – in most cases by at least one order of magnitude. This discrepancy may be due to chloride binding. The formation factor theory assumes that there is no interaction between the chlorides and the cement matrix. However, this is not the case; depending on the composition of the cement, especially the C_3A content, there may be considerable binding, which the bulk diffusion test accounts for.

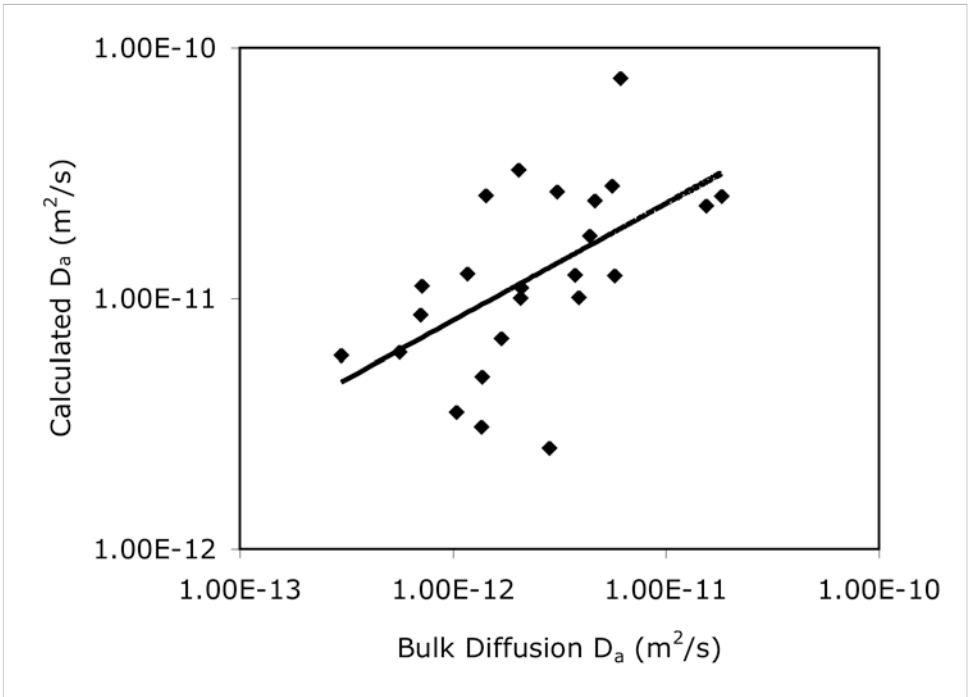

Figure 5.14: Calculated vs. measured diffusion coefficients based on Wenner Probe resistivity

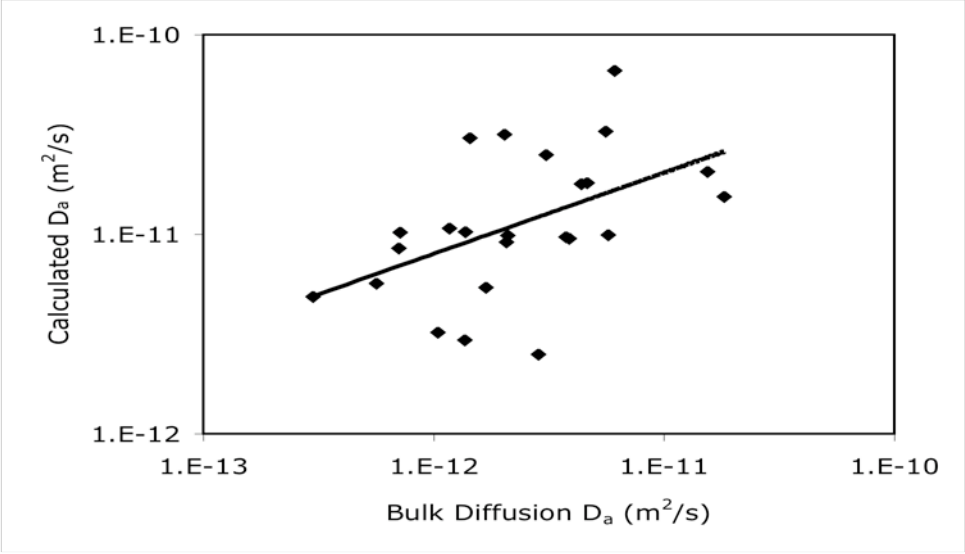

Figure 5.15: Calculated vs. Measured diffusion coefficients based on //Plate-200mm resistivity

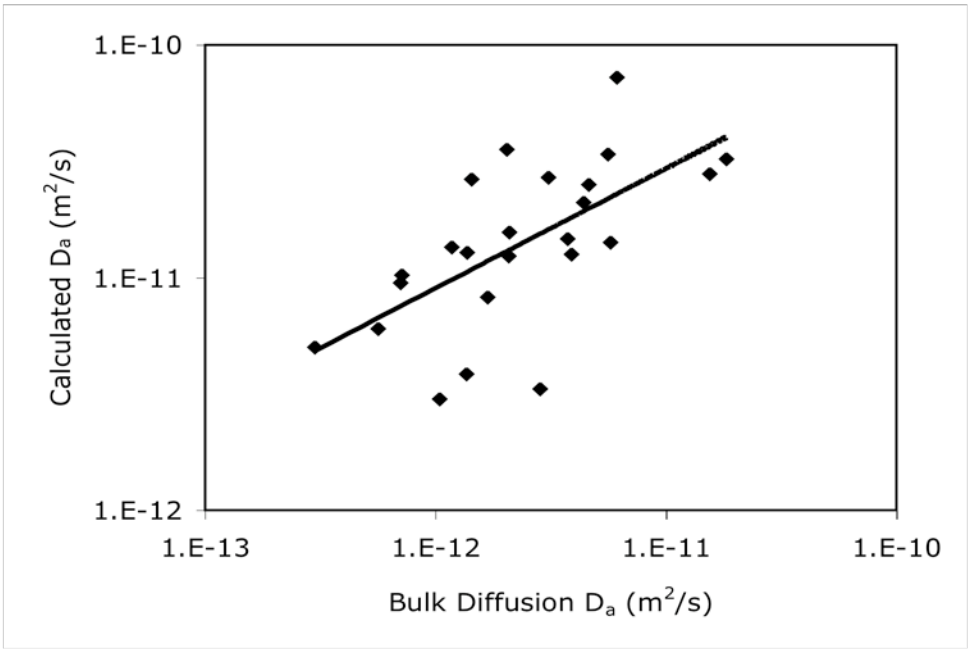

Figure 5.16: Calculated vs. Measured diffusion coefficients based on //Plate-50mm resistivity

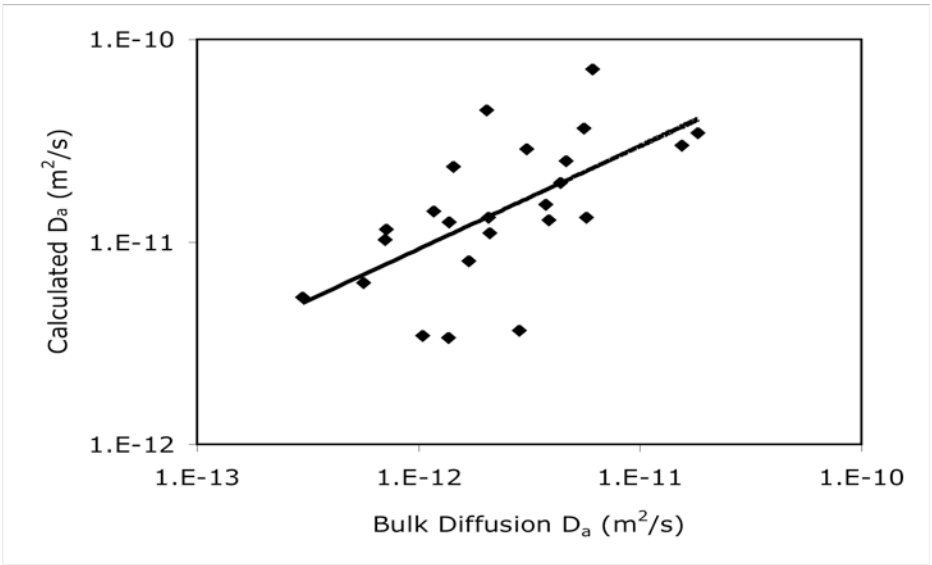

Figure 5.17: Calculated vs. Measured diffusion coefficients based on AC-Cell resistivity

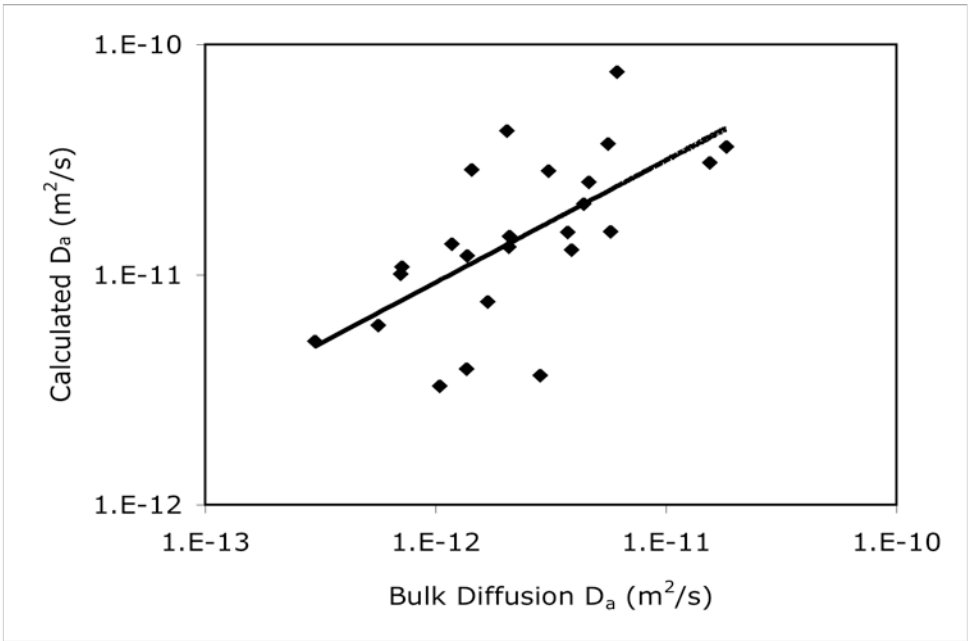

Figure 5.18: Calculated vs. Measured diffusion coefficients based on DC-Cell resistivity

5.6. Recommended Quality Control Values

As is well shown, there is a very strong correlation between the charge passed in the RCP test and the resistivity of the concrete. Resistivity techniques have many advantages over the widely used RCP test including reduced sample preparation time, reduced testing time, no risk of spurious results due to heating, and the measurement of resistivity has potential use in the field. Table 5.5 gives recommended ranges of resistivity, corresponding to the currently used ranges of charge passed (ASTM C 1202) for classifying the risk of chloride ion penetrability. These ranges are recommended for non-reinforced, saturated concrete only. The ranges for each test method examined in this thesis were determined by the equations set out in Table 5.2.

Table 5.5: Recommended Chloride Ion Penetrability Based on Resistivity

Risk	RCPT (Coulombs)	Wenner (Ω-m)	//Plate – 200mm (Ω-m)	//Plate – 50mm (Ω-m)	AC-Cell (Ω-m)	DC-Cell (Ω-m_
High	>4000	<50	<70	<50	<50	<50
Moderate	2000-4000	100-50	130-70	100-50	80-50	100-50
Low	1000-2000	200-100	250-130	200-100	170-80	200-100
Very Low	100-1000	2300-200	2300-250	2600-200	2000-170	2000-200
Negligible	<100	>2300	>2300	>2600	>2000	>2000

6.0 Conclusions

There were two main goals of this project; the first was to develop a rapid quality control test to replace current methods, and the second was to examine the feasibility of using electrical techniques to predict diffusion coefficients of chlorides through concrete. The first goal has been achieved as is demonstrated throughout this thesis, however, before diffusion coefficients can be predicted through electrical resistivity the effect of chloride binding needs to be studied.

This project also examined various techniques for measuring the electrical resistivity and determining the chloride diffusion coefficient of concrete. Various factors affecting resistivity measurements were also examined. The conclusions reached through this project are as follows:

1. The various resistivity tests did give relatively consistent results, however it appears as though the results from the //Plate-200 test were a somewhat higher than the others.
2. A very strong relationship exists between resistivity and the amount of charge passed in the Rapid Chloride Permeability test. Therefore, resistivity can be used in place of the RCP test for quality control measures.
3. Reinforcing steel does influence surface resistivity measurements when the cover depth is less than the inter-point spacing of the probe.
4. The impact of reinforcing steel on surface resistivity measurements is greatly reduced when the probe is aligned perpendicular to the direction of the rebar.

5. The influence on surface saturation due to wetting and drying in the field is such that this effect must be accounted for when taking surface resistivity measurements.

6. There is a weak relationship between resistivity and the rate of chloride diffusion in saturated concrete, however, this relationship is not strong enough to predict diffusion rates by resistivity.

7. The conductivity of concrete pore solution cannot be determined by the in-situ method, as tested. It is possible that improved results may be obtained if the test is conducted on new concrete.

8. The use of the formation factor does not improve the predictability of diffusion coefficients by resistivity. This prediction may be improved if the effect of chloride binding can be accounted for.

9. Diffusion coefficients determined by monitoring the change in chloride concentration both upstream and downstream of the concrete in the electrical migration test gave similar results.

10. The diffusion coefficients determined through electrical migration techniques tend to be lower than those found by the bulk diffusion test.

7.0 Recommendations

Upon completion of this project the following recommendations are made.

1. Standards committees such as American Society for Testing and Materials (ASTM) and Canadian Standards Association (CSA) should adopt electrical resistivity tests as an alternative to the Rapid Chloride Permeability Test.
2. The ranges of resistivity set out in Table 5.5, corresponding to ranges established in the RCP test, should be used to classify the risk of chloride ion penetration of concrete.
3. Researchers need to carry out a full-scale study to determine the viability of surface resistivity measurements on field concrete as a quality control method. Factors affecting resistivity that need to be examined in this study include wetting and drying of the surface concrete, carbonation and curing methods used, such as curing compounds, moist curing and no curing at all.
4. A more extensive study needs to be carried out to determine if pore solution conductivity can be determined by in-situ methods.
5. The effect of chloride binding needs to be determined before resistivity can be used to predict diffusion rates.
6. The upstream monitoring method of the electrical migration test needs to be further studied. It must be determined is accurate diffusion coefficients can be determined given solution analysis available in typical concrete testing laboratories.

7. Laboratory technicians should measure the electrical resistivity of a concrete sample prior to conducting the RCP test in an effort to increase the body of work supporting the relationship between the two test methods.

8.0 References

American Society for Testing and Materials. (2000). Standards on Disc, Vol. 04.02, October 2000, Concrete and Aggregates. West Conshohocken, PA, United States

C 39/C 39M Standard Test Method for Compressive Strength of Cylindrical Concrete Specimens

C 1202-97 Standard Test method for Electrical Indication of Concrete's Ability to Resist chloride Ion Penetration.

C 1556 – 03 Standard Test method for Determining the Apparent Chloride Diffusion Coefficient of Cementitious Mixtures by Bulk Diffusion

"Florida Method of Test for Concrete Resistivity as an Electrical Indicator of its Permeability", *Designation: FM 5-578*, January 27, 2004.

Andrade, C. "Calculation of Chloride Diffusion Coefficients in Concrete from Ionic Migration Measurements" *Cement and Concrete Research* Vol. 23. pp. 724-742, 1993.

Broomfield, J.B., *Corrosion of Steel in Concrete,* FN Spon, an Imprint of Chapman & Hall, London, UK, 320 pages, 1997.

Burden, Donald "The Durability of Concrete Containing High Levels of Fly Ash" *M.Sc Thesis,* Department of Civil Engineering, University of New Brunswick, 2006.

Chatterji, S. et al. "On the Applicability of Fick's Second Law to Chloride Ion Migration Through Portland Cement Concrete", *Cement and Concrete Research,* Vol. 25 No. 2 pp. 299-303, 1995.

Crank, John *The Mathematics of Diffusion 2ed.* Claredon Press, Oxford England, 1975.

Csizmadia, Jolan et al "Chloride Ion Binding Capacity of Aluminoferrites" *Cement and Concrete Research* Vol 31 pp 577-588, 2001.

Evans, Christopher "The Influence of Fly Ash and Early-age Curing Temperature on Durability and Strength of High-performance Concrete" *M.A.Sc. Thesis,* University of Toronto, 1997.

Friedmann, H. et al, " a direct method for Determining Chloride Diffusion Coefficient by using Migration Test", *Cement and Concrete Research*, Vol. 34, pp. 1967-1973, 2004.

Hansson, I. L. H. and Hansson, C. M. "Electrical Resistivity Measurements of Portland Cement Based Systems", *Cement and Concrete Research,* Vol. 13, pp. 675-683, 1983.

Hope, Brian b. and Ip, Alan K. "Corrosion and Electrical Impedance in Concrete" *Cement and Concrete Research* Vol 15, pp 525-534, 1985.

Horvath, A.L, *Handbook of Aqueous Electrolyte Solutions* Ellis Horwood Limited Publishers, Chichester, 1985.

Joshi, Prakash and Chan, Cesar, "Rapid Chloride Permeability Testing: A test that can be used for a wide range of applications and quality control purposes if the inherent limitations are understood", Publication #C02l037 Hanely-Wood, LLC, 2002

Kemp, Marwin K. *Physical Chemistry, a Step by Step Approach* Marcel Dekker, Inc, New York and Basel, 1979.

Lide, David R. (editor-in-chief), *Handbook of Chemistry and Physics 82nd edition*, CRC Press, New York, 2001-2002.

Liu, Zheng, and Beaudoin, J.J., "The Permeability of Cement Systems to Chloride Ingress and Related Test Methods", *Cement, Concrete and Aggregates,* pp 16-23, 2000.

Liu, Zheng, and Beaudoin, J. J., "An Assessment of the relative Permeability of Cement Systems using AC Impedance Techniques", *Cement and Concrete Research,* Vol. 29, pp. 1085-1090, 1999.

Martys, Nicos S. "Survey of Concrete transport Properties and their Measurements", *NISTIR 5592,* February, 1995.

McGrath, Patrick F. "Development of Test methods for Predicting Chloride Penetration into High Performance Concrete" *Ph.D Thesis*, Department of Civil Engineering, University of Toronto, 1996.

Morris, W. Practical Evaluation of Resistivity of Concrete Test Cylinders using a Wenner Array Probe", *Cement and Concrete Research,* Vol. 26, No. 12, pp 1779-1787, 1996.

Naik, T. R., Ramme, B. W., and Kraus, R. N. "Performance of High-volume Fly Ash Concrete Pavements Constructed since 1984", *The Indian Concrete Journal*, pp. 137-143, February 2004.

Obla, K. H., Hill, R. L. Thomas, M. D. A., Shashiprakash, S. G. and Perebatova, O. "Properties of Concrete Containing Ultra-Fine Fly Ash" *ACI Materials Journal* pp. 426-433, September-October 2003.

Polder, Rob B. "Test method for Onsite measurement of Resistivity of Concrete – a RILEM TC-154 Technical Recommendation", *Construction and Building Materials*, Vol. 15, pp. 125-131, 2001.

Prince, W. and Gagne, R. "The Effects of Types of Solutions used in Accelerated Chloride Migration Tests for Concrete", *Cement and Concrete Research,* Vol. 31, pp. 775-780, 2001.

Prince, William et al, "Mechanisms Involved in the Accelerated test of Chloride Permeability", *Cement and Concrete Research*, Vol. 29, pp. 687-694, 1999.

Saleem, M. et al, "Effect of Moisture, Chloride and Sulphate Contamination on the Electrical resistivity on Portland Cement Concrete" *Construction and building Materials,* Vol. 10, No. 3, pp. 209-214, 1996.

Shi, Cajun, "Effect of mixing proportions of concrete on its electrical conductivity and the rapid chloride permeability test (ASTM C 1202 or ASSHTO T277) results" *Cement and Concrete Research,* Vol. 34, pp 537-545, 2003.

Snyder, K. A. et al, "Using Impedance Spectroscopy to Assess the Viability of the Rapid Chloride test for Determining Concrete Conductivity", *Journal of Research of the National Institute of Standards and Technology,* Vol. 105, No. 4, pp. 497-509, July-August 2000.

Snyder, K. A. and Feng, X. "Estimating the Electrical Conductivity of Cement Paste Pore Solutions from OH^- , K^+ and Na^+ Concentrations" *Cement and Concrete Research* Vol. 33, No. 6, pp. 793-798, June 2003.

Stanish, Kyle David, "The Migration of Ions in concrete" *Ph.D. Thesis*, Department of Civil Engineering, University of Toronto, 2002.

Stanish, K. D. et al, "Testing the Chloride Penetration Resistance of Concrete: A Literature Review", *FHWA Contract DTFH61-97-R-00022 "Prediction of Chloride Penetration in Concrete,* 31 pages, 1997.

Stanish, K et al, " A Novel Approach for Describing Chloride Ion Transport due to an Electrical Gradient in Concrete: Part 1. Theoretical Description" *Cement and Concrete Research* Vol. 34 pp.43-49, 2004.

Stanish, K. et al, " A Novel method for Describing Chloride Ion Transport Due to an Electrical Gradient in Concrete: Part 2. Experimental Study" *Cement and Concrete Research* Vol. 34, pp. 51-57, 2004

Stanish, Kyle and Thomas, Michael, "The use of Bulk Diffusion Tests to Establish Time-dependant Concrete Chloride Diffusion Coefficients"*, Cement and Concrete Research* Vol. 33 pp. 55-62, 2005.

Streicher, P.E. and Alexander, M.G. "A Chloride Conduction Test for Concrete" *Cement and Concrete Research,* Vol. 25, No. 6, pp. 1284-1294, 1995.

Su, Jin-Kiang et al, "Effect of Moisture Content on Concrete Resistivity Measurement", *Journal of the Chinese Institute of Engineers,* Vol. 25, No. 1 pp. 117-122, 2002.

Tong, L. and Gjorv, O.E. "Chloride Diffusivity Based on Migration Testing", *Cement and Concrete Research,* Vol. 31 pp. 973-982, 2001.

Truc, O. et al, "A new way for determining the Chloride Diffusion Coefficient in Concrete from Steady State Migration Test" *Cement and Concrete Research,* Vol. 30, pp. 217-226, 2000.

Tumidajski, P.J. et al, "On the Relationship Between Porosity and Electrical Resistivity in Cementitious Systems", *Cement and Concrete Research,* Vol. 26, No. 4, pp. 539-544, 1996.

Tumidajski, Peter J., "Relationship Between Resistivity, Diffusivity abd Microstructural Descriptors for Mortars with Silica Fume" *Cement and Concrete Research,* Vol. 35, pp. 1262-1268, 2005.

Whiting, David A. and Nagi, Mohamad A. "Electrical Resistivity of Concrete – A Literature Review" *PCA R&D No. 2457,* 2003.

Yang, C.C and Huang, S. W. ChoR "The Relationship between Charge Passed and the Chloride-ion Concentration in Concrete using Steady-state Chloride Migration Test", *Cement and Concrete Research* Vol. 32, August, pp. 217-222, 2001.

Appendix A: Wenner Probe Test Method

Designation: FM 5-578

1. SCOPE

1.1 This non-destructive laboratory test method measures the electrical resistivity of water-saturated concrete and provides an indication of its permeability. The test result is a function of the electrical resistance of the specimen.

2. APPLICABILITY

2.1 This test method is applicable to concretes formulated with various combinations of cementitous materials (fly ash, slag, silica fume, or metakaolin), but can produce misleading results when calcium nitrite, reinforcing steel, conductive fibers or other embedded electrically conductive materials are present in the concrete. This test method is not applicable to cores, as these can be contaminated with conductive chloride ions.

3. APARATUS

3.1 Surface Resistivity meter with a Wenner linear four-probe array. The meter should have a range of 0 to 100 KOhm-cm, with a resolution of 0.1 KOhm-cm and an Accuracy of +/- 2% of reading. The Wenner probe array spacing should be set at 1.5 inches (38.1 mm).

3.2 Test Specimen Molds - 4.0 x 8.0 inches (100 x 200 mm) cylindrical molds meeting the requirements of ASTM C-470.

4. SAMPLE PREPARATION

4.1 Cast three 4.0 x 8.0 inches concrete cylinder specimens, as identified in 3.2, in accordance with ASTM C192 or ASTM C31.

4.2 All specimens shall be moist cured in accordance with ASTM C-192, except as noted below, from the time of molding to testing in a moist room. The specimens should not be cured in a saturated lime water tank, as this curing condition decreases the resistivity of the concrete.

4.3 Allow the specimens to cure in the molds for approximately 24 +/- 8 hours at 73 +/- 3°F (23 +/- 2°F) before removing from the molds. Immediately after demolding, make four indelible marks on the top circular face of the specimen marking the 0, 90, 180, and 270 degree points of the circumference of the circle. Extend the marks into the longitudinal sides of the specimens. The marks serve as visual aids during the resistivity readings.

5. PROCEDURE

5.1 Place Wenner array probe longitudinally on the side of the specimen at the 0 degree mark. Ensure the probe is centered on the side of the specimen (Figure 1). Make sure all the points of the array probe are in contact with the concrete. Wait 3 to 5 seconds or until a stable reading is obtained, record the resistivity measurement on the form shown in Table 1. Negative, unstable or obviously erroneous readings are indicative of problems with the instrument or the probe array, which need to be addressed before proceeding. A reading is considered unstable if it drifts by more than 1 kOhm-cm.

5.2 Repeat step 5.1 for the 90, 180, and 270 degree marks.

5.3 Repeat steps 5.1 and 5.2 for the same specimen.

5.4 Average all eight readings obtained in steps 5.1 to 5.3 for this specimen. Record this value on the form shown in Table 1.

5.5 Repeat steps 5.1 to 5.4 for the remaining two specimens.

5.6 Calculate average resistivity for the set of samples by averaging the average resistivity of the three specimens. Record this value on the form shown in Table 1. Use table 2 to characterize the permeability of the concrete.

FIGURE 1

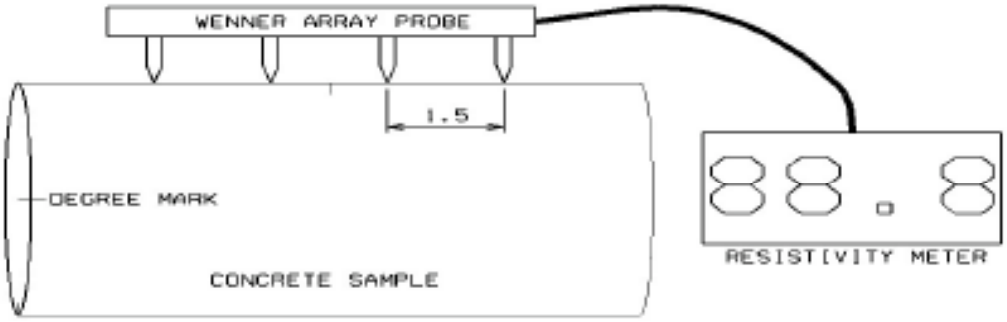

6. Report

Mix Description:

Cast Date:

Test Date:

Age:

Technician Name:

Table 1 Surface Resistivity Readings									
Sample	0°	90°	180°	270°	0°	90°	180°	270°	Average
A									
B									
C									
							Set Average		

Table 2 Surface Resistivity - Permeability	
Chloride Ion Permeability	Surface Resistivity Test kΩ–cm
High	< 12
Moderate	12 – 21
Low	21 – 37
Very Low	37 – 254
Negligible	> 254

Permeability Based on Surface Resistivity:

7. REFERENCE

7.1 Chini, A., ""Determination of Acceptance Permeability Characteristics for Performance-Related Specifications for Portland Cement Concrete," BC 354-41, School of Building Construction, University of Florida, 2003. Table 5.9 from this report is partially reproduced here for information purposes only.

Table 5.9 Equivalent Surface Resistivity Values Rounded for Utilization

Chloride Ion Permeability	RCP Test Charged Passed (coulombs)	Surface Resistivity Test 28 day test kΩ–cm
High	> 4,000	< 12
Moderate	2,000-4,000	12 - 21
Low	1,000-2,000	21 - 37
Very Low	100-1,000	37 - 254
Negligible	< 100	> 254

8. PRECISION AND BIAS

8.1 Single-Operator Precision – the single operator coefficient of variation of a single test result has been found to be 8.2%. Therefore, the results of two properly conducted tests by the same operator on concrete samples from the same batch and the same diameter should not differ by more than 23.1%.

8.2 Bias – The procedure of this test method for measuring the resistance of concrete to chloride ion penetration has no bias because the value of this resistance can be defined only in terms of a test method.

Appendix B: Resistivity Meter Schematic (Designed and constructed by Stanley Bowser, Department of Electrical Engineering, UNB**)**

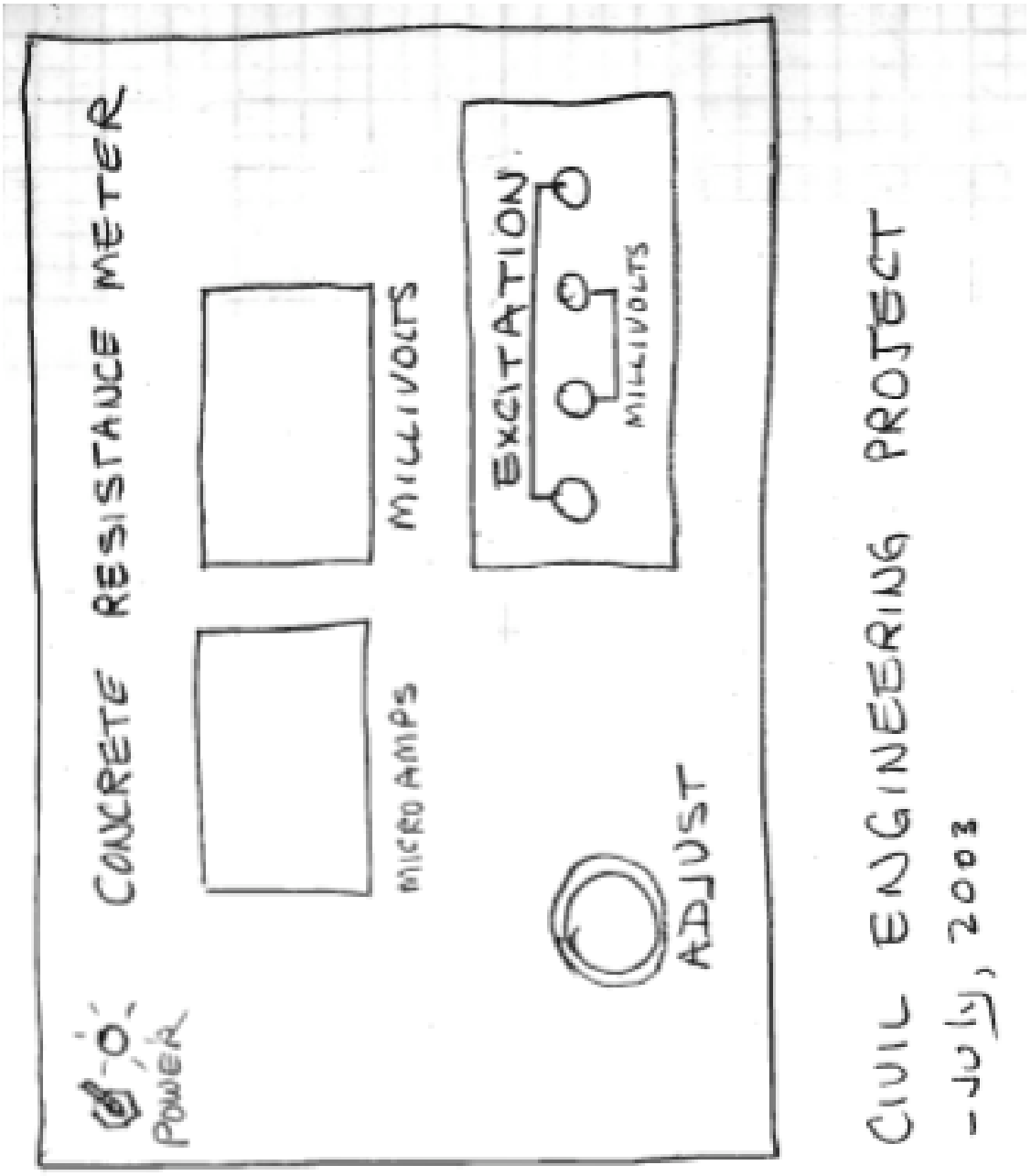

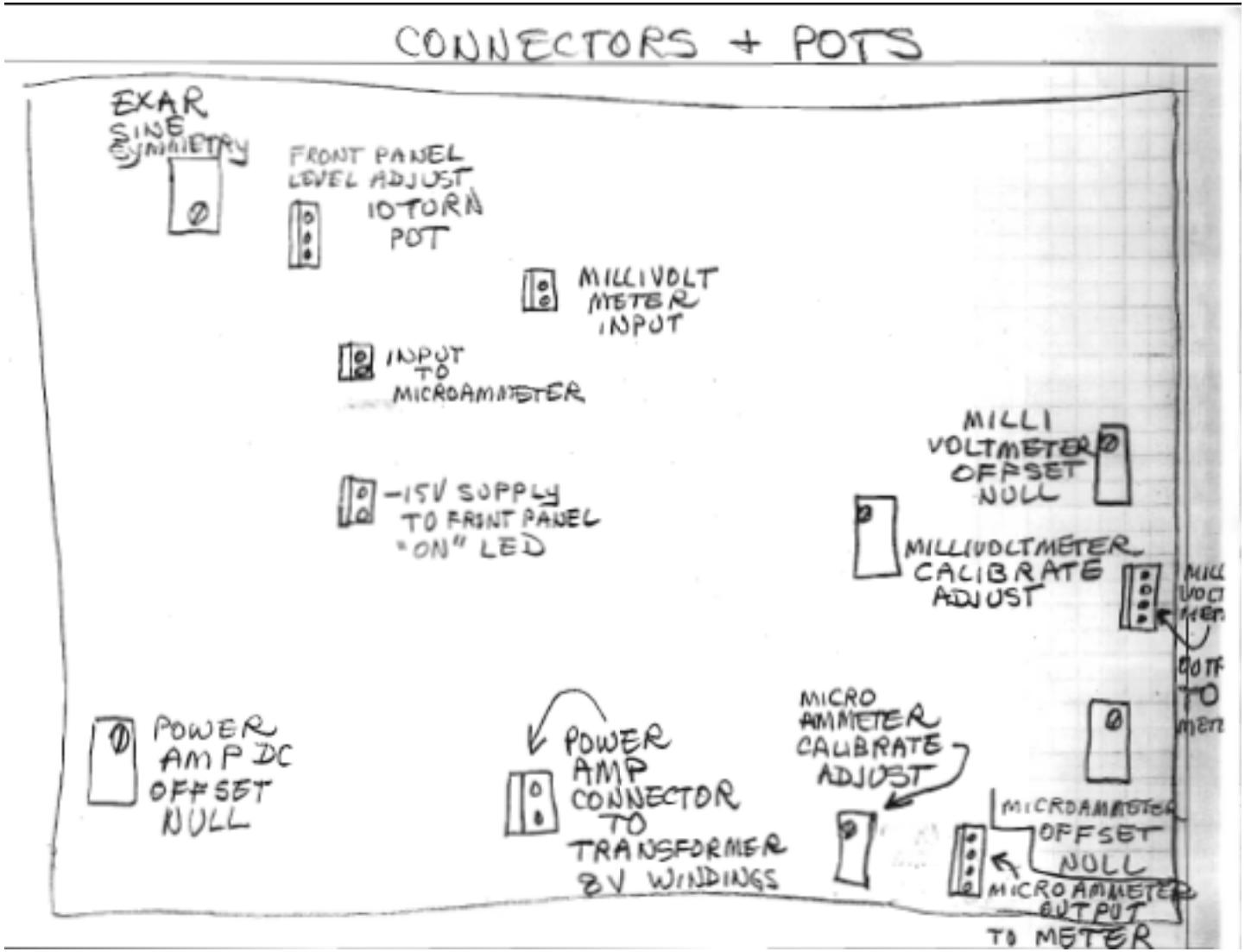
CONNECTORS + POTS
EXAR SINE SYMMETRY
FRONT PANEL LEVEL ADJUST 10 TURN POT
MILLIVOLT METER INPUT
INPUT TO MICROAMMETER
-15V SUPPLY TO FRONT PANEL "ON" LED
MILLI VOLTMETER OFFSET NULL
MILLIVOLTMETER CALIBRATE ADJUST
POWER AMP DC OFFSET NULL
POWER AMP CONNECTOR TO TRANSFORMER 8V WINDINGS
MICRO AMMETER CALIBRATE ADJUST
MICROAMMETER OFFSET NULL
MICROAMMETER OUTPUT TO METER

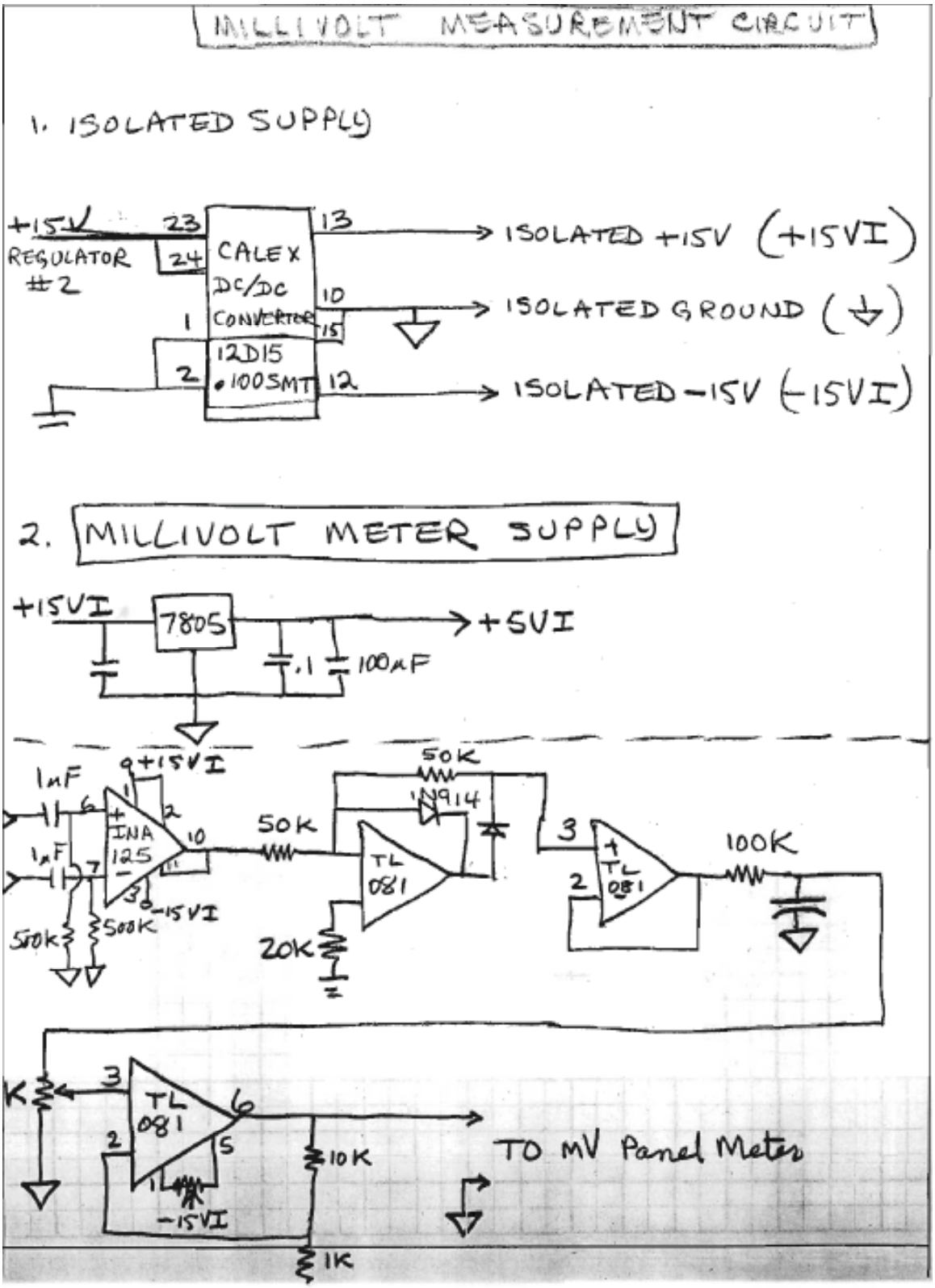
MILLIVOLT MEASUREMENT CIRCUIT
1. ISOLATED SUPPLY
+15V REGULATOR #2
23
24
1
2
CALEX DC/DC CONVERTER
12D15 • 100SMT
13
10
15
12
ISOLATED +15V (+15VI)
ISOLATED GROUND
ISOLATED -15V (-15VI)
2. MILLIVOLT METER SUPPLY
+15VI
7805
+5VI
.1
100μF
1μF
1μF
INA 125
+15VI
-15VI
50K
50K
50K
1N914
TL 081
20K
100K
TL 081
10K
1K
TO MV Panel Meter

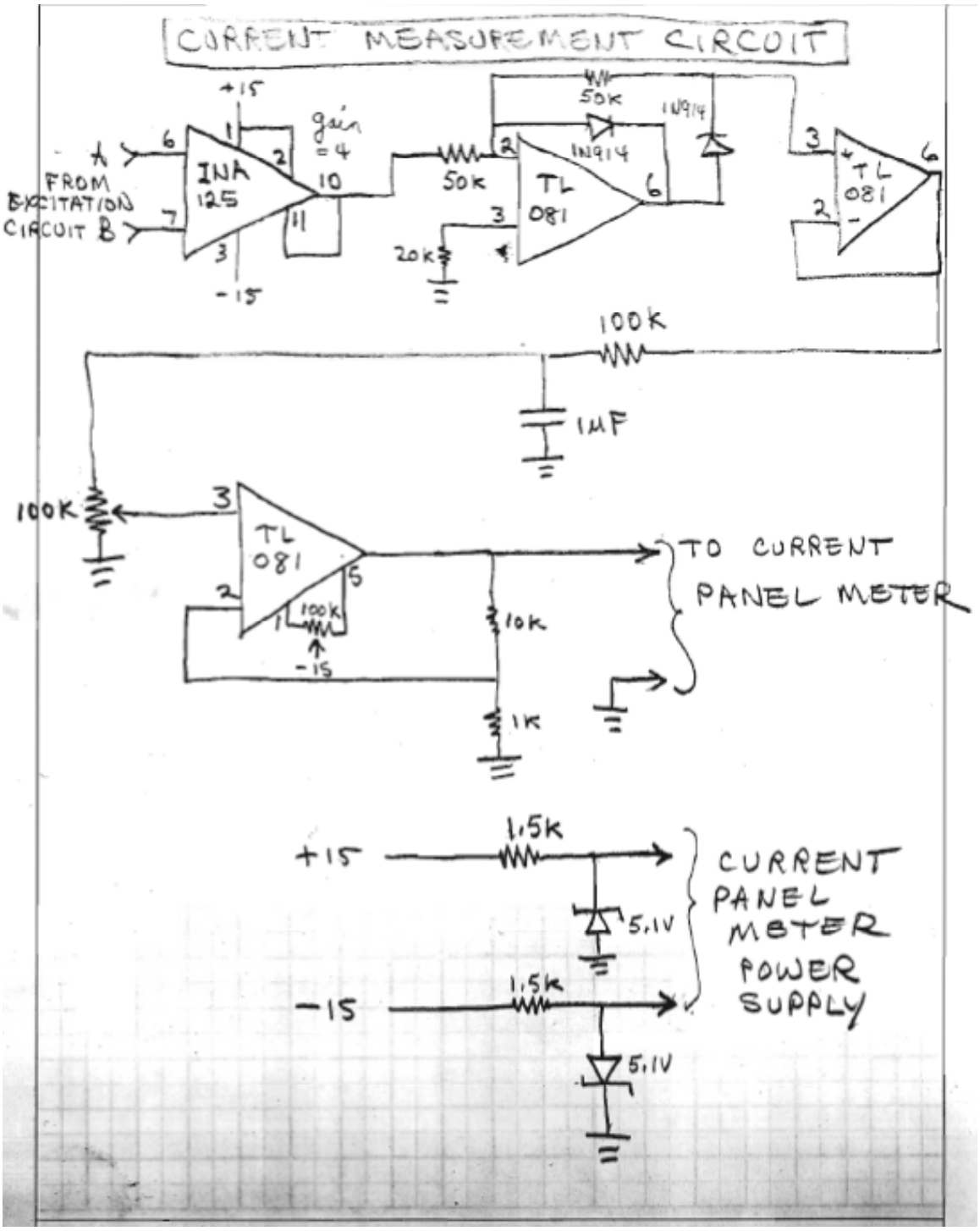
CURRENT MEASUREMENT CIRCUIT
+15
gain = 4
INA 125
FROM EXCITATION CIRCUIT B
-15
50K
1N914
50K
TL 081
20K
TL 081
100K
1MF
100K
TL 081
100K
-15
10K
1K
TO CURRENT PANEL METER
+15
1.5K
5.1V
CURRENT PANEL METER POWER SUPPLY
-15
1.5K
5.1V

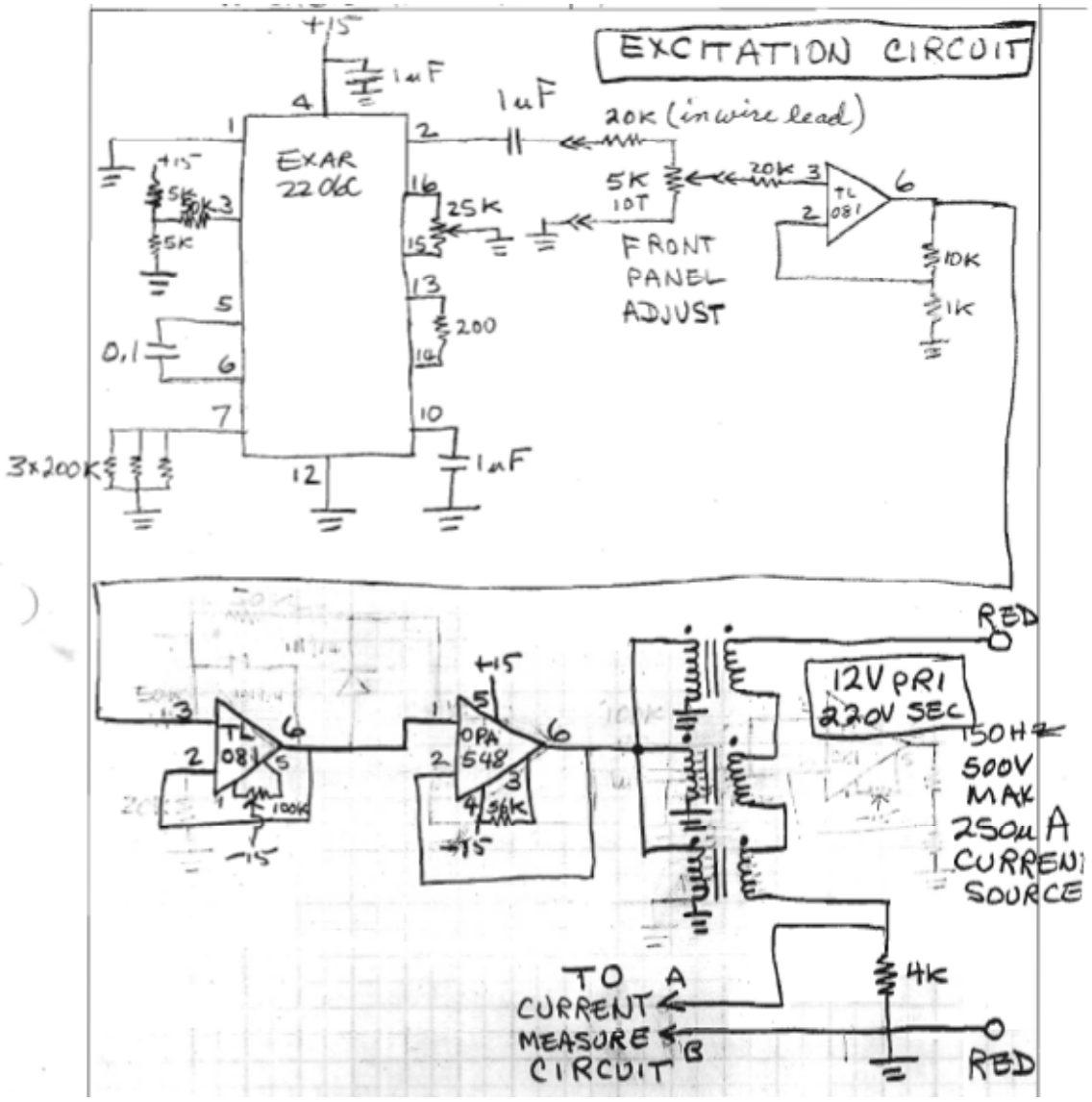
EXCITATION CIRCUIT
+15
1uF
1uF
20K (in wire lead)
EXAR
2206
5K
10T
FRONT
PANEL
ADJUST
25K
200
0.1
3x200K
1uF
TL
081
10K
1K
20K
5K
50K
100K
-15
OPA
548
56K
RED
12V PRI
220V SEC
150H
500V
MAX
250mA
CURRENT
SOURCE
4K
TO
CURRENT
MEASURE
CIRCUIT
A
B
RED

Appendix C : Bulk Diffusion Data

Depth (m)	0.37PC	0.37SF	0.37SF/CNI	0.6PC	0.37SF/FA	0.37FA
0.0005	0.809%	0.606%	0.543%	1.329%	0.680%	0.995%
0.0015	0.522%	0.500%	0.271%	1.095%	0.591%	0.943%
0.0025	0.408%	0.378%	0.169%	0.877%	0.416%	0.697%
0.0035	0.341%	0.206%	0.112%	0.664%	0.278%	0.559%
0.0045	0.281%	0.104%	0.059%	0.522%	0.184%	0.443%
0.0055	0.214%	0.046%	0.035%	0.416%	0.115%	0.368%
0.0065	0.155%	0.031%	0.023%	0.358%	0.087%	0.321%
0.0075	0.108%	0.019%	0.017%	0.309%	0.050%	0.280%
0.0085	0.081%	0.012%	0.018%	0.280%	0.040%	0.254%
0.0095	0.051%	0.010%	0.013%	0.248%	0.026%	0.221%
C_s (%)	0.654%	0.826%	0.419%	1.264%	0.8400%	1.0380%
D_a (m^2/s)	4.38E-12	1.37E-12	1.43E-12	5.57E-12	2.03E-12	6.11E-12
R^2	0.998	0.994	0.997	0.978	0.998	0.984

90d

Depth (m)	0.37PC	0.37SF	0.37SF/CNI	0.6PC	0.37SF/FA	0.37FA
0.0005	0.443%	0.465%	0.371%	0.352%	0.679%	0.963%
0.0015	0.437%	0.419%	0.483%	0.548%	0.567%	1.036%
0.0025	0.450%	0.301%	0.337%	0.628%	0.428%	0.827%
0.0035	0.403%	0.185%	0.248%	0.568%	0.334%	0.604%
0.0045	0.360%	0.098%	0.184%	0.494%	0.252%	0.425%
0.0055	0.308%	0.033%	0.139%	0.439%	0.195%	0.365%
0.0065	0.256%	0.019%	0.091%	0.409%	0.159%	0.292%
0.0075	0.192%	0.015%	0.062%	0.409%	0.109%	0.234%
0.0085	0.128%	0.012%	0.032%	0.402%	0.089%	0.180%
0.0095	0.100%	0.001%	0.037%	0.319%	0.062%	0.134%
C_s (%)	0.647%	0.568%	0.632%	0.712%	0.7020%	1.2820%
D_a (m^2/s)	5.72E-12	1.36E-12	2.09E-12	1.82E-11	3.88E-12	3.08E-12
R^2	0.989	0.989	0.998	0.962	0.998	0.988

180d

Depth (m)	0.37PC	0.37SF	0.37SF/CNI	0.6PC	0.37SF/FA	0.37FA
0.0005	0.479%	0.418%	0.485%	1.077%	0.922%	1.013%
0.0015	0.319%	0.382%	0.284%	0.983%	0.585%	1.014%
0.0025	0.212%	0.348%	0.134%	0.833%	0.390%	0.784%
0.0035	0.146%	0.234%	0.071%	0.738%	0.301%	0.598%
0.0045	0.106%	0.153%	0.047%	0.674%	0.214%	0.483%
0.0055	0.070%	0.089%	0.027%	0.595%	0.145%	0.357%
0.0065	0.042%	0.042%	0.021%	0.567%	0.057%	0.257%
0.0075	0.027%	0.024%	0.017%	0.515%	0.059%	0.177%
0.0085	0.020%	0.024%	0.015%	0.457%	0.037%	0.159%
0.0095	0.010%	0.022%	0.004%	0.430%	0.024%	0.088%
C_s (%)	0.444%	0.505%	0.584%	1.071%	0.9740%	1.2830%
D_a (m^2/s)	2.07E-12	2.84E-12	7.03E-13	1.54E-11	1.68E-12	3.74E-12
R^2	0.999	0.988	0.987	0.993	0.99	0.998

365d

Depth (m)	*0.37PC*	*0.37SF*	*0.37SF/CNI*	*0.6PC*	*0.37SF/FA*	*0.37FA*
0.0005	1.113%	0.532%	0.603%	1.028%	0.749%	0.683%
0.0015	0.798%	0.395%	0.557%	0.762%	0.450%	0.482%
0.0025	0.535%	0.254%	0.266%	0.543%	0.227%	0.286%
0.0035	0.230%	0.163%	0.032%	0.402%	0.089%	0.190%
0.0045	0.234%	0.064%	0.044%	0.345%	0.033%	0.106%
0.0055	0.177%	0.045%	0.034%	0.296%	0.021%	0.057%
0.0065	0.114%	0.032%	0.018%	0.297%	0.013%	0.035%
0.0075	0.082%	0.020%	0.012%	0.286%	0.010%	0.021%
0.0085	0.057%	0.018%	0.013%	0.278%	0.008%	0.014%
0.0095	0.047%	0.011%	0.011%	0.287%	0.008%	0.013%
C_s (%)	1.240%	0.617%	0.789%	0.920%	0.9190%	0.7830%
D_a (m^2/s)	1.17E-12	1.04E-12	7.12E-13	4.62E-12	2.99E-13	5.62E-13
R^2	0.96	0.99	0.91	0.889	0.998	0.998

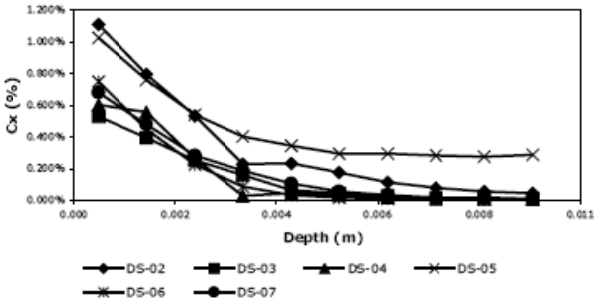

Fly Ash Pavement Cores

Depth (m)	*0.37PC*	*0.37SF*	*0.37SF/CNI*	*0.6PC*	*0.37SF/FA*	*0.37FA*	*PW-1*
0.0005	0.978%	0.805%	0.878%	0.851%	0.971%	0.888%	1.000%
0.0015	0.532%	0.372%	0.498%	0.520%	0.565%	0.626%	0.775%
0.0025	0.329%	0.223%	0.317%	0.343%	0.492%	0.337%	0.554%
0.0035	0.223%	0.164%	0.195%	0.198%	0.417%	0.337%	0.369%
0.0045	0.183%	0.089%	0.144%	0.113%	0.359%	0.242%	0.252%
0.0055	0.135%	0.089%	0.120%	0.099%	0.302%	0.149%	0.184%
0.0065	0.089%	0.090%	0.106%	0.077%	0.254%	0.099%	0.163%
0.0075	0.063%	0.074%	0.097%	0.067%	0.213%	0.079%	0.155%
0.0085	0.094%	0.083%	0.094%	0.060%	0.187%	0.053%	0.078%
0.0095	0.086%	0.079%	0.091%	0.059%	0.136%	0.054%	0.146%
C_s (%)	1.043%	0.912%	0.940%	0.943%	0.6610%	0.9280%	1.067%
D_a (m^2/s)	5.22E-13	3.32E-13	5.44E-13	5.29E-13	3.66E-13	8.92E-13	1.11E-12
R^2	0.99	0.98	0.99	0.99	0.998	0.96	0.97

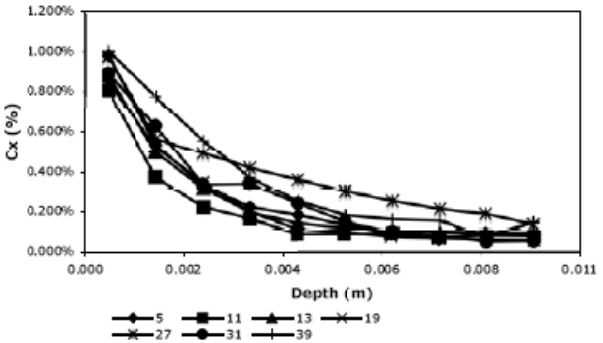

Chris Evans

Depth (m)	*SF1*	*CIJ25FS-MDAT*	*56FS-MDAT*	*SF1-MDAT*	*40FS*	*56FS*	*40FS-MDAT*	*SF2*
0.0005	-	0.651%	0.591%	0.494%	0.491%	0.893%	0.283%	0.828%
0.0015	0.633%	0.277%	0.600%	0.417%	0.359%	0.709%	0.101%	0.648%
0.0025	0.475%	0.135%	0.236%	0.373%	0.168%	0.479%	0.043%	0.502%
0.0035	0.361%	0.081%	0.066%	0.372%	0.162%	0.303%	0.039%	0.449%
0.0045	0.296%	0.096%	0.035%	0.253%	0.071%	0.245%	0.028%	0.298%
0.0055	0.262%	0.083%	0.026%	0.241%	0.059%	0.217%	0.014%	0.231%
0.0065	0.243%	0.085%	0.021%	0.206%	0.044%	0.203%	0.017%	0.216%
0.0075	0.213%	0.088%	0.019%	0.303%	0.034%	0.176%	0.015%	0.160%
0.0085	0.160%	0.013%	0.016%	0.320%	0.018%	0.163%	0.013%	0.036%
0.0095	0.096%	0.069%	0.014%	0.139%	0.015%	0.112%	0.026%	0.035%
C_s (%)	0.702%	0.584%	1.506%	0.467%	0.5540%	0.9040%	0.376%	0.870%
D_a (m^2/s)	6.05E-12	7.03E-13	4.55E-13	1.84E-11	1.34E-12	3.22E-12	3.22E-13	3.65E-12
R^2	0.97	0.67	0.995	0.64	0.95	0.95	0.75	0.97

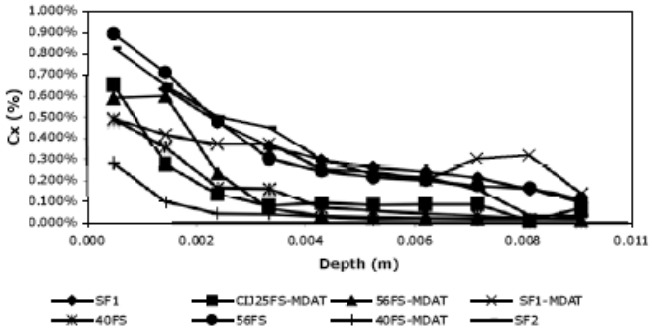

Curriculum Vitae

Candidate's Full Name

David Eric Smith

Universities Attended

Acadia University 1999 – 2001 (CAS)

University of New Brunswick 2001 – 2004 (B.Sc.E)

Publications

N/A

Conference Presentations

Portland Cement Association Educational Fellowship Annual Meeting, Sept. 2006

Awards

Bremner Scholarship in Concrete Materials 2005/2006

Portland Cement Association Educational Fellowship 2004

Ken Vaughn Memorial Bursary 2004

Atlantic Chapter – ACI Award for best Senior Report in Concrete Materials

J. Nairn McCaffery Memorial Scholarship 2002/2003 and 2003/2004